

THESIS ON CHEMISTRY AND CHEMICAL ENGINEERING G28

**Thermal Analysis of Crystallization  
Behaviour of Polyethylene  
Copolymers and Their Blends**

TRIINU POLTIMÄE

**TUT**  
**PRESS**

TALLINN UNIVERSITY OF TECHNOLOGY  
Faculty of Chemical and Materials Technology  
Department of Polymer Materials

**Dissertation was accepted for the defence of the degree of Doctor of Philosophy in Engineering on June 17, 2011.**

**Supervisor:** Prof. Andres Krumme, Department of Polymer Materials,  
Tallinn University of Technology

**Co-supervisor:** Ph. D. Elvira Tarasova, Department of Polymer Materials,  
Tallinn University of Technology

**Opponents:** Prof. Vincent B.F. Mathot, SciTe B.V., Netherlands  
Katholieke Universiteit Leuven, Belgium

Ph. D. Ants Lõhmus, Institute of Physics,  
University of Tartu

**Defence of the thesis:** 26<sup>th</sup> September 2011 at 11:00, lecture hall X-212,  
Tallinn University of Technology

Declaration:

Hereby I declare that this doctoral thesis, my original investigation and achievement, submitted for the Degree of Doctor of Philosophy at Tallinn University of Technology, has not been submitted for any academic degree.

Triinu Poltimäe



Euroopa Liit  
Euroopa Sotsiaalfond



Eesti tuleviku heaks

This work has been partially supported by graduate school “Functional materials and processes” receiving funding from the European Social Fund under project 1.2.0401.09-0079 in Estonia.

Copyright: Triinu Poltimäe, 2011  
ISSN 1406-4774  
ISBN 978-9949-23-143-0  
ISBN 978-9949-23-144-7 (PDF)

KEEMIA JA KEEMIATEHNIKA G28

**Polüetüleenil kopolümeeride ja nende segude  
kristallisatsioonikäitumise  
termiline analüüs**

TRIINU POLTIMÄE



# CONTENTS

|   |     |
|---|-----|
| LIST OF PUBLICATIONS.....   | 6   |
| INTRODUCTION.....   | 7   |
| ABBREVIATIONS AND SYMBOLS .....   | 9   |
| 1. LITERATURE SURVEY .....  | 10  |
| 1.1. Theory of crystallization .....  | 10  |
| 1.2. Thermodynamics.....  | 14  |
| 1.3. Linear low-density polyethylene: structure, catalyst, thermal behaviour ..     | 16  |
| 1.3.1. Structure, catalyst, synthesis.....  | 16  |
| 1.3.2. Crystallization of copolymers.....   | 17  |
| 1.3.3. Triple crystallization behaviour of ethylene/ $\alpha$ -olefin copolymers .. | 19  |
| 1.3.4. Crystallization of blends .....  | 21  |
| 2. EXPERIMENTAL .....   | 23  |
| 2.1. Materials .....  | 23  |
| 2.1.1. Preparative fractionation.....   | 23  |
| 2.1.2. Blending by dissolving method .....  | 26  |
| 2.2. Differential scanning calorimetry .....  | 26  |
| 2.3. Miscellaneous analyses .....   | 27  |
| 3. RESULTS AND DISCUSSION .....   | 28  |
| 3.1. Crystallization of whole copolymers .....                                      | 28  |
| 3.1.2. Dependence on comonomer content.....   | 30  |
| 3.2. Crystallization of fractionated copolymers .....                               | 33  |
| 3.2.1. Dependence on comonomer content.....   | 35  |
| 3.2.2. Dependence on molar mass .....   | 37  |
| 3.2.2.1. Crystallinity.....   | 37  |
| 3.2.2.2. Crystallization peak temperature.....                                      | 38  |
| 3.3. Crystallization of blends .....  | 41  |
| CONCLUSIONS.....  | 47  |
| REFERENCES.....   | 49  |
| KOKKUVÖTE.....  | 55  |
| ABSTRACT .....  | 57  |
| APPENDIX I: PUBLICATIONS.....   | 59  |
| APPENDIX II: CURRICULUM VITAE.....  | 101 |

## LIST OF PUBLICATIONS

- I T. Poltimäe, E. Tarasova, A. Krumme, A. Lehtinen, A. Viikna. Behaviour of the very-low-temperature crystallization peak of linear low-density polyethylene. *Proceedings of the Estonian Academy of Sciences*, 2009, 58 (1), 58-62.
- II E. Tarasova, T. Poltimäe, A. Krumme, A. Lehtinen, A. Viikna. Study of very low temperature crystallization process in ethylene/ $\alpha$ -olefin copolymers. *Macromolecular Symposia*, 2009, 282 (1), 175–184.
- III E. Tarasova, T. Poltimäe, A. Krumme, A. Lehtinen, A. Viikna. Triple crystallization behavior of fractionated ethylene/ $\alpha$ -olefin copolymers of different catalyst type. *Journal of Polymer Research*, 2011, 18 (2), 207-216.
- IV T. Poltimäe, E. Tarasova, A. Krumme, J. Roots, A. Viikna. Thermal analyses of blends of hyperbranched LLDPE with HDPE and LLDPE prepared by dissolving method. *Material Science (Medžiagotyra)*, accepted 03 December 2010.

### The author's contribution to the publications:

- I The author fulfilled the experiments and analyses, analysed the results and wrote the paper.
- II The author fulfilled the experiments and analyses, analysed the results and wrote the paper together with E. Tarasova.
- III The author fulfilled the experiments and analyses, analysed the results and wrote the paper together with E. Tarasova.
- IV The author fulfilled the experiments and analyses, analysed the results and wrote the paper.

## INTRODUCTION

Polyethylene (PE) is one of the most important semicrystalline synthetic polymers. Semicrystalline polymers consist of two or more solid phases, in at least one of them molecular chain segments are organized into a regular three-dimensional array, and in one or more other phases, chains are disordered. When molten polyethylene solidifies, the chains in some regions become organized into small crystals, known as crystallites. Disordered chains surround the crystallites; this is the essence of semicrystallinity. Term “amorphous” is often used to describe regions with no discernible ordering.

PE is a commodity polymer that has become widely used over the past several decades because of its low price and good mechanical properties. Polyethylene is available with a wide array of engineering properties to provide toughness, ease of processing, shrinkable grades as well as chemical, abrasion and impact resistance. The properties are largely determined by the characteristics of the polymer such as molar mass (MM), molar mass distribution (MMD), comonomer type and content. The relationship between microstructure and properties of polymers requires, among other factors, investigation of melting and crystallization behaviours. The microstructure plays an important role in determining the polymer mechanical, optical, rheological and thermal properties.

Differential scanning calorimetry (DSC) has been the main technique used to study melting and crystallization behaviour and this method is powerful enough to analyze very small quantities, sometimes only 1-2mg of material and to detect very small changes in crystallinity.

Despite the fact that polyethylene crystallization is very widely studied there are still some questions which need to be answered. Polyethylene crystallizes at the temperatures around 110-120°C (high temperature crystallization). Often this high temperature crystallization peak (HTCP) in DSC has a shoulder around 90°C, so called low temperature crystallization peak (LTCP). This is primary crystallization where crystal superstructures are formed. Between crystallites exists amorphous region. Under certain conditions, additional crystallization, at temperatures around 60-75°C, takes place. It is not clear what causes this phenomenon of very low temperature crystallization (VLTC) and it is not satisfactorily studied.

Commercial materials have usually broad MMD and composition distribution (CD). Before going on to the end-use properties of the materials and how this crystallization behaviour at very low temperature influences the products it is important to understand how its macromolecular constituents influence the VLTC process.

Therefore, the main objective of the present study was to examine the crystallization behaviour of linear low density polyethylene (LLDPE) at very low temperature using DSC. For better understanding what causes the very low temperature crystallization peak (VLTCP), components with different comonomer contents were blended together. Another interest in blending is the synergy and segregation of the components.

The aim of the work was to study the effect of:

structure

MM and MMD

polydispersity (PD)

comonomer type

comonomer concentration

on the behaviour of the VLTCP.

The results of the work have been published in four papers.

## **Acknowledgements**

I thank my supervisor Prof. Andres Krumme for his contribution to this work. I express my deepest gratitude to Ph.D. Elvira Tarasova for her continuous support and help. I also express my gratitude to Prof. Jaan Roots for the pleasant cooperation and giving me the chance to practice in University of Oslo. I would like to thank Ph.D. Arja Lehtinen for her valuable comments and Mrs. Raija Vainikka for her help in chromatography. Also, I thank former master students M.Sc. Veronika Gavrilkina, M.Sc. Maris Leirost and M.Sc. Kairi Kivistik for helping in laboratory work. I express warm thanks to Mrs. Piret Lees for revising the language of the manuscript and finally I thank all my colleagues from Department of Polymer Materials for their support.

Borealis Polymers OY, Finland is acknowledged for structural characterization of the studied materials. The Estonian Science Foundation is acknowledged for support under grant No. 6553 and ETF8134, as well as Graduate School of Tartu University and Tallinn University of Technology "Functional Materials and Technologies".

## ABBREVIATIONS AND SYMBOLS

|                      |   |
|----------------------|---|
| ASL                  | average sequence length                   |
| BC                   | branching content                         |
| $C_{\text{com}}$     | comonomer content                         |
| CD                   | composition distribution                  |
| DSC                  | differential scanning calorimetry         |
| $\Delta H$           | change of enthalpy                        |
| HDPE                 | high density polyethylene                 |
| HTCP                 | high temperature crystallization peak     |
| HTMP                 | high temperature melting peak             |
| LDPE                 | low-density polyethylene                  |
| LLDPE                | linear low density polyethylene           |
| LPE                  | linear polyethylene                       |
| LTCP                 | low temperature crystallization peak      |
| LTMP                 | low temperature melting peak              |
| MM                   | molar mass                                |
| MMD                  | molar mass distribution                   |
| $M_w$                | weight average molar mass                 |
| PD                   | polydispersity                            |
| PE                   | polyethylene                              |
| PTFE                 | polytetrafluoroethylene                   |
| SCB                  | short chain branching                     |
| SCBD                 | short chain branching distribution        |
| SS                   | single site                               |
| ZN                   | Ziegler-Natta                             |
| $T_{\text{HTCP}}$    | HTCP temperature                          |
| $T_m$                | melting temperature                       |
| $T_m^0$              | equilibrium melting temperature           |
| $T_{\text{VLTCP}}$   | VLTCP temperature                         |
| VLTC                 | very low temperature crystallization      |
| VLTCP                | very low temperature crystallization peak |
| VLTMP                | very low temperature melting peak         |
| X                    | degree of crystallinity                   |
| $X_{\text{overall}}$ | overall degree of crystallinity           |
| $X_{\text{VLTCP}}$   | partial degree of crystallinity of VLTCP  |

# 1. LITERATURE SURVEY

## 1.1. Theory of crystallization

Despite this relatively broad subject area, it needs to be discussed within the general framework of the **crystallization behaviour** of copolymers. Therefore, brief summary of the general principles that govern copolymer crystallization is presented before some of the specific thermodynamic and structural properties are discussed.

Polymer crystallites are microscopic crystals that are embedded in a matrix of noncrystalline material. Solid polyethylene consists of a three-phase morphology: submicroscopic crystallites are surrounded by a non-crystalline phase comprising a partially ordered layer adjacent to the crystallites and disordered material in the intervening spaces as shown in Figure 1. In crystalline phase the molecular chain segments are packed in regular arrays. Disordered molecular segments in the non-crystalline regions are normally continuous with those in the crystallites. Noncrystalline segments can traverse the intercrystalline zone to connect to an adjacent crystallite (known as “tie chains”), they can double back and attach themselves to the crystallite from which they originated (“loops”), or they can terminate in a chain end (“cilia”). The three types of noncrystalline segments are shown in Figure 2. Between disordered regions and crystallite surfaces a third phase exists, made up of chain segments that exhibit varying degrees of order as they traverse it. The third phase is termed the interfacial region (Peacock 2000).

There are several models of crystallization. The **fringed micelle** model was one among the earliest morphological models of semi-crystalline polymers (Flory 1953). In this model, crystallites are envisaged as small bundles of parallel extended linear chain segments disposed randomly in a matrix of disordered chains. This is a model of crystallinity in which the crystallized segments of a macromolecule belong predominantly to different crystals. In the fringed micelle model noncrystalline chain segments are attached to the crystalline stems via partially aligned noncrystalline chain segments. Schematic picture of fringed micelle model can be seen in Figure 3.

The modern view of initial step in crystallization process is based on the model of **chain folding** which was first introduced by Storks (1938). Storks concluded that the chains of semicrystalline polymer had to fold back and forth. But at that time this proposal was left unnoticed until in the mid 1950's it was discovered by Keller (1957), Till (1957) and Fischer (1957) that various polymers could form crystals with lateral dimensions, several orders of magnitude greater than their thickness. Such crystals were called «lamellae». First this type of crystals were discovered in crystallization from solution but then it was observed that

also melt-crystallized samples had structure similar to solution crystals (Gedde 1995).

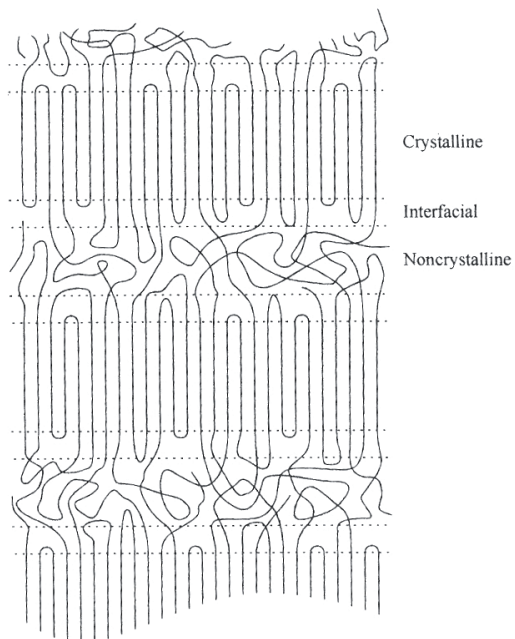


Figure 1. Three-phase morphology of polyethylene (Peacock 2000)

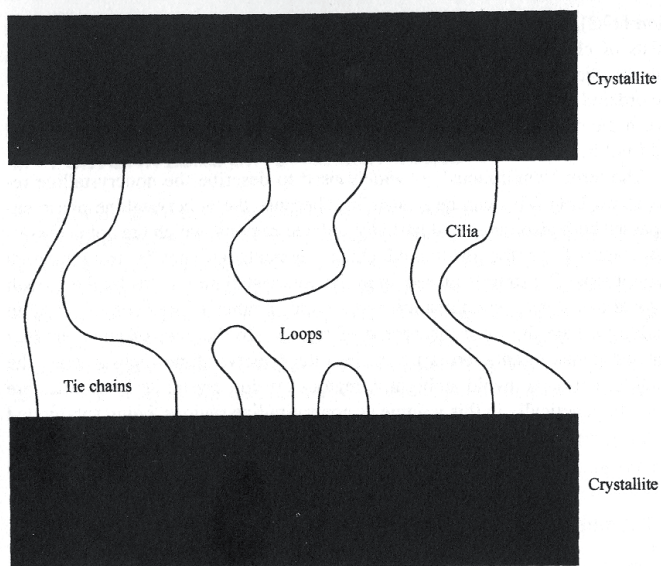
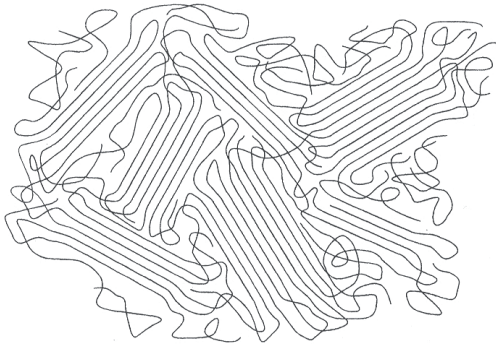


Figure 2. Tie chains, loops and cilia in the non-crystalline phase of polyethylene (Peacock 2000)



*Figure 3. Fringed micelle model (Peacock 2000)*

When polyethylene crystallizes from a very dilute solution it forms lamellar crystals with thicknesses of the order of  $0.01\mu\text{m}$  and lateral dimensions varying from a few micrometers up to more than  $100\mu\text{m}$  (Sharma and Mandelkern 1969). The surface of solution crystals was observed to be microscopically smooth, leading to the suggestion that the crystals were composed of crystalline stems linked to their neighbours by a series of regular tight folds (Basset et al. 1963, Keller 1959, Lindenmeyer 1962). This model required that consecutive chain segments from a single molecule be laid down successively on the growing face of the crystal in a mode known as adjacent reentry (see Fig.4a).

An opposing view held that many molecules contributed chain segments to each layer of the growing face. It has been said that no more than half of the chains emanating from the lamellar crystal surface can be accommodated by the neighbouring disordered amorphous phase. As a result, more than half of those sequences must return to the crystal face from which they departed. This re-entry has been proposed to occur via loops of varying lengths that are present in the spaces between the crystal and the amorphous regions. There are also a number of chains that do not re-enter a given crystallite, but leave the basal plane of the crystal to become part of a disordered amorphous region. These chains could eventually enter another neighbouring crystallite. Such a possibility of chain folding is often referred to as the "switchboard model" (see Figure 4b). Model shown in Figure 4c is called loose loops with adjacent reentry and 4d is called departure of chains from immediate environs of crystallite.

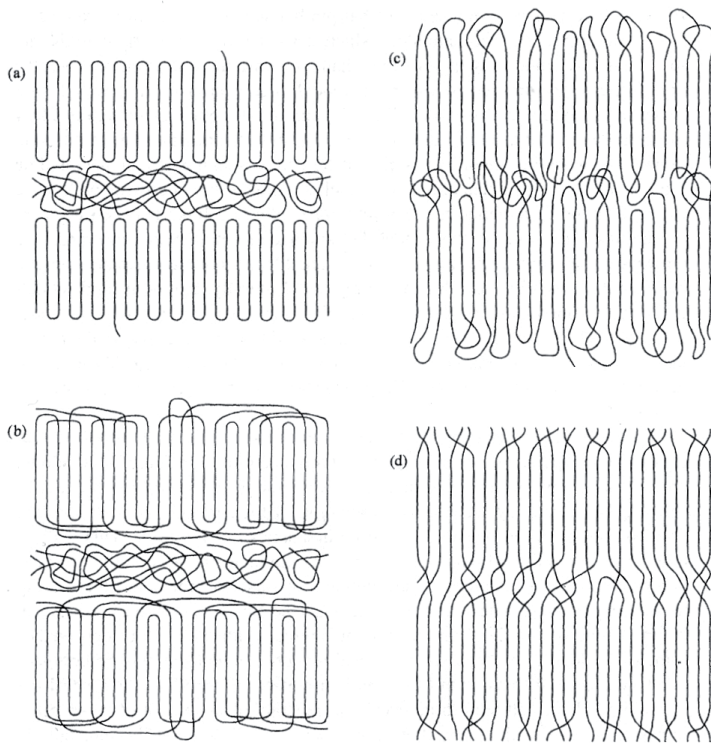


Figure 4. Different chain-folding models: *a*-adjacent reentry, *b*-switchboard model, *c*-loose loops with adjacent reentry, *d*-departure of chains from immediate environs of crystallite (Peacock 2000)

Strobl (2000) has argued that in all processes of polymer crystallization, a mesomorphic precursor phase is formed before the crystalline phase. Blocks of this mesomorphic state then attach to the growth front, as seen in Figure 5.

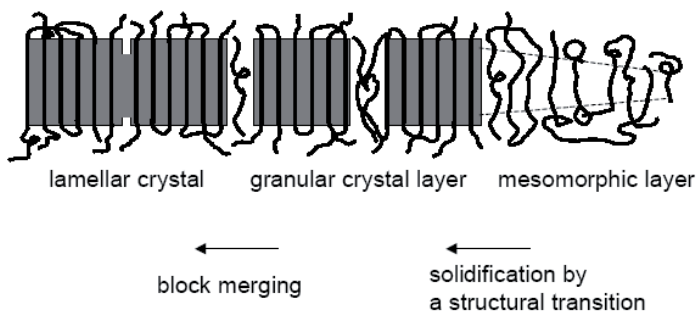


Figure 5. Strobl's model (Reiter and Strobl 2007)

## 1.2. Thermodynamics

When semicrystalline polymer is cooled to a temperature that is below the melting temperature  $T_m$  but above the glass transition temperature  $T_g$ , the polymers undergo crystallization. Processes that increase enthalpy such as melting or evaporation are endothermic while those that lower like crystallization are called exothermic. The change in enthalpy is measured with calorimeter, by recording the displacement of the heat flux  $Q$  from a baseline. The baseline is a linear section of the curve that represents conditions in which no reaction or transition occurs.

One of the powerful methods for studying the thermal properties of crystallisable polymers is DSC. DSC measures the heat flow into or from a sample under heating, cooling or isothermal conditions. DSC provides valuable information on such key parameters as enthalpy of fusion, melting and crystallization temperatures, time to reach maximum rate of crystallization etc.

Crystallization is the change that occurs when a material in the (usually liquid) amorphous state is transformed into a solid crystalline state. It can occur only after the temperature has fallen below the equilibrium melting temperature  $T_m^0$ , for PE  $T_m^0=142^\circ\text{C}$  (Wunderlich 1980). The crystallisation peak temperature  $T_c^p$  is the temperature at which the crystallization rate is at maximum.

Polyethylene crystallizes from the molten state when the prevailing conditions make the crystalline state more stable than the disordered one. The processes by which polyethylene crystallizes, reflect the properties of the disordered state from which the ordered phase condenses. Thus levels of chain entanglements, molecular dimensions, and viscosity all play important roles. The factors affecting the structure of disordered state are molar mass average, MMD, and concentration, type, and distribution of branches.

The driving force behind the crystallization is thermodynamic. The system strives to achieve the lowest possible free energy state. As with all thermodynamic processes occurring at constant pressure, the direction of change is covered by the free energy of competing states according to

$$\Delta G = \Delta H - T\Delta S \quad (1)$$

where  $\Delta G$  is change of Gibbs free energy,  $\Delta H$  is change of enthalpy,  $T$  is absolute temperature and  $\Delta S$  is change of entropy (Peacock 2000).

Melting is a change from solid, crystalline state into an amorphous liquid state. No loss of mass or chemical change occurs. Semicrystalline polymers consist of crystallites of different lamellar thicknesses and degree of perfection. The

melting curve reflecting this non-uniform structure is shown in Figure 6. At the onset temperature  $T_{im}$  the thinner or less perfect crystallites begin to melt and at the melting end temperature  $T_{fm}$  all crystallites are melted and the crystalline order has been destroyed. Therefore the melting curve indirectly characterizes the lamellar thickness distribution. The melting peak temperature  $T_{pm}$  is the temperature at which most of the crystallites melt.

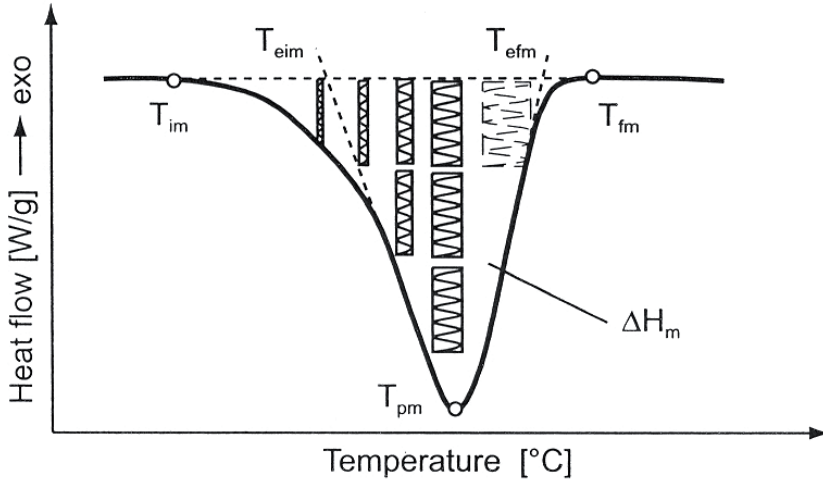


Figure 6. Melting curve and lamellar thickness distribution for a semicrystalline thermoplastic (Ehrenstein et al 2004)

One of the important relationships for crystalline polymers is the Thompson-Gibbs equation which relates melting point and crystal thickness:

$$T_m = T_m^0 \left[ 1 - \frac{2\sigma}{\Delta H^0 \rho_c L_c} \right] \quad (2)$$

$\sigma$  is the specific fold surface free energy,  $\Delta H^0$  is the heat of fusion;  $\rho_c$  is the crystal phase density;  $L_c$  is crystal thickness. From this equation it is possible to estimate the initial crystal thickness,  $L_c^*$  (Gedde 1995):

$$L_c^* = \frac{2\sigma T_m^0}{\Delta H^0 \rho_c (T_m^0 - T_c)} \quad (3)$$

where  $T_c$  is the crystallization temperature.

## 1.3. Linear low-density polyethylene: structure, catalyst, thermal behaviour

### 1.3.1. Structure, catalyst, synthesis

Conventionally, PE is classified into three types according to its density and structure: high density polyethylene (HDPE), low-density polyethylene (LDPE), and LLDPE. Because the current study treats ethylene/1-olefin copolymers, representing class of LLDPE, the literature review also focuses only on these materials. HDPE can be viewed as a LLDPE with no comonomer.

Figure 7 shows schematic structures of HDPE and LLDPE. In Table 1 are listed some key properties of those materials.



Figure 7. Different polyethylenes

Table 1. Properties of different types of polyethylenes (Peacock 2000)

| Property                           | HDPE      | LLDPE     |
|------------------------------------|-----------|-----------|
| Density ( $\text{g}/\text{cm}^3$ ) | 0.94-0.97 | 0.90-0.94 |
| Degree of crystallinity %          | 62-82     | 34-62     |

The LLDPE is produced from the reaction of ethylene with an  $\alpha$ -olefin such as 1-butene, 1-hexene, 1-octene and others. Production of LLDPE with conventional Ziegler–Natta (ZN) catalysts is difficult because of the much greater reactivity in the ethylene to polymerize than the  $\alpha$ -olefin. ZN catalyst systems contain a variety of active sites. Each type of site behaves differently, having a unique activity level to cause branching, chain transfer, or rearrangement of molecular chains. Accordingly, each site will produce polyethylene molecules with different distribution of chain lengths, branching, saturation, etc. Single site (SS) catalysts allow control increase on the type, amount and distribution of the  $\alpha$ -olefin comonomer within the chains. SS catalyst contains only one type of active site which polymerizes available monomers in an identical fashion (Müller and Arnal 2005, Razavi-Nuori 2006, Brüll et al. 2001, Razavi-Nuori and Hay 2001, Faldi and Soares 2001, Islam et al. 2007, Peacock 2000).

The single-site catalysts involved in the synthesis of such copolymers permit a uniform distribution of comonomers in various polymer chains, i.e., the

distributions of comonomers in different polymer chains are identical to each other, irrespective of chain length (Hseih et al. 1997). This is in sharp contrast to the ZN based systems that yield a broad distribution of comonomers among various polymer chains. There is also a difference in MMD due to catalyst used: ZN catalyst gives broad MMD and SS catalyst gives narrow MMD.

The structure of LLDPE can be carefully manipulated by varying the manufacturing conditions according to the application desired (Brüll et al. 2001). The branches in LLDPE not only lower the degree of crystallinity compared to HDPE but also lower the density of the material. LLDPE is comprised only of branches of a constant length leading to potentially higher crystallinity and higher rigidity compared to a LDPE (Subramaniam 1999).

### 1.3.2. Crystallization of copolymers

From the point of view of the crystallization behaviour, the definition of a copolymer can be subtle. In copolymers two or more chemically dissimilar monomers or co-units incorporated into the chain will constitute a copolymer. Unlike a homopolymer, a copolymer is fragmented into a number of sequences by the occurrence of branches along the backbone.

Generally, a copolymer can be considered as being comprised of two types of units - crystallizable A units, and B co-units. The latter represent the comonomers (or branches) in an actual copolymer. The presence of co-units gives rise to the possibility of these units being either completely rejected from a crystal lattice, or being uniformly included in the lattice.

The equilibrium theory of the fusion of copolymers has been developed by Flory (1949, 1955) for the case where the crystalline phase remains pure. In his theory the co-units are considered as defects that are completely excluded from the growing crystal. All sequences of a crystallite are composed only of A units, while the melt includes both A and B units. The presence of B units results in the partitioning of the polymer into sequences of A units of varying lengths that can aggregate in an ordered fashion to form a crystallite.

The Flory theory also gives expectations to the level of crystallinity for random copolymers. The degree of crystallinity,  $X_c$ , is estimated as the sum of all sequences involved in the formation of crystallites and is given by the following expression:

$$X_c = \sum_{\zeta^*}^{\infty} X_{\zeta}^c = \sum_{\zeta^*}^{\infty} (X_{\zeta}^0 - X_{\zeta}^e) \quad (4)$$

where  $\zeta^*$  is the limiting sequence length of the crystallite that can be in equilibrium with the melt at given temperature,  $X_\zeta^0$  is the weight fraction of  $\zeta$  sequences of A units in the completely molten copolymer, and  $X_\zeta^e$  is the weight fraction of  $\zeta$  sequences of A units in the melt in equilibrium with the crystallites. The degree of crystallinity is severely reduced as the concentration of non-crystallizing units increases. This is in contrast to the crystallinity of a homopolymer. A broad range of melting temperatures may be expected for the copolymers. The crystallization process in copolymers is further influenced by the fact that branches longer than the methyl are predominantly excluded from the growing crystal. As a result, the crystals formed are much thinner and less perfect compared to those formed from the corresponding linear material.

Flory (1962) pointed out that a demarcation between the ordered crystalline region and the disordered liquid-like region could not be sharply defined in a semicrystalline polymer. Consequently an interfacial region develops that involves a partially ordered set of chain units. Molar mass and crystallization conditions significantly alter the content of the interface (Alamo and Mandelkern 1994). The interfacial content increases with increasing co-unit content in the copolymer (Alamo and Mandelkern 1994, Alamo et al. 1993).

In general, melt-crystallization in semicrystalline polymers can be described by the following structural hierarchy: (a) crystal lamellae of folded chains; (b) stacks of almost parallel crystal lamellae, each crystal separated by a thin, amorphous interlayer; (c) supermolecular structures which are polycrystalline structures, e.g. spherulites (Gedde 1995). Spherulites may be viewed as spherical aggregates of lamellae that originate from a common center and radiate outwards.

The process involving the formation of a spherulitic superstructure may be roughly classified as **primary crystallization**. However, it has been widely reported that the physical and mechanical properties as well as the degree of crystallinity of many polymers continue to vary considerably with time, after the completion of this step. The process involving the time-dependent evolution of the crystallinity of the material is termed as **secondary crystallization**. It may be viewed as a slow process of completion of the crystallization process in polymers.

The changes associated with a secondary crystallization are modest in comparison with those of primary crystallization. The degree of crystallinity is unlikely to increase by more than 2-3%. Samples crystallized slowly at higher temperatures are unlikely to exhibit secondary crystallization, because their chain segments initially have the opportunity to adopt thermodynamically stable conformations (Peacock 2000). For highly crystalline polymers the long time evolution of crystallinity has been associated with a lamellar thickening process

(Schultz and Scott 1969, Hoffman and Weeks 1965, Wunderlich and Mellilo 1968). For polymers having bulky unit structures and for copolymers with branches along the backbone, the lamellar thickening process may be dismissed as being highly unfavorable on the basis of the reorganization required at the lamellar fold surface. Generation of new lamellae (Bell and Murayama 1969), crystal perfection (Fakirov et al. 1977, Fischer and Fakirov 1976), and a combination of thickening and recrystallization (Groeninckx et al. 1980) have also been proposed for secondary crystallization. The exact nature of the process involved depends on factors such as chain mobility, stiffness of chains, level of primary crystallinity, degree of constraint in the amorphous regions etc.

### **1.3.3. Triple crystallization behaviour of ethylene/ $\alpha$ -olefin copolymers**

The molecular architecture of the distribution of the short chain branching (SCB) for LLDPE is an important parameter which determines many of the properties as it controls the crystallization and hence the final morphological structure (Chau and The 2005). An important element of phase structure is the degree of crystallinity. Alamo et al. (1984) studied the crystallinity of polyethylene copolymers and noticed a decrease of crystallinity with increasing comonomer content. The chemical nature of the branch does not influence the crystallinity values for a given co-unit content. It was suggested that the dependence of crystallinity on comonomer content is associated with the severe restrictions imposed on the length of the crystallizable sequences with the random addition of comonomer units. Mathot et al. (1998) have examined the comonomer effect on the crystallinity of a variety of ethylene copolymers via thermal analysis. The crystallization process in samples with comonomer content  $< \sim 5$  mole-% branches was found to be largely influenced by cooling rate, whereas the higher branch content materials remained mostly invariant. Peeters et al. (1997) suggested that lower branched samples may crystallize more perfectly if the time available for crystallization is prolonged via a slower cooling rate. No such effect was seen for the highly branched copolymers.

Increasing branch content also causes a decrease in the melting temperatures  $T_m$  of ethylene/ $\alpha$ -olefin copolymers (Alamo and Mandelkern 1994). However, the  $T_m$ 's were found to be independent of the chemical nature of the co-unit. According to Flory's theory, the melting point of a copolymer ( $T_m$ ) does not bear a unique dependence on composition, nor is it significantly influenced by the nature of the co-unit, as long as the comonomer is non-crystallizable and is excluded from the crystal lattice.  $T_m$  is influenced mostly by the sequence distribution of the co-unit in the copolymer.

Many properties of crystalline polymers are dependent on the molar mass. Alamo and Mandelkern (1994) have studied the influence of molar mass on the

crystallization and melting behaviours of random copolymers. They reported a decrease in the degrees of crystallinity and melting temperatures of quenched random ethylene-olefin copolymers with increasing molar mass up to 100 kg/mol, while being independent of the chemical nature of co-unit. The explanation was that the increased entanglement density in the melt at higher molar masses considerably slows down the disentanglement of chains and hinders the ability of the chains to participate in the crystal formation process. Thus, the kinetic constraints imposed by the higher molar mass not only reduce the level of crystallinity, but also leads to the formation of thinner and smaller crystals that melt at lower temperatures (Alamo et al. 1992, Mandelkern et al. 1968, Mandelkern 1971).

The results of thermal analysis study on heterogeneous ZN ethylene/a-olefin copolymers clearly indicate the existence of a triple crystallization mechanism: a sharp HTCP, a broad LTCP next to HTCP and often a VLTCP. The phenomenon of VLTCP has been noticed by several authors (Alizadeh et al. 1999, Hussein 2008, Kim and Philips 1998, Marand et al. 2000, Mathot 1994, Mathot et al. 1998, Minick et al. 1995, Hussein 2008 and Islam et al. 2007). For SS copolymers, and in general for homogeneous copolymers, just HTCP and, often, VLTCP are observed. HTCP is usually associated with a primary crystallization process, whereas VLTCP is associated with secondary crystallization process that occurs during longer period of time and at lower temperatures. Islam et al. (2007) suggested that branching content (BC) hinders longitudinal chain diffusion through the crystals, thus suppresses crystal thickness growth. So, a very slow further lateral extension of lamella can occur during secondary crystallization.

For SS LLDPE samples Zhang et al. (2002) and Mirabella (2008) suggested that HTCP corresponds to the crystallization of ethylene with a large linear average sequence length (ASL) and VLTCP is related to the crystallization with a relatively short ASL. As it is said that crystallization in copolymers is predominantly governed by the crystallizable sequence length distribution Alizadeh et al. (1999) suggested that while longest sequences form part of the lamellar crystals, they impose a constraint on the remaining crystallizable sequences in these chains. As the number of segments participating in lamellar formation increase, so do the restrictions imposed on the mobility of the remaining sequences. At a very high degrees of constraint, the shorter sequences are unable to participate in the reeling-in process required for chain-folded crystal formations. The easiest way for those short segments to crystallize is to aggregate into thin bundles. They aggregate with neighbouring sequences to form stable clusters or bundled crystals.

Another point of view on the problem of VLTCP arises from the investigation of homogeneous nucleation of PE. For this purpose Kraack et al. (2001) emulsified

low MM PEs to separate the nucleation from the growth process and to remove macroscopic heterogeneous nucleation sites. Both a VLTCP and a HTCP were observed for the emulsified samples during DSC cooling scans. The degree of undercooling from the equilibrium melting temperature of linear PE,  $T_m^0=142^\circ\text{C}$  (Wunderlich 1980), for the VLTCP was several tens of degrees (80–100°C) in contrast to non-emulsified samples, which had only a HTCP at a few degrees of undercooling. It was suggested that the HTCP in the cooling scans is due to heterogeneous nucleation of aggregated droplets and the VLTCP is related to the homogeneous nucleation of the un-aggregated emulsion droplets.

#### **1.3.4. Crystallization of blends**

One of the problems that has to be solved is the phase segregation between the components of the blends. Blends of HDPE with LDPE show segregation between two components when cooled slowly from the melt (Wignall et al. 1995, Agamalian et al. 1999, Morgan et al. 1999). Only quenching of the melts showed a uniformly mixed crystalline sample, or a co-crystallized sample. For the blend of LDPE with LLDPE a formation of separated crystals of phase segregation was suggested (Kyu et al. 1987). For the blend between HDPE and slightly branched LLDPE the co-crystallization was reported even under the condition of slow cooling (Tashiro et al. 1994a, Tashiro et al. 1994b, Tashiro et al. 1992, Wignall et al. 2000). Therefore the crystal segregation and co-crystallization are dependent in a complicated manner upon the couples of the selected PEs, the crystallization conditions, etc.

The molar mass of the components in the blends, as it has been suggested elsewhere (Tashiro et al. 1994a, Tashiro et al. 1995), is of secondary importance in determining the occurrence or extent of co-crystallization. At the same time the amount of SCB and type of catalyst seems to be important factors (Tanem and Stori 2001a, Puig 2001, Tanem and Stori 2000). The higher the branching content, the lower is the possibility of co-crystallization between the components. Zhao et al. (1997) conclude that the upper branching limit still allowing co-crystallization to occur is probably much lower in blends with SS catalyst synthesised materials than in blends with ZN based materials. Zhao et al. (1997) argue that in ZN LLDPE long segments exist between branches that can easily co-crystallize with HDPE or linear polyethylene (LPE), but the more uniform SCB distribution in single site LLDPE makes co-crystallization more difficult.

Many works presented in literature have focused on blends between LPE or HDPE and the LLDPE (Tashiro et al. 1994a, Tashiro et al. 1994b, Tashiro et al. 1992, Wignall et al. 2000, Tashiro et al. 1995, Tanem and Stori 2001b, Shanks and Amarasinghe 2000). Moreover, in performed works the mixtures are

generally prepared by melt-blending, which may not ensure the initial homogeneity of the components, because it is not certain that sufficient time was allowed for the molecules to inter-diffuse to the homogeneous state.

## 2. EXPERIMENTAL

### 2.1. Materials

Nine commercial ethylene/1-butene and ethylene/1-hexene copolymers were chosen for the study of VLTC process. Five of them were produced using SS catalyst and four using ZN catalyst. All these materials had similar density,  $923\text{kg/m}^3$ , and weight average MM ( $M_w$ )  $126\text{kg/mol}$ . Comonomer content varied from 2.3 to 8.5 wt-%. One ZN HDPE (ZN-0) was taken for comparison. Material SS-6 was used only in blends and is only discussed regarding blends. All materials were obtained in pellet form. Molecular characteristics and producers of whole copolymers are listed in Table 2.

Table 2. Properties of whole copolymers

| Sample name | Manufacturer                  | Type of co-monomer | $C_{\text{com}}$ , wt-% | Density, $\text{kg/m}^3$ | $M_w$ , $\text{kg/mol}$ | Poly-dispersity $M_w/M_n$ |
|-------------|-------------------------------|--------------------|-------------------------|--------------------------|-------------------------|---------------------------|
| SS-1        | Exxon Chemical Co.            | 1-hexene           | 5.4                     | 923                      | 84                      | 2.1                       |
| SS-2        | Borealis                      | 1-hexene           | 3.6                     | 927                      | 140                     | 3.1                       |
| SS-3        | Exxon Mobile                  | 1-hexene           | 5.0                     | 923                      | 140                     | 2.3                       |
| SS-4        | Exxon Mobile                  | 1-hexene           | 6.9                     | 920                      | 115                     | 2.4                       |
| SS-5        | Chevron Phillips              | 1-butene           | 2.3                     | 922                      | 136                     | 2.3                       |
| ZN-1        | Borealis                      | 1-hexene           | 5.6                     | 930                      | 125                     | 4.5                       |
| ZN-2        | Borealis                      | 1-hexene           | 7.6                     | 924                      | 125                     | 4.4                       |
| ZN-3        | Westlake Chemical Corporation | 1-hexene           | 8.5                     | 917                      | 150                     | 3.8                       |
| ZN-4        | Borealis                      | 1-butene           | 7.2                     | 920                      | 122                     | 4.0                       |
| ZN-0        | Rhone-Poulenc                 | -                  | 0                       | 960                      | 94.5                    | 8.3                       |
| SS-6        | Mitsui Chemicals              | 1-butene           | 17.8                    | 888                      | 87.9                    | 2.0                       |

#### 2.1.1. Preparative fractionation

For fractionation were chosen materials SS-1, SS-4, ZN-2, ZN-4 and ZN-0. Fractionation was carried out in a glass reactor, heated by silicon oil thermostat. Inside the reactor there a stainless steel net was placed and the bottom of reactor was covered with glass wool in order to prevent the obstruction of out flow tap.

For mixing the solution inside the reactor vibromixer was used. Nitrogen was blown into reactor to prevent oxidation.

Before fractionation polymer pellets were dissolved in xylene at 130°C for 30min. The obtained polymer solution was allowed to cool to room temperature and the polymer was precipitated by adding acetone, then filtered using polytetrafluoroethylene (PTFE) filters with pore size 0.45µm and dried in vacuum at room temperature for 24h. Obtained material was a powder.

Fractionation by MM was carried out according to Holtrup technique which is a solvent/non-solvent extraction (Holtrup 1977). Polymer powder was extracted in a 200ml of solvent/non-solvent mixture of xylene/ethylene glycol monoethyl ether in different ratios (see Table 3). Antioxidant 2,6-di-tert-butyl-4-methylphenol (BHT) was added in concentration of 6ppm. Dissolution time for each dissolution step was 10min. The collected polymer solutions were allowed to cool to room temperature and then polymers were precipitated by adding acetone, then filtered using PTFE filters with pore size 0.45µm and dried at room temperature first 24h in air and next 24h in vacuum. Obtained material was a powder.

Fractionation by SCB (composition) was carried out by multiple solvent extraction technique (Lehtinen and Paukkeri 1994). The dissolution time for each step was 30min. The solvents used in the fractionation were: n-pentane at 35°C, n-hexane at 65°C, n-heptane at 75°C and 90°C, n-octane at 100°C, toluene at 105°C and xylene at 130°C. The first two fractions were separated by evaporation of the solvent in a rotavaporizer and the other ones by precipitation in acetone.

In the text fractions are named after whole copolymer following “*M*” or “*C*” for molarmass or compositional fractions respectively and the fraction number.

Table 3. Properties of fractionated copolymers

| Sample | ZN-4<br>(butene) |                |                  |                   |                |                  | ZN-2<br>(hexene) |                |                  |                   |                |                  | ZN-0<br>(HDPE) |                |                  |                   |                |                  | SS-1<br>(hexene) |                |                  |                   |                |                  | SS-4<br>(hexene) |                |                  |                   |                |                  |   |
|--------|------------------|----------------|------------------|-------------------|----------------|------------------|------------------|----------------|------------------|-------------------|----------------|------------------|----------------|----------------|------------------|-------------------|----------------|------------------|------------------|----------------|------------------|-------------------|----------------|------------------|------------------|----------------|------------------|-------------------|----------------|------------------|---|
|        | MM fractions     |                |                  | Compos. fractions |                |                  | MM fractions     |                |                  | Compos. fractions |                |                  | MM fractions   |                |                  | Compos. fractions |                |                  | MM fractions     |                |                  | Compos. fractions |                |                  | MM fractions     |                |                  | Compos. fractions |                |                  |   |
|        | Solv.            | M <sub>w</sub> | C <sub>com</sub> | Solv.             | M <sub>w</sub> | C <sub>com</sub> | Solv.            | M <sub>w</sub> | C <sub>com</sub> | Solv.             | M <sub>w</sub> | C <sub>com</sub> | Solv.          | M <sub>w</sub> | C <sub>com</sub> | Solv.             | M <sub>w</sub> | C <sub>com</sub> | Solv.            | M <sub>w</sub> | C <sub>com</sub> | Solv.             | M <sub>w</sub> | C <sub>com</sub> | Solv.            | M <sub>w</sub> | C <sub>com</sub> | Solv.             | M <sub>w</sub> | C <sub>com</sub> |   |
| whole  |                  | 122            | 7.2              |                   | 125            | 7.6              |                  | 125            | 7.6              |                   | 7.6            |                  |                |                |                  |                   |                |                  |                  |                |                  |                   |                |                  |                  |                |                  |                   |                |                  |   |
| 1      | 20               | 2.1            | NA               | 43.3              | 5.1            | NA               | 43.3             | 61             | 27.8             | 43.3              | 0              | 46.7             | 9.4            | -              | 45               | 5.1               | -              | -                | 45               | 5.1            | -                | -                 | 5.1            | -                | -                | -              | -                | -                 | -              | -                | - |
| 2      | 40               | 5.3            | NA               | 48.3              | 8.1            | NA               | 46.7             | 66.9           | 18.9             | 46.7              | 0              | 53.3             | 14.2           | -              | 51.7             | 13.6              | -              | -                | 51.7             | 13.6           | -                | -                 | 13.6           | -                | -                | 56.1           | 9.2              | -                 | -              | -                | - |
| 3      | 46               | 9.1            | NA               | 53.3              | 14.3           | NA               | 50               | 92.9           | 12.3             | 50                | 0              | 56.7             | 23.1           | -              | 55               | 20.1              | -              | -                | 55               | 20.1           | -                | -                 | 20.1           | -                | -                | 98.5           | 6.5              | -                 | -              | -                | - |
| 4      | 50               | NA             | NA               | 55                | 17.5           | NA               | 53.3             | 128            | 4.5              | 53.3              | 0              | 58.3             | 32.4           | -              | 56.7             | 25.4              | -              | -                | 56.7             | 25.4           | -                | -                 | 25.4           | -                | -                | 100            | 5.9              | -                 | -              | -                | - |
| 5      | 53.95            | NA             | NA               | 56.7              | 24             | NA               | 55               | 136            | 3.2              | 55                | 0              | 60               | 44             | 5.2            | 58.3             | 35                | 5.6            | 5.2              | 58.3             | 35             | 5.6              | 5.2               | 35             | 5.6              | 5.2              | 96             | 5.4              | -                 | -              | -                | - |
| 6      | 56               | NA             | NA               | 58.3              | 33             | 9.3              | 56.7             | 232            | 1.3              | 56.7              | 0              | 61.7             | 54             | 5.2            | 60               | 43.4              | 5.8            | 5.2              | 60               | 43.4           | 5.8              | 5.2               | 43.4           | 5.8              | 5.2              | 99.5           | 3.9              | -                 | -              | -                | - |
| 7      | 58               | 29             | NA               | 60                | 42.7           | 7.9              | 58.3             | 227            | 1.5              | 58.3              | 0              | 63.3             | 78.8           | 5.1            | 61.7             | 66.5              | 6.3            | 5.1              | 61.7             | 66.5           | 6.3              | 5.1               | 66.5           | 6.3              | 5.1              | -              | -                | -                 | -              | -                | - |
| 8      | 59.5             | 35.8           | NA               | 61.7              | 53             | 6.9              | 60               | 50.2           | 0                | 60                | 0              | 65               | 89.3           | 5.1            | 63.3             | 82.4              | 6.2            | 5.1              | 63.3             | 82.4           | 6.2              | 5.1               | 82.4           | 6.2              | 5.1              | -              | -                | -                 | -              | -                | - |
| 9      | 80               | 125            | NA               | 63.3              | 78.7           | 6.2              | 61.7             | 73.9           | 0                | 61.7              | 0              | 66.7             | 86.1           | 5.2            | 65               | 128               | 6.2            | 5.2              | 66.7             | 128            | 6.2              | 5.2               | 128            | 6.2              | 5.2              | -              | -                | -                 | -              | -                | - |
| 10     |                  |                |                  | 65                | 152            | 5.9              | 63.3             | 111            | 0                | 63.3              | 0              | 70               | 90             | 5.2            | 66.7             | 117               | 6.4            | 5.2              | 66.7             | 117            | 6.4              | 5.2               | 117            | 6.4              | 5.2              | -              | -                | -                 | -              | -                | - |
| 11     |                  |                |                  | 66.7              | 303            | 5.7              | 65               | 211            | 0                | 65                | 0              | 73.3             | 90.2           | 5.1            | 70               | -                 | -              | 5.1              | 70               | -              | -                | 5.1               | -              | -                | -                | -              | -                | -                 | -              | -                | - |
| 12     |                  |                |                  | 68.3              | 207            | 5.1              | 66.7             | 571            | 0                | 66.7              | 0              | -                | -              | -              | -                | -                 | -              | -                | -                | -              | -                | -                 | -              | -                | -                | -              | -                | -                 | -              | -                | - |
| 13     |                  |                |                  | 70                | 194            | 5.2              | 68.3             | 606            | 0                | 68.3              | 0              | -                | -              | -              | -                | -                 | -              | -                | -                | -              | -                | -                 | -              | -                | -                | -              | -                | -                 | -              | -                | - |

NA – not analysed

### 2.1.2. Blending by dissolving method

SS catalyzed highly branched LLDPE SS-6 was taken as common component for all the blends. The SS-6 is a copolymer of ethylene with 1-butene. For a second component different ZN catalyzed polyethylene samples with different degrees of branching were chosen: ZN-2, ZN-2-M1 and ZN-0-M1. The molecular parameters of pure components can be seen in Table 2 and 3.

Blends were prepared by dissolving components, approximately 15mg, in 4ml xylene at 130°C by stirring with magnetic stirrer for 2h. To avoid oxidation nitrogen was blown into vessel. After dissolving, the mixtures were quenched in liquid nitrogen and then freeze dried in vacuum for 48h. Blends were obtained as powders/fluffy materials.

### 2.2. Differential scanning calorimetry

Perkin Elmer Diamond DSC and DSC-7 calorimeters were used for thermal analysis. Temperature and heat flow calibrations were done by indium and tin at all used heating rates. In Diamond DSC helium (20ml/min) was used as furnace purge gas and in DSC-7 nitrogen (20ml/min) was used.

For calorimetry sample preparation plates from whole copolymer pellets were pressed at 180°C and then cooled to room temperature. Flat samples of  $1\pm 0.02$ mg were cut from the plates and packed into aluminium foil to maximise thermal contact between the sample and calorimetric furnace. Fractions and blends were compacted manually and flat samples of  $1\pm 0.02$ mg were packed into aluminium foil.

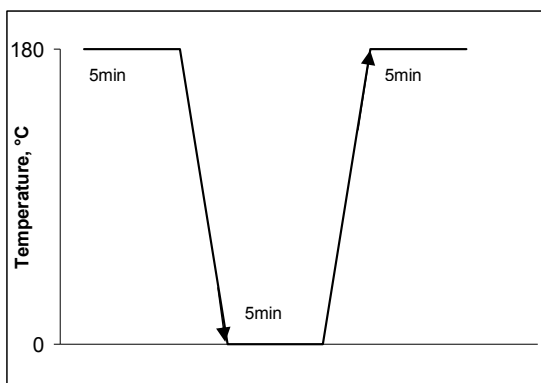


Figure 8. Thermal program for non-isothermal measurements

During the non-isothermal measurement, the sample was first kept at 180°C for 5min for deleting its thermal history. Then it was cooled to 0°C (–50°C for highly branched samples) at constant scanning rate, kept at this temperature for 5min and then heated to 180°C at the same rate. Thermal program is shown in Figure 8.

The enthalpy change  $\Delta H$  of a specimen, expressed in terms of initial specimen mass [J/g], is calculated from the area bounded by the curve and the line connecting the onset temperature to the end temperature, that means baseline. The enthalpy change is called heat of fusion  $\Delta H_f$  and is the energy needed to melt the existing crystalline fraction. The crystalline fraction is expressed as a percentage of a value representing complete crystallization. Overall degree of crystallinity  $X_{overall}$  was calculated from the heat of fusion using the peak area determination method, i.e., by integration of the area under the normalized melting peak after subtraction of an arbitrary straight baseline; a value of  $\Delta H_m^0=293$  J/g was used as the reference melting enthalpy of fusion for 100% crystalline PE. The partial degree of crystallinity estimated from the area of VLTCP,  $X_{VLTCP}$ , was obtained from cooling traces by dividing the crystallization enthalpy of VLTCP by  $\Delta H_m^0$ .

$$X_{overall} = \frac{\Delta H_m}{\Delta H_m^0} \times 100 \quad (5)$$

### 2.3. Miscellaneous analyses

The MM averages and MMD of the samples were determined by Waters 150C size exclusion chromatography (SEC) using 1,2,4-trichlorobenzene (TCB) stabilized with 2,6-di-tert-butyl-4-methylphenol (BHT) as an eluent at 140°C. A set of two mixed bed and one  $10^7$  Å TSK-Gel columns from TosoHaas was used and the system was calibrated with polystyrene standards with narrow MMD and well-characterised PEs having a broad MMD.

Comonomer contents of the samples were determined by Fourier transform infrared spectroscopy (FTIR) (Usami and Takayama 1984). The method was calibrated with samples analysed by  $^{13}\text{C}$  NMR spectroscopy.

### 3. RESULTS AND DISCUSSION

#### 3.1. Crystallization of whole copolymers

VLTCP is still an open question and poorly studied so therefore mostly crystallization behaviour of copolymers at very low temperature is discussed. Whole copolymers with different comonomer content ( $C_{com}$ ) were studied at different scanning rates: 5, 10, 100 and 300°C/min. In all used scanning rates three crystallization peaks (HTCP, LTCP, and a small VLTCP) are observed and the character of dependences on the same molecular parameters is similar for all scanning rates. It was found that the area of VLTCP increases with decreasing scanning rate and the shape of this peak broadens. The higher the scanning rate, the better the resolution of VLTCP: the peak becomes sharper and higher. It allows to obtain the more precise values of partial degree of crystallinity,  $X_{VLTCP}$  and peak temperatures of VLTCP. Figure 9 shows the dependence of VLTCP temperature,  $T_{VLTCP}$ , on scanning rate. The VLTCP depends on scanning rate, as it is evident from the Figure 9: the higher the cooling rate the lower is the  $T_{VLTCP}$ . The temperature corresponding to the main sharp crystallization peak ( $T_{HTCP}$ ) shows the same rate-dependency, shifting to lower temperatures at higher cooling rates.

Also the partial degree of crystallinity calculated from VLTCP,  $X_{VLTCP}$ , displays slight scanning rate dependence. Crystallinity value decreases with increasing scanning rate, and appear to reach a nearly constant value when scanning rate is higher than 100°C/min. It can be suggested that at low scanning rate there is enough time for chains to be incorporated into the crystal lattice and more perfect and larger crystals are formed in comparison to those obtained at high cooling rate. Therefore, 100°C/min cooling/heating rate was chosen for all other experiments.

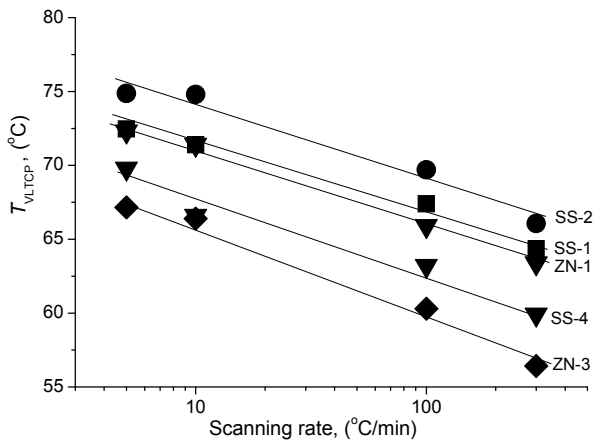


Figure 9. Dependence of temperature of the VLTCP,  $T_{VLTCP}$  on scanning rate

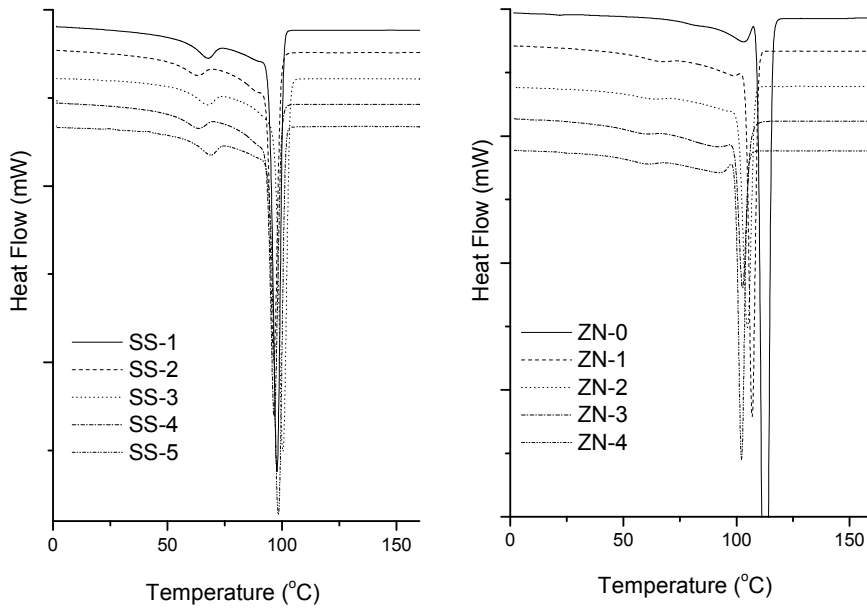


Figure 10. DSC cooling curves of whole copolymers

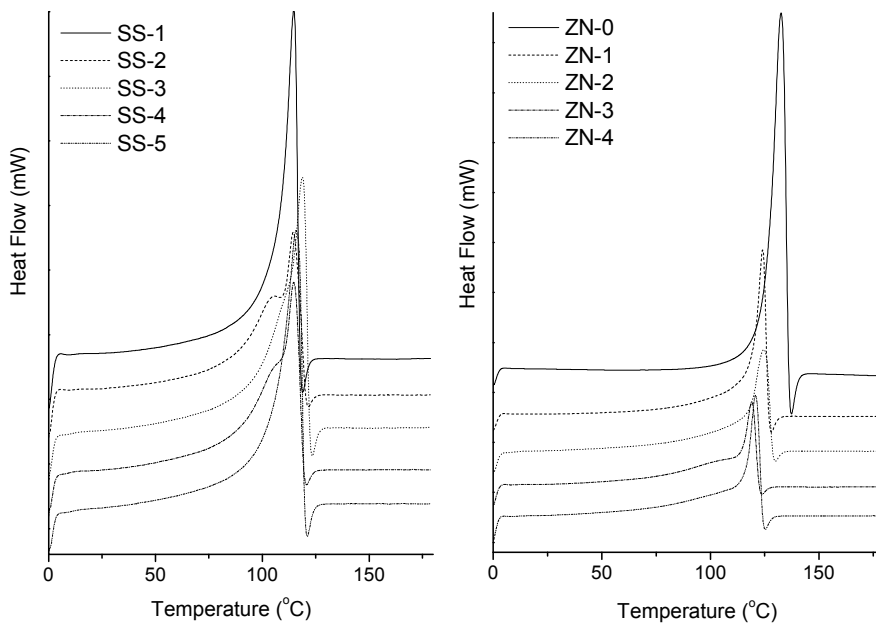


Figure 11. DSC heating curves of whole copolymers

The non-isothermal crystallization and melting thermograms for nine copolymers that were studied are shown in Figure 10 and 11 respectively. The presence of

two distinct peaks in the crystallization curves of copolymers can be seen: a sharp HTCP and a much broader and less in magnitude VLTCP at temperatures around 65-70°C. The melting of the materials has only one endothermic peak corresponding to their HTCP.

### 3.1.2. Dependence on comonomer content

The pronounced effect of  $C_{com}$  on  $T_{VLTCP}$  is observed for all studied copolymers. Figure 12 shows the dependence of the peak temperature of VLTCP,  $T_{VLTCP}$ , on the comonomer content,  $C_{com}$ , for ethylene-1-hexene copolymers. As  $C_{com}$  increases,  $T_{VLTCP}$  decreases, which is in agreement with the finding reported Mathot (1994). An interesting fact is that  $T_{VLTCP}$  vs.  $C_{com}$  for copolymers that have the same comonomer type can be represented by a single line, irrespective of the catalyst type by which the materials were produced. This differs from the behaviour of the HTCP. The temperatures of the main peak  $T_{HTCP}$  for SS materials were lower than for ZN materials as is seen from the inset in Figure 12. The ZN copolymers are known to be structurally heterogeneous. Therefore, more and longer ethylene sequences are available leading to thicker lamellae and consequently to higher crystallization and melting temperatures according to the Thompson–Gibbs equation.

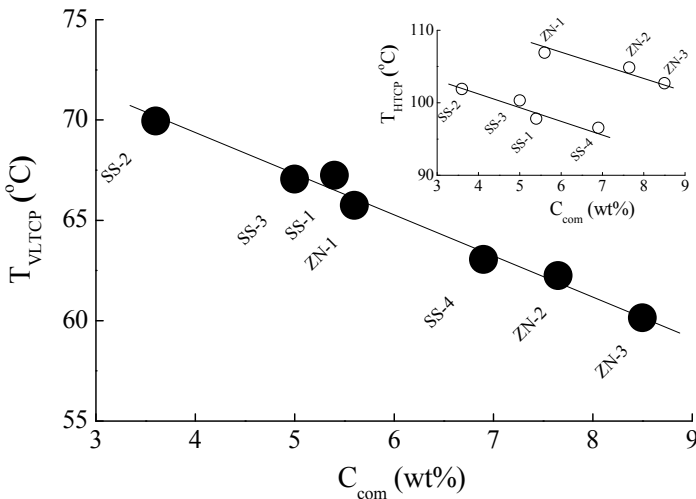


Figure 12. Dependence of peak temperature  $T_{VLTCP}$  on  $C_{com}$

For ZN catalyst it was suggested by Wilfong and Knight (1990) that the HTCP is due to the crystallization of high MM constituent having low branching content, whereas the LTCP is caused by low MM constituent with high branching content. The VLTCP was also referred to the highly branched low MM chains (Zhang et al. 2002, Mirabella 2008, Alizadeh et al. 1999). However,

the branching distribution is homogeneous in materials synthesized by SS catalysis, without the localization of branch along the main chain as in ZN copolymers, and there should be no relation between MM and branch content. However, the experimental results uniquely indicate that there is still a low temperature crystallization process, leading to a formation of VLTCP.

The dependence of  $T_{VLTCP}$  on  $C_{com}$  of whole copolymers can be seen also in Figure 12. When  $C_{com}$  increases,  $T_{VLTCP}$  decreases for all scanning rates in agreement of the finding reported in works (Mathot 1994, Wilfong 1989). A decrease in  $T_{VLTCP}$  (and consequently in crystallite size) is expected with increasing the number of branches in a given chain due to the decreased number of crystallizable units.

Taking into account similar MM of the used materials (see Table 2), the conclusion can be made that SS and ZN copolymers possess approximately the same thickness of crystallites associated with the VLTCP. Such behaviour differs from that of HTCP (See Figure 12 inset). The temperatures of the main peak ( $T_{HTCP}$ ) for SS materials are essentially lower than for ZN materials if  $C_{com}$  is fixed, due to the structural heterogeneity of ZN copolymers. Therefore, more and longer ethylene sequences are available in ZN materials leading to thicker lamellae and consequently to higher crystallization and melting temperatures according to the Thompson-Gibbs equation.

On further comparison between copolymers of different catalyst types the plots of  $X_{VLTCP}$  vs.  $T_{VLTCP}$  for all the copolymers are presented. As shown in Figure 13 in spite of identical  $T_{VLTCP}$ ,  $X_{VLTCP}$  is approximately two times higher for the SS copolymers compared to the ZN materials.

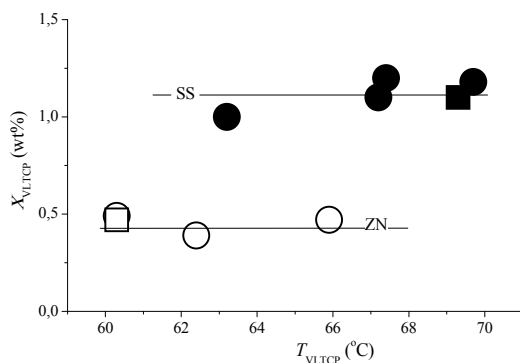


Figure 13. The degree of crystallinity  $X_{VLTCP}$  vs. peak temperature  $T_{VLTCP}$ , for all used SS and ZN based ethylene/1-butene (squares) and ethylene/1-hexene (circles) copolymers.

Figure 13 also shows that  $X_{VLTCP}$  does not depend on  $T_{VLTCP}$  and comonomer type within the same type of catalyst. The independence of crystallinity on

nature of the comonomer (except for methyl branches) is well known for the HTCP, because the degree of crystallinity mostly determined by the crystallizable sequence length distributions (Kim and Philips 1998, Alamo and Mandelkern 1989). In its turn, the sequence distributions are influenced by the type of catalyst. It is evident, that homogeneous CD facilitates formation of the VLTCP.

On further comparison between copolymers of different catalyst types, it is found that the type of catalyst ZN and SS, influence the crystallization process in the low-temperature range. These observations are verified by comparing the fractional degree of crystallinity of  $X_{VLTCP}$  vs  $C_{com}$ . Plots for all the copolymers are shown in Figure 14. It is found that  $X_{VLTCP}$  does not depend either on the comonomer type and its content or on the polydispersity of MM within the same type of catalyst. The overall degree of crystallinity is known to be independent of the nature of the comonomer (except for methyl branches), while being largely determined by the crystallizable sequence length distributions (Alamo and Mandelkern 1989, Kim and Philips 1998). In turn, the sequence distributions are influenced by the type of catalyst (e.g., ZN-based systems result in broader distributions compared to SS catalyst based copolymers). The fractional degree of crystallinity calculated from VLTCP is two times higher for the SS copolymers than for the ZN materials as seen in Figure 14. It is evident that homogeneous CD facilitates the formation of a VLTCP.

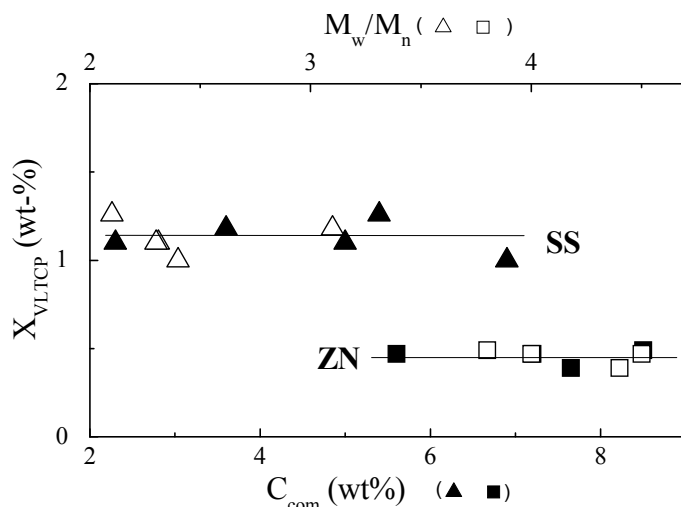


Figure 14. The degree of crystallinity  $X_{VLTCP}$  vs comonomer content  $C_{com}$  and polydispersity  $M_w/M_n$  for the SS and ZN copolymers

Important fact detected in calorimetric cooling and heating scans is that no low-temperature melting peaks corresponding to the VLTCP were found for the studied LLDPE materials. Hence, the origin and properties of the VLTCP cannot

be explained only in terms of the crystallization of ethylene sequences having a relatively short average sequence length ASL. In this case the lamellae population formed at low temperature should be thin (Mirabella 2008) and therefore should melt at a considerably low temperature. This is not observed for the studied materials, which have essentially large VLTCs at undercoolings  $\sim 80^{\circ}\text{C}$ .

### 3.2. Crystallization of fractionated copolymers

Many properties of crystalline polymers are dependent on chain length (Alamo and Mandelkern 1989, 1994, Ergoz et al. 1972, Kim and Philips 1998, Mandelkern 1971, Mandelkern et al. 1990). The phase structure that defines the crystalline state can be varied by changing the MM and/or crystallization conditions (Alamo et al. 1992, Alamo and Mandelkern 1994, Ergoz et al. 1972, Simanke et al. 2001, ).

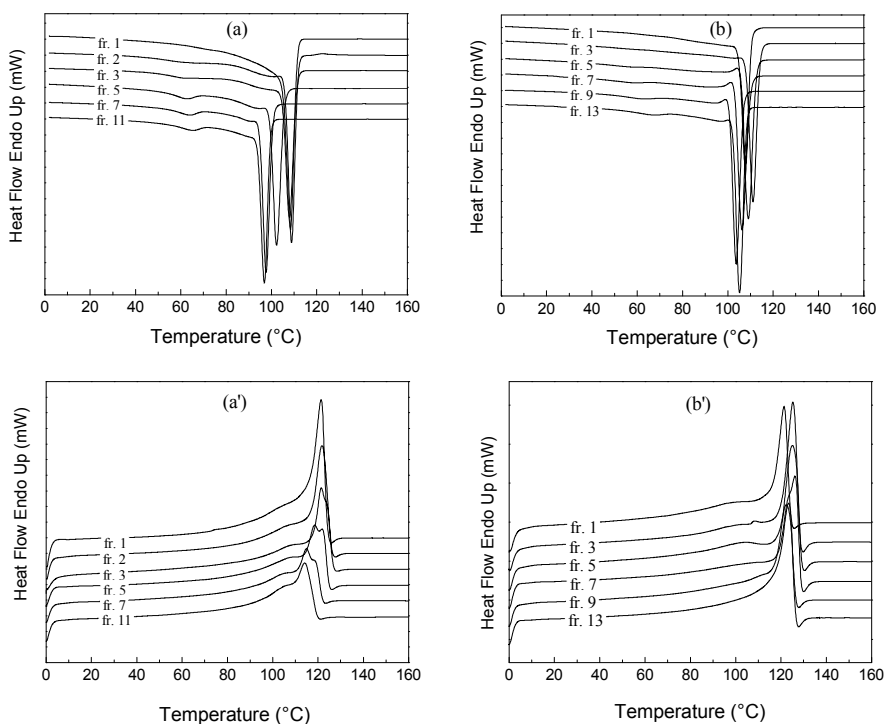


Figure 15. Selected heat flow curves for MM fractions of SS-4 (a, a') and ZN-2 (b, b'). The numbers of fractions are listed in the plots.

Since whole copolymers represent a mixture of chains with different MMD and short chain branching distribution (SCBD), the influence of MM as an independent variable has to be investigated. The best way for studying the influence of MM on copolymer structure and properties is the fractionation of copolymer. As a result several chosen copolymers were fractionated both by MM and composition. The characteristics of fractionated copolymers are listed in Table 3. The obtained fractions have narrow MMD and SCBD.

The crystallization and melting behaviour of the selected SS and ZN molar mass fractions are shown in Figure 15. It is clearly demonstrated that no VLTCP is detected for the first fractions. The next fractions have, as usual, three crystallization peaks: HTCP, LTCP and VLTCP. The crystallization behaviours of the SS and ZN fractions are rather similar. The important finding is that the identical crystallization behaviour is also detected for MM fractions of HDPE, namely ZN-0: the first fractions with lowest MM have no VLTCP but fractions with highest MM also demonstrate the presence of VLTCP.

Nevertheless, the melting curves of the LLDPE materials and HDPE as well have only one or seldom two endothermic peaks corresponding to primary crystallization process presented by HTCP and secondary LTCP. No additional very low temperature peaks, unambiguously related to the VLTCP, were detected, as it is obvious from the Figure 15a' and 15b'. Due to this fact no melting temperature and partial crystallinity directly corresponding to the VLTCP can be obtained from the melting traces. For that reason in this work only data obtained from exotherms is used.

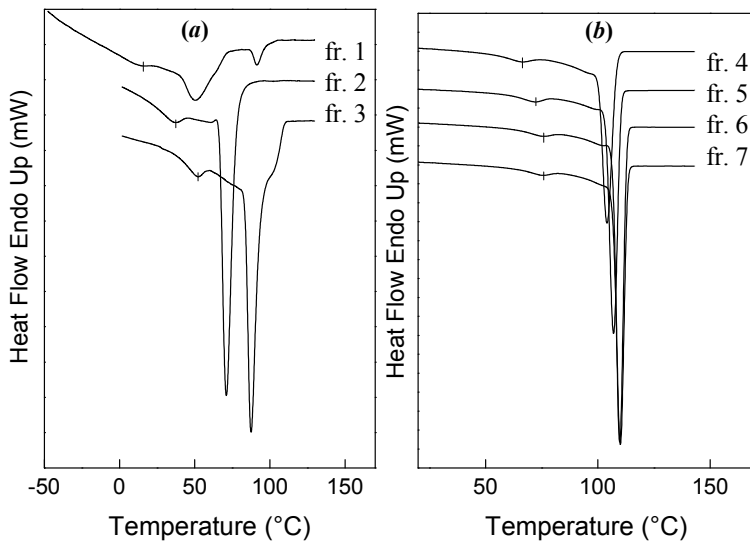


Figure 16. DSC cooling thermograms of compositional ZN-2 fractions. Numbers of fractions are listed in the figure

### 3.2.1. Dependence on comonomer content

The heat flow curves for compositional ZN-2 fractions are shown in Figure 16. It is shown that the compositional fraction has also VLTCF along with HTCF. The relationship between the crystallization peak temperatures and the comonomer content for the HTCF and VLTCF is shown in Figure 17 for ZN and SS compositional fractions. At fixed branch content the values of  $T_{VLTCF}$ , as well as  $T_{HTCF}$ , are identical for the SS and ZN fractions. Increase in  $C_{com}$  leads to decreasing of the peak temperatures. Important fact is that the temperature interval between HTCF and VLTCF remains constant. Thus, crystallization of the macromolecules associated with the VLTCF is influenced by the prior crystallization of macromolecules represented by the HTCF. Such comonomer content dependence for fractions is rather similar to that of whole copolymers.

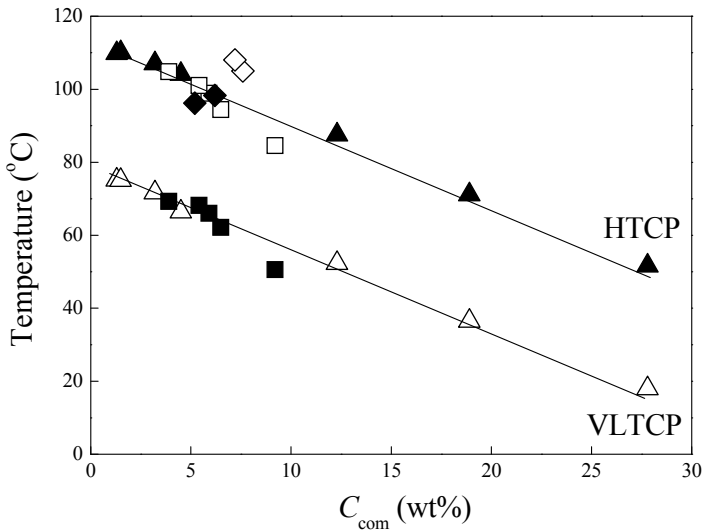


Figure 17. Crystallization peak temperatures as a function of comonomer content  $C_{com}$  for the compositional SS-4 (solid and open squares) and ZN-2 (solid and open triangles) fractions

Moreover, the Figure 17 shows that the less branched copolymers display the higher values of  $T_{VLTCF}$  and extrapolation of  $T_{VLTCF}$  to  $C_{com}=0$  gives the value of  $T_{VLTCF} \cong 80$  °C, which is found to be  $T_{VLTCF}$  for ZN-0 (HDPE).

In spite of  $T_{VLTCF}$ , which is presumably related to the crystallite thickness of the very-low temperature crystallized structures, decreases with increasing  $C_{com}$ , the  $X_{VLTCF}$  does not show any systematical change with  $C_{com}$ . In Figure 18 the  $X_{VLTCF}$  is plotted as a function of  $C_{com}$  for compositional fractions of SS-4 and ZN-2 copolymers. MM of these samples is similar, around 100kg/mol. It is evident that the introduction of the non-crystallizing co-units into the chain does

not influence strongly the level of  $X_{VLTCP}$  within the same type of catalyst. This fact is understandable when you consider that the degree of crystallinity that is attained in an actual crystallization process, is not a measure of the minimum or maximum sequence that participates in the crystallization, which is directly related to  $C_{com}$ . Rather it is the sum over all possibilities, which can lead to independence of crystallinity on  $C_{com}$  up to a definite value.

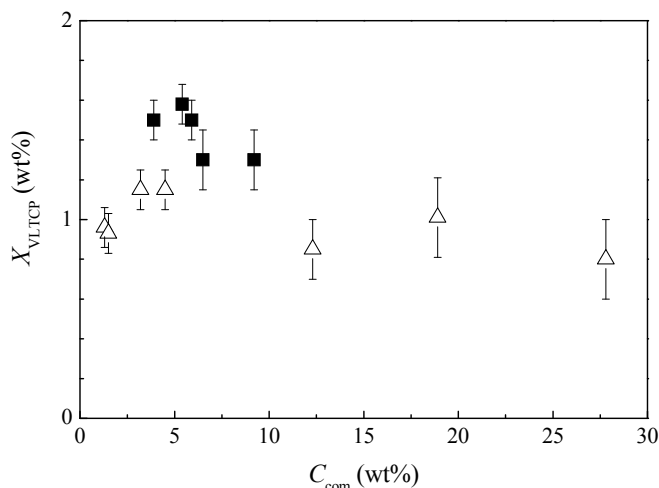


Figure 18. Plots of VLTCP partial crystallinity  $X_{VLTCP}$  vs.  $C_{com}$  for SS-4 (solid squares) and ZN-2 (open triangles) fractions obtained by fractionation according to structure

Wilfong (1989) suggested that the co-units in the macromolecule may have been distributed in a blocky manner during the copolymerization of ethylene and  $\alpha$ -olefin. Hence, the HTCP and the VLTCP may arise from the crystallization of ethylene rich and hexene/butene rich portions of the macromolecule, respectively. That is, the HTCP can be associated with crystallization of the linear portions of the macromolecule into the chain folded lamellae. The branched segments of macromolecule are exiled into the inter-lamellar or interfacial regions and crystallized there upon further undercooling into thin lamellae. However, the blocky intramolecular distribution of co-monomers in chain is recognized for ZN (Hosoda 1988), but not for SS samples. Additionally, VLTCP has also been detected by us for HDPE having extremely low number of branches. Moreover, thin lamellar crystallites should melt at considerable low temperature and could be detected in melting traces by DSC. But no melting peaks related to VLTCP were found in all the studied materials.

### 3.2.2. Dependence on molar mass

#### 3.2.2.1. Crystallinity

Since the effect of  $C_{com}$  has been studied, the effect of MM as an independent variable can be investigated. Figure 19 represents the dependences of the degrees of overall ( $X_{overall}$ ) and partial VLTCF ( $X_{VLTCF}$ ) crystallinities of MM fractions for all the samples on weight average MM ( $M_w$ ). The decrease in  $X_{overall}$  of the fractions with MM is well-known (Alamo et al. 1984, Ergoz et al. 1972, Rastogi et al. 2005). Increasing MM increases the density of chain entanglements in the melt (Alamo et al. 1992, Alamo and Mandelkern 1994, Fan et al. 2003, Lippits et al. 2007, Psarski et al. 2000, Rastogi et al. 2005, Simanke et al. 2001, ). It gives the opportunity to suggest that increasing chain entanglements reduces the ability of chains to participate in the primary crystallization process at high temperature and as a result restrict the formation of large dominant crystallites.

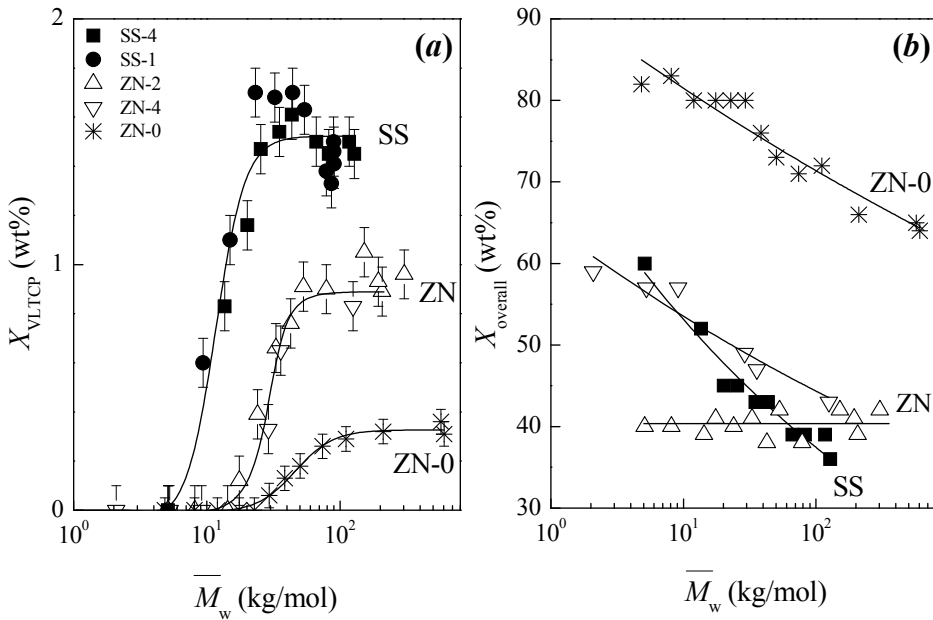


Figure 19. Dependence of  $X_{VLTCF}$  (a) and  $X_{overall}$  (b) on  $M_w$  of both SS and ZN molar mass fractions.

This means that the proportion of non-crystallized chains in the amorphous regions, which further can participate in the secondary crystallization at lower temperature, increases. As it is evident from the Figure 19, in the range of  $M_w$  from 5 up to 60–100 kg/mol  $X_{VLTCF}$  sharply increases. At  $M_w > 60$ –100 kg/mol, named as critical MM, the degree of crystallinity  $X_{VLTCF}$  does not increase

anymore. Within the same catalyst type (ZN) there is an essential difference in  $X_{\text{VLTCP}}$  values for different material types—LLDPE or HDPE. It is well known that in case of HDPE in comparison with LLDPE the major part of chains take part in primary crystallization process that gives the value of overall crystallinity for HDPE more than 70% against 30–60% for LLDPE. Therefore it can be concluded that the value of critical MM and maximum level of  $X_{\text{VLTCP}}$  are sensitive to polymer (LLDPE or HDPE) and catalyst (ZN or SS) types. The most probable that the VLTCP crystallinity depends on whether the fraction of crystallizable sections of polymer macromolecules is incorporated into the primary crystallization process associated with HTCP. Less incorporation in primary crystallization will cause crystallites, associated with the VLTCP, to grow in size or/and amount and reach some kind of equilibrium with dominant crystallites at critical  $M_w \approx 60\text{--}100\text{kg/mol}$ . An identical behaviour as presented in Figure 19 is observed for the dependence of  $X_{\text{VLTCP}}$  on  $T_{\text{VLTCP}}$ .

### 3.2.2.2. Crystallization peak temperature

For the lowest MM fractions as seen from the inset to the Figure 20, crystallization temperature of the HTCP,  $T_{\text{HTCP}}$ , slightly increases with MM due to the decrease in number of end-groups per 1000 C atoms (Mathot 1994). The VLTCP is not detected for such fractions. Further, after an initial expected increase the  $T_{\text{HTCP}}$  decreases at  $M_w \approx 10\text{--}20\text{kg/mol}$  to become more or less constant at  $M_w \approx 60\text{--}100\text{kg/mol}$ . The reduction of the  $T_{\text{HTCP}}$  with increasing MM is a consequence of the decreased crystallite thickness of dominant lamellae (Alamo et al. 1984, Alamo et al. 1992, Basiura et al. 2006, Fan et al. 2003, Lippits et al. 2007, Mathot 1994, Psarski et al. 2000, Rastogi et al. 2005). An explanation for the formation of smaller crystals with increasing MM is due to the increase in entanglements: as the number of intermolecular entanglements increases with the increase in MM, the mobility of segments is increasingly hindered. In this case, a higher undercooling is required to produce a larger driving force for crystallization to overcome the influence of entanglements, and then the crystallization temperature shifts to lower temperature (Fan et al. 2003).

VLTCP behaves in opposite manner than HTCP: while the  $T_{\text{HTCP}}$  decreases, the  $T_{\text{VLTCP}}$  grows with the increasing MM (see Figure 20). According to Smith and Manley (1979), for quenched PE fractions with  $M_w = 4\text{kg/mol}$ , that is MM above which the entanglements are operative, the chains are extended. In the domain  $4 < M_w < 100\text{kg/mol}$  the amorphous phase increases with the MM. For monodisperse and polydisperse samples of MM greater than  $100\text{kg/mol}$ , the long period and the crystalline lamellar thickness do not change any more (Robelin-Souffache and Rault 1989, Rousseaux and Lemonnier 1980). These results are in accordance with this finding. Indeed,  $T_{\text{VLTCP}}$  steeply increases in the range of MM  $10\text{--}100\text{kg/mol}$ , and tends to level off at  $M_w = 60\text{--}100\text{kg/mol}$ . Within the

same catalyst and polymer types the value of critical MM depends on PD: the larger the PD, the higher the value of critical MM. When  $MM < 60\text{--}100\text{kg/mol}$  the slope of the dependence  $T_{VLTCP}$  on  $M_w$  is defined by  $C_{com}$ . It is obvious for ZN-2 sample, in which the less branched fractions have higher MM (see Table 3), that  $T_{VLTCP}$  decreases with  $M_w$  steeper than that of SS-1 fractions, having the same  $C_{com}$ .

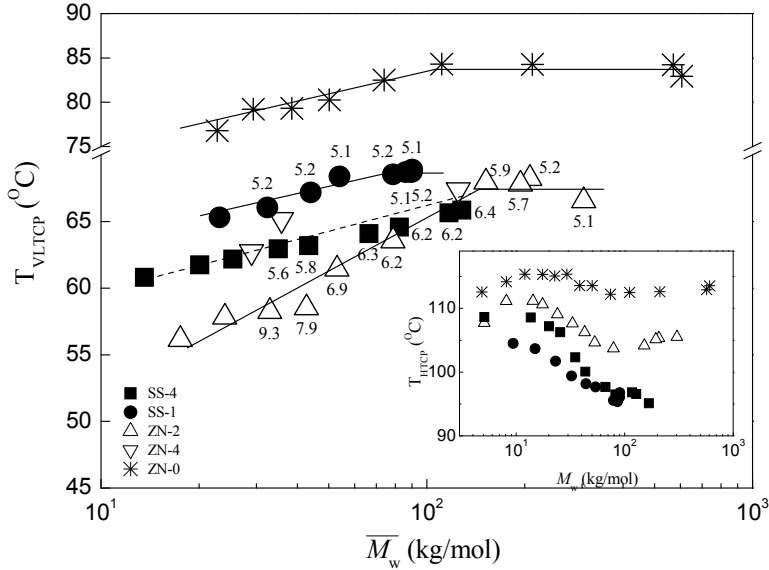


Figure 20. Plot of  $T_{VLTCP}$  against  $M_w$  for MM fractions of SS and ZN copolymers (the data labels represent the values of  $C_{com}$ ); inset shows the dependence of  $T_{HTCP}$  vs.  $M_w$  for the same fractions

For copolymers produced using ZN catalyst the most popular explanation for VLTCP is that the molecular fractionation or segregation of macromolecules by MM during crystallization implies that the HTCP is due to the crystallization of high MM macromolecules having low branching content, whereas VLTCP can be comprised of the less crystallizable, lower MM, more highly branched polymer chains (Alamo and Mandelkern 1994, Alizadeth et al. 1999, Canetti and Bertini 2010, Crist and Claudio 1999, Mandelkern 1971, Marand et al. 2000, Mirabella 2008, Rabiej et al. 2004, Simanke et al. 2001, Tashiro et al. 1995, Zhang et al. 2002). However, based on the results it can be said that if there was the possibility, for ZN fractions the polymer molecules associated with the VLTCP would be mostly present in the first fractions. Hence, fractions with higher MM would be expected to exhibit only the HTCP. However, as it is seen from the Figure 15b the first MM fractions of ZN copolymer having low MM and high  $C_{com}$  do not show any VLTCP at all. The fractions with higher MM display both the HTCP and the VLTCP. This suggests that the polymer chains associated with the HTCP are also related to the VLTCP, which is in agreement

with the results on crystallization temperatures. Moreover, it can be seen from Figure 16 that even the first highly branched compositional fractions, which presumably should have only VLTCP, demonstrate the HTCP along with VLTCP in DSC thermograms.

To understand the effect of MM and  $C_{com}$  on the behaviour of VLTCP two different LLDPEs were blended together: 80% of ZN-2-M1 having no VLTCP and 20% of SS-6 having only VLTCP. Melting and crystallization thermograms for both pure components are shown in Figure 21.

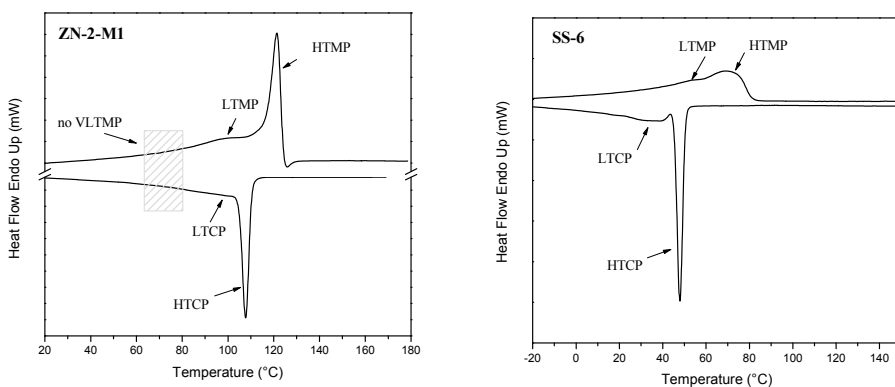


Figure 21. Melting and crystallization thermograms for pure components

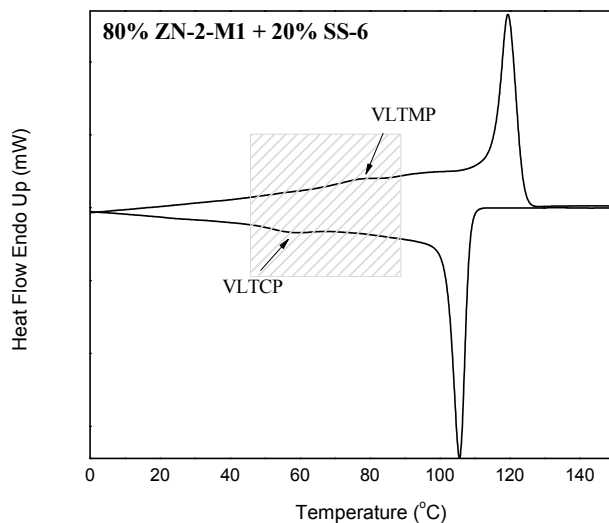


Figure 22. Melting and crystallization thermogram of blend

Blend of those components shows both VLTCP and very low temperature melting peak (VLTMP) as it is seen in Figure 22. Based on that can be said if VLTCP was caused by highly branched molecules why VLTMP cannot be seen in any of whole copolymers and their fractions thermograms. Most probably the key role on formation of VLTCP is entanglements of high MM chains.

Because there is a clear correlation of both peaks with molar mass (see Figure 20), it is implicit that these exotherms (especially the VLTCP) are also a consequence of melt topology; in other words, entanglements. Then, the key to the presence of VLTCP exotherm will not be the sequence distribution caused by the comonomer, but a melt topology that restricts further crystallization after a primary nucleation and further (usually spherulitic) growth in most semicrystalline polymers. The increase in  $X_{\text{VLTCP}}$  with MM leads to a suggestion that inter-crystalline links are responsible for the formation of the VLTCP. During crystallization numerous tie molecules are formed especially at rather large supercooling. These tie molecules can aggregate locally to form intercrystalline links (named as bundles). However, the formation of inter-crystalline links also has its optimum MM limit equal to 60–100kg/mol, above which the crystallinity level of so-named bundles does not strongly change or even slightly decreases.

### 3.3. Crystallization of blends

After analysing the VLTCP blends were also analysed in the point of view how they will co-crystallize. Based on the result found in literature (Puig 2001, Shanks and Armasinghe 2000, Tanem and Stori 2000, 2001a and 2001b, Zhao et al. 1997) it is expected that blends studied in this work will show two separate crystal populations. DSC melting endotherms of the blends ZN-0-M1/SS-6 with various ratios of components are shown in Figure 23. The heating and cooling rates were 10°C/min. The DSC result clearly indicates the existence of two crystal populations in these blends. Two melting peaks are found in all studied blends. The mixtures with a high concentration of the high-density polymer (>50%) show a sharp high temperature melting peak (HTMP) with a small peak in the low-temperature region. This low temperature melting peak (LTMP) further develops into a well-defined peak for the mixtures with high concentration of the hyper-branched component. The form and position of the low-temperature peak indicates that this peak represents melting of mainly the component rich in SS-6. The HTMP seems to represent the ZN-0-M1-rich component. It should be noticed that HTMP has a small shoulder, sub-peak, generated at slightly lower temperature. Similar behaviour is detected for all the blends of ZN-2 with SS-6, as is obvious from the Figure 24 where their crystallization and melting thermograms are shown.

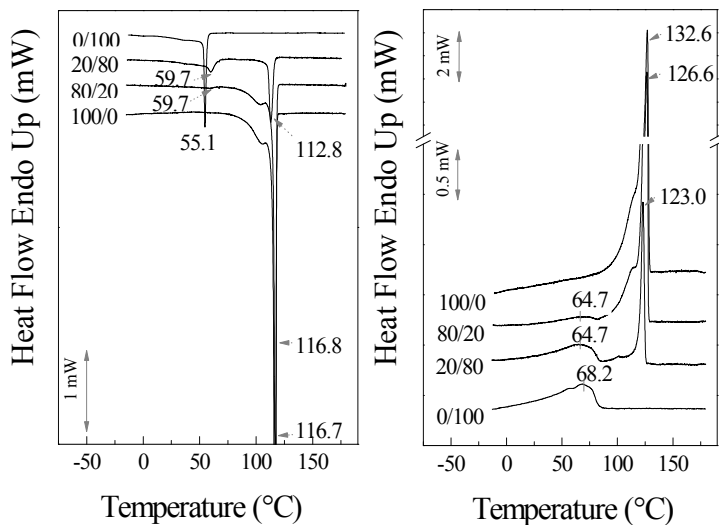


Figure 23. DSC cooling and melting traces of the ZN-0-M1/SS-6 blends with various component ratios. Cooling and heating rate 10 °C/min.

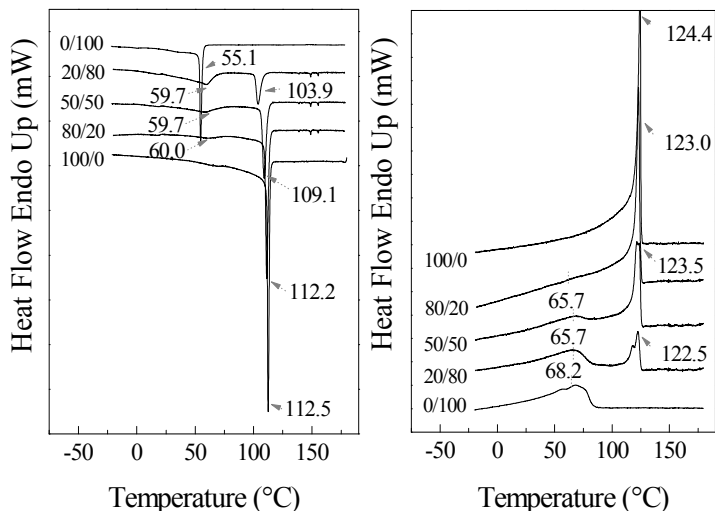


Figure 24. DSC cooling and melting traces of the ZN-2/SS-6 blends with various component ratios. Cooling and heating rate 10 °C/min.

The origin of sub-peak observed at high temperatures can be understood from the thermograms of pure components, also presented in Figures 23 and 24. Pure ZN-0-M1 component has mainly one melting peak but the shoulder extent to lower temperatures is present, indicating some degree of heterogeneity in sequence lengths. The same is found for pure ZN-2. If the compositional and MM heterogeneity of conventional whole ZN-2 is expected, the heterogeneity of ZN-0-M1 seems to be unusual. Taken into account that ZN-0-M1 used in this

study is the first fraction of the whole ZN-0 obtained by fractionation according to MM and it is catalyzed by ZN technique, this first fraction contains branched chains with low MM. The degree of branching in the first fractions is therefore higher than present in whole polymer. Therefore ZN-0-M1 can contain chains that can be excluded from the largest lamellae during primary crystallization and generate a secondary crystal sub-population. This can result in an appearance of sub-peak in melting traces. SS-6 has also rather wide SCBD and contains chains having much lower branching content than averaged value (17.8 wt-%, see Table 2) Presence of chains forming the secondary crystals gives the possibility of mixing them with that part of SS-6 chains which have very low branch content. As seen from the Figures 23 and 24, the increase in the amount of SS-6 component in the blends results in a better separation of HTMP and sub-HTMP. The position and broadness of these peaks indicates partial chain segregation of ZN-0-M1-rich peak and possibility of a formation of mix crystals.

In order to understand the origin of LTMP and HTMP in blends the cooling rate during the cooling scans was varied. The heating rate was constant, 10°C/min. The thermograms of the blends at 1 and 200°C/min cooling rates show identical behaviour as it was observed for cooling rate of 10°C/min. It is clearly seen from the Figure 25 where melting traces of 20/80 ZN-0-M1/SS-6 and 50/50 ZN-2/SS-6 blends at different cooling rates are shown as illustrations. Two main melting peaks, HTMP and LTMP, with additional sub-peak sub-HTMP at high temperature were recorded.

From the heat of fusion, the degree of crystallinity  $X$  by weight was obtained for low and high temperature peak. These values are given in Table 4 for the 20/80 ZN-0-M1/SS-6 blend as example. First of all the degree of crystallinity of each peak does not depend on scanning rate indicating that the observed peaks are not associated with the recrystallization or reorganization process but consistent with the formation of separate crystals from both components. The other blends of ZN-0-M1/SS-6 and ZN-2/SS-6 were found to possess a similar behaviour and the same conclusion can be done for them. Rapidly crystallized samples show usually one peak but slowly crystallized show two peaks. Thus, in comparison with HDPE/LLDPE and LDPE/LLDPE discussed in literature (Agamalian 1999, Hill et al. 1992, Kyu et al. 1987, Martinez-Salazar et al. 1991, Morgan et al. 1999, Puig 2001, Tanem and Stori 2000, 2001b, Tashiro et al. 1992, 1994a, 1994b, 1995, Wignall 1995, 2000), in blends studied in this work two crystal populations are forming even in rapidly crystallized mixtures at 200°C/min similar to slowly cooled samples at 1°C/min.

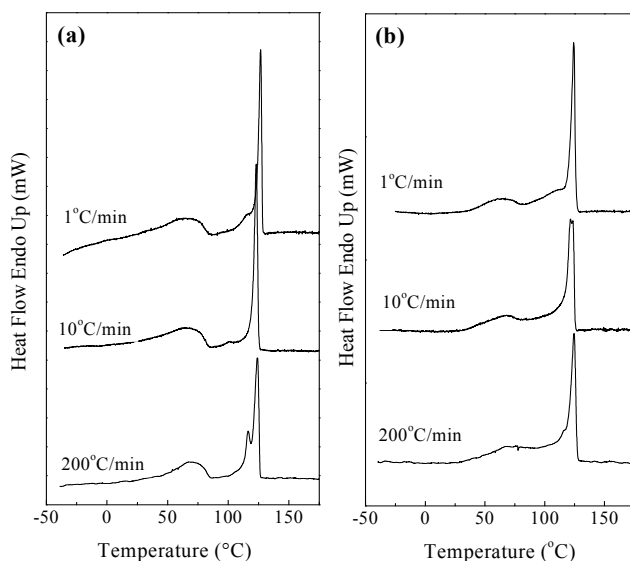


Figure 25. DSC melting thermograms for (a) 20/80 ZN-0-M1/SS-6 and (b) 50/50 ZN-2/SS-6 blends crystallized at various cooling rates.

To find out whether the observed melting peaks correspond to completely separated crystallites, formed independently, the degree of crystallinity of low and high temperature peaks was compared with the expected value in the blends if both components had crystallized independently. Table 4 shows that the crystallinity of the SS-6-rich low-temperature peaks is lower than that calculated assuming independent crystallites. Overall degree of crystallinity of both peaks is also lower than that calculated by mentioned above method. Lower crystallinity of the blends compared to the pure blend components has been taken elsewhere as an argument in favor of co-crystallization (Morgan et al. 1999, Puig 2001, Tanem and Stori 2000, 2001a, 2001b, Tashiro et al. 1992, 1994a, 1994b, 1995, Wignall 2000, Zhao et al. 1997). The observed melting behaviour of the blends therefore suggests that slight co-crystallization to some limited extent is present in the blends.

Table 4. The degree of crystallinities  $X$  for 20/80 ZN-0-M1/SS-6 blends obtained from melting thermograms at various cooling rates.

| Cooling rate<br>°C/min | $X_{\text{overall}}$<br>(wt%) |       | $X_{\text{LTMP}}$<br>(wt%) |       | $X_{\text{HTMP}}$<br>(wt%) |       |
|------------------------|-------------------------------|-------|----------------------------|-------|----------------------------|-------|
|                        | extpl.*                       | calc. | extpl.                     | calc. | extpl.                     | calc. |
| 1                      | 27                            | 37    | 11                         | 18    | 16                         | 19    |
| 10                     | 26                            | 31    | 11                         | 12    | 15                         | 19    |
| 200                    | 25                            | 35    | 10                         | 16    | 15                         | 19    |

\* *extpl.* means measured from DSC melting endotherms  
*calc.* means calculated assuming independently crystallized crystals

Furthermore, the low-temperature peaks in all the blends have almost the same melting points. However this melting point is around 4°C lower than observed for the pure SS-6 component as also obvious from the Figures 23 and 24. This result might indicate that even in SS-6 there are chain segments that are able to co-crystallize with branched chains of ZN-0-M1 or ZN-2 (Shanks and Armasinghe 2000). Most probably that these chain segments of SS-6 have the lowest branching content compared to overall SS-6 branch content. In that case remaining SS-6 chains, not incorporated in ZN-0-M1- (ZN-2-) rich crystals, can be suggested to have a higher overall content of branches than the pure ZN-0-M1 (ZN-2) and should melt consequently at a lower temperature; and this is in fact observed from Figures 23 and 24.

The melting point of the high-temperature peak in the ZN-0-M1/SS-6 and ZN-2/SS-6 is significantly lower (~10°C and 2°C maximum, respectively) compared to that of the pure ZN-0-M1 and ZN-2 component. Other authors have observed a similar depression of the melting temperature of the high-temperature peak in a blend of LPE/LDPE (Puig et al 1993, Puig 2001) and LPE/LLDPE (Tanem and Stori 2001a and 2001b) and suggest that such behaviour can be explained by both the co-crystallization of the branched component into the LPE crystal and a lower lamellae thickness of the LPE component in the blend. Based on this conclusion, the depression of the high-temperature peak in the blends most probably has a complex reason but could be explained, at least partly, from a limited degree of co-crystallization among the blend components.

Therefore, a limited degree of co-crystallization is believed to be present in blends used in this work, at least in the blends rich in SS-6 ( $\geq 50\%$ ).

One more interesting behaviour can be seen from the crystallization traces of the blends. From Figure 23 it is observed that the crystallization temperature of the SS-6-rich component in separated blends locates at a higher temperature than the crystallization point of the corresponding pure SS-6 component. This observation seems to be in a conflict with the observation of melting point behaviour. This effect can be explained based on comments and observations made by others (Tanem and Stori 2001b). Crystallization curves for both pure blend components show sharp leading edges, characteristic of primary crystallization. Additionally, both components have an extended tail to lower temperatures, reflecting a secondary crystallization process into thinner lamellae. In the blends it is obvious from Figures 23 and 24 that the ZN-0-M1- as well as ZN-2-rich component crystallizes first. The crystallization curves show rather sharp and narrower peak at high temperature. The low-temperature peak, however, reflecting a secondary crystallization process of mainly SS-6-rich component, shows rather broad leading edge very different from the sharp peak observed for pure SS-6. Therefore it can be suggested that the primary

crystallization in blend is associated with the crystallization of ZN-0M1-rich or ZN-2-rich component in ZN-0-M1/SS-6 and ZN-2/SS-6 blends, respectively. SS-6-rich component crystallizes in a secondary crystallization processes within the structure determined by crystallization of ZN-0-M1- or ZN-2-rich component (Ueda and Register 1996). Therefore as others have suggested the crystallization of ZN-0-M1 or ZN-2 will generate the crystallization of SS-6 at higher temperature than the pure SS-6 would otherwise crystallize. The lamellae thickness of the resulting SS-6-rich component in the blends and the subsequent melting behaviour indicate that this enhanced crystallization at higher temperature occurs without forming thicker lamellae, as normally would be expected due to higher crystallization temperature.

## CONCLUSIONS

Low temperature crystallization behaviour of single site (SS) and Ziegler-Natta (ZN) catalyst based ethylene- $\alpha$ -olefin whole copolymers and their fractions was analyzed. DSC curves of whole copolymers, molar mass (MM) and compositional fractions of SS and ZN materials uniquely show the presence of an additional crystallization process occurring at temperatures around 60–75°C. The very low temperature crystallization peak (VLTCP) was not detected in the fractions having lowest MM. The VLTCP is much broader and less in magnitude than the main sharp high temperature crystallization peak (HTCP). Moreover, the melting curves do not show any additional peaks clearly related to the VLTCP. Results of this work give a better understanding of the matter compared to the mixed opinions in literature.

Based on DSC measurements following conclusions can be made:

- The comonomer content ( $C_{\text{com}}$ ) does not strongly influence the partial degree of crystallinity of VLTCP ( $X_{\text{VLTCP}}$ ) while the pronounced decrease in peak temperatures of VLTCP ( $T_{\text{VLTCP}}$ ) with  $C_{\text{com}}$  is observed. However, the  $X_{\text{VLTCP}}$  and  $T_{\text{VLTCP}}$  are independent of the chemical nature of the co-monomers (1-butene or 1-hexene).
- The  $X_{\text{VLTCP}}$  is influenced by the type of catalyst. For the SS materials the  $X_{\text{VLTCP}}$  is approximately 2 times higher than for the ZN samples. For ZN high density polyethylene (HDPE) the obtained values of  $X_{\text{VLTCP}}$  are much lower than those of ZN linear low density polyethylene (LLDPE). At the same time,  $T_{\text{VLTCP}}$  did not depend on the catalyst type used.
- In the range of  $5 < M_w < 100$  kg/mol the partial degree of crystallinity  $X_{\text{VLTCP}}$  calculated from the VLTCP and the crystallization peak temperature  $T_{\text{VLTCP}}$  increase with increasing  $M_w$ .

At the same time the crystallinity of HTCP decreases with  $M_w$  that involves a molecular correlation between the primary and secondary crystallization processes. When  $M_w$  is higher than 100 kg/mol, the  $X_{\text{VLTCP}}$  and  $T_{\text{VLTCP}}$  level off. Such behaviour can be a result of increasing amorphous layer with  $M_w$  due to the increase in number of entanglements. It implies the less incorporation of the fraction of crystallizable sections of polymer macromolecules into the primary crystallization process associated with HTCP. The chains or/and segments of chains, remaining in the melt after primary crystallization, can aggregate locally forming the bundle-like inter-crystalline links.

Blends of LLDPE with high  $C_{\text{com}}$  with HDPE and LLDPE had in addition to a VLTCP also a corresponding melting peak. Based on these results, it can be said:

– VLTCP in copolymers is not caused by highly branched component of the materials but due to the entanglements of high  $M_w$  chains which melt at higher temperatures.

From thermal analysis of rapidly and slowly cooled blends can be concluded that both components form two crystal populations. The limited degree of co-crystallization is present in all studied blends having the content of LLDPE with high  $C_{\text{com}}$  component of 80%.

## REFERENCES

- Agamalian, M.; Alamo, R.; Kim, M.; Londono, J.; Mandelkern, L.; Wignall, G.** 1999. Phase Behavior of Blends of Linear and Branched Polyethylenes on Micron Length Scales via Ultra-Small-Angle Neutron Scattering. – *Macromolecules*. 32, 3093-3096.
- Alamo, R., Domszy, R., Mandelkern, L.** 1984. Thermodynamic and structural properties of copolymers of ethylene – *J. Phys.Chem.* 88, 6587-6595.
- Alamo, R.G., Chan, E.K.M., Mandelkern, L., Voigt-Martin, I.G.** 1992. Influence of molecular weight on the melting and phase structure of random copolymers of ethylene – *Macromolecules* 25, 6381-6394.
- Alamo, R.G., Mandelkern, L.** 1994. The crystallization behavior of random copolymers of ethylene – *Thermochim Acta*, 238, 155-201.
- Alamo R.G., Viers B.D., Mandelkern L.** 1993. Phase structure of random ethylene copolymers: a study of counit content and molecular weight as independent variables – *Macromolecules* 26, 5740-5747.
- Alamo, R. G., Mandelkern, L.** 1989. Thermodynamic and structural propeties of ethylene copolymers. – *Macromolecules*. 22, 1273–1277.
- Alizadeh A., Richrdson L., Xu J., McCartney S., Marand H.** 1999. Influence of Structural and Topological Constraints on the Crystallization and Melting Behavior of Polymers. 1. Ethylene/1-Octene Copolymers – *Macromolecules* 32, 6221-6235.
- Basiura, M., Gearba, R.I., Ivanov, D.A., Janicki, J., Reynaers, H., Groeninckx, G., Bras, W., Goderis, B.** 2006. Rapidly cooled polyethylenes: on the thermal stability of the semicrystalline morphology. – *Macromolecules*. 39, 8399–8411.
- Bell, J. P., Murayama, T.** 1969. Relations between dynamic mechanical properties and melting behavior of nylon 66 and poly(ethylene terephthalate) – *J. Polym. Sci. Part A-2*, 7, 1059-1073.
- Brüll, R., Pasch, H., Raubenhaimer, H. G., Sanderson, R., van Reenen, A. J., Wahner, U. M.** 2001. Investigation of the melting and crystallization behavior of random propene/a-olefin copolymers by DSC and CRYSTAF. – *Macromol. Chem. Phys.*, 202, 1281-1288.
- Canetti, M., Bertini, F.** 2010. Crystalline and supermolecular structure evolution of poly(ethylene terephthalate) during isothermal crystallization and annealing treatment by means of wide and small angle X-ray investigation. – *European Polym. J.* 46, 270–276.
- Chau, J., The, J.** 2005. Successive self-nucleation and annealing in the solvated state of ethylene copolymers. – *Journal of Thermal Analysis and Calorimetry*, 81, 217-223.
- Crist, B., Claudio, E.S.** 1999. Isothermal crystallization of random ethylene-butene copolymers: bimodal kinetics. – *Macromolecules* 32, 8945–8951.

- Ehrenstein, G. W., Riedel, G., Trawiel, P.** 2004. Thermal Analysis of Plastics: Theory and Practice. Munich, Carl Hanser Verlag.
- Ergoz, E., Fatou, J.G., Mandelkern, L.** 1972. Molecular weight dependence of the crystallization kinetics of linear polyethylene. I. Experimental results. – *Macromolecules* 5,147–157.
- Fakirov, S., Fischer, E. W., Hoffmann, R., Schmidt, G. F.** 1977. Structure and properties of poly(ethylene terephthalate) crystallized by annealing in the highly oriented state: 2. Melting behaviour and the mosaic block structure of the crystalline layers – *Polymer*, 18, 1121-1129.
- Faldi, A., Soares, J. B. P.** 2001. Characterization of the combined molecular weight and composition distribution of industrial ethylene/α-olefin copolymers. – *Polymer*, 42, 3057-3066.
- Fan, Z., Wang, Y., Bu, H.** 2003. Influence of intermolecular entanglements on crystallization behavior of ultra-high molar mass polyethylene. – *Polym. Eng. Sci.* 43, 607–614.
- Fischer, E. W., Fakirov, S.** 1976. Structure and properties of poly(ethylene terephthalate) crystallized by annealing in the highly oriented state. Part 1. Morphological structure as revealed by SAXS. – *J. Mat. Sci.*, 11, 1041-1065.
- Flory P. J.** 1949. Thermodynamics of Crystallization in High Polymers. IV. A Theory of Crystalline States and Fusion in Polymers, Copolymers, and Their Mixtures with Diluents. – *The Journal of Chemical Physics*, 17 (3), 223-240.
- Flory P. J.** 1953. Principles of Polymer Chemistry. Ithaca, N.Y., Cornell University Press
- Flory P. J.** 1955. Theory of crystallisation in copolymers. – *Trans. Faraday Soc.*, 51, 848-857.
- Flory P. J.** 1962. On the Morphology of the Crystalline State in Polymers. – *J. Am. Chem. Soc.*, 84, 2857-2867.
- Galante, M.; Alamo, R.; Mandelkern, L.** 1998. The crystallization of blends of different types of polyethylene: The role of crystallization conditions. – *Polymer* 39(21), 5105-5119.
- Gedde, U.** 1992. Crystallization and morphology of binary blends of linear and branched polyethylene. – *Progress in Colloid Polymer Science* 87, 8-15.
- Gedde U. W.** 1995. Polymer Physics. First edition. London: Chapman & Hall.
- Groeninckx, G., Reynaers, H. Berghmans, H., and Smets, G.** 1980. Morphology and melting behavior of semicrystalline poly(ethylene terephthalate). I. Isothermally crystallized PET – *J. Polym. Sci. Polym. Phys. Ed.*, 18, 1311-1324.
- Hill, M.; Barham, P.; Keller, A.** 1992. Phase segregation in blends of linear with branched polyethylene: the effect of varying the molecular weight of the linear polymer – *Polymer* 33(12), 2530-2541.
- Hoffman, J. D., Weeks, J. J.,** 1965. X-Ray Study of Isothermal Thickening of

Lamellae in Bulk Polyethylene at the Crystallization Temperature – J. Chem. Phys., 42, 4301.

**Holtrup W.** 1977. Zur fraktionierung von polymeren durch direktextraktion. – Makromol. Chem., 178, 2335–2349.

**Hosoda, S.** 1988. Structural distribution of linear low-density polyethylenes. – Polym. J. 20, 383–386.

**Hsieh, E. T., Tso, C. C., Byers, J. D., Johnson, T. W., Fu, Q. and Cheng, S. Z. D.** 1997. Intermolecular structural homogeneity of metallocene polyethylene copolymers – J. Macromol. Sci. - Phys., B36, 615-628.

**Hussein, I. A.** 2008. Nonisothermal crystallization kinetics of linear metallocene polyethylenes. – Journal of Applied Polymer Science, 107, 2802-2808.

**Islam, M. A., Hussein, I. A., Atiqullah, M.** 2007. Effects of branching characteristics and copolymer composition distribution on non-isothermal crystallization kinetics of metallocene LLDPEs. – European Polymer Journal, 43, 599-610.

**Keller A.** 1959. The morphology of crystalline polymers – Makromol. Chem., 34, 1-28.

**Kim, M., Philips, P. J.** 1998. Nonisothermal melting and crystallization studies of homogeneous ethylene/ $\alpha$ -olefin random copolymers. – J. Appl. Polym. Sci., 70, 1893–1905.

**Kraack, H., Sirota, E. B., and Deutsch, M.** 2001. Homogeneous crystal nucleation in short polyethylenes – Polymer, 42, 8225–8233.

**Kyu, T.; Hu, S.; Stein, R.** 1987. Characterization and properties of polyethylene blends II. Linear low-density with conventional low-density polyethylene – Journal of Polymer Science Polymer Physics 25(1), 89-103.

**Lehtinen A., Paukkeri R.** 1994. Fractionation of polypropylene according to molecular weight and tacticity. – Macromol. Chem. Phys., 195, 1539–1556.

**Lindenmeyer, P.H.** 1965. Crystallization and Molecular Folding – Science 147, 1256-1262.

**Lippits, D.R., Rastogi, S., Hahne, G., Mezari, B., Magusin, P.** 2007. Heterogeneous distribution of entanglements in the polymer melt and its influence on crystallization. – Macromolecules 40, 1004–1010.

**Mandelkern, L., Alamo, R.G., Kennedy, M.A.** 1990. The interphase thickness of linear polyethylene. – Macromolecules 23, 4721–4723.

**Mandelkern L.** 1971. Thermodynamic and morphological properties of crystalline polymers – J.Phys.Chem. 75, 3909-3920.

**Mandelkern, L., Allou, A.L.Jr., Gopalan, M.** 1968. Enthalpy of fusion of linear polyethylene – J.Phys.Chem. 72, 309-318.

**Marand, H., Alizadeh, A., Farmer, R., Desai, R., Velikov, V.** 2000 Influence of structural and topological constraints on the crystallization and melting behavior of

- polymers. 2. Polyarylene ether ether keton. – *Macromolecules*, 33, 3392–3403.
- Martinez-Salazar, J.; Sanchez Cuesta, M.; Plans, J.** 1991. On phase separation in high- and low-density polyethylene blends: 1. Melting-point depression analysis – *Polymer* 32(16), 2984-2988.
- Mathot, V. B. F., Scherrenberg, R. L., Pijpers, T. F. J.** 1998. Metastability and order in linear, branched and copolymerized polyethylenes – *Polymer*, 39, 4541-4559.
- Mathot, V. B. F.** 1994. *Calorimetry and Thermal Analysis of Polymers*. Munich, Hanser Publishers
- Minick, J., Moet, A., Hiltner, A., Baer, E., Chum, S.P.** 1995. Crystallization of very low density copolymers of ethylene with  $\alpha$ -olefins. – *J Appl Polym Sci*, 58,1371–1384.
- Mirabella F. M.** 2008. Crystallization and melting of a polyethylene copolymer: *In situ* observation by atomic force microscopy – *J. Appl. Polym. Sci.*, 108, 987-994.
- Morgan, R.; Hill, M.; Barham, P.** 1999. Morphology, melting behaviour and co-crystallization in polyethylene blends: the effect of cooling rate on two homogeneously mixed blends – *Polymer* 40, 337-348.
- Müller, A. J., Arnal, M. L.** 2005. Thermal fractionation of polymers. – *Progress in Polymer Science*, 30, 559-603.
- Peacock, A.J.** 2000. *Handbook of Polyethylene. Structure, Properties and Applications*. New York: Marcel Dekker.
- Peeters, M., Goderis, B., Vonk, C., Reynaers, H., Mathot, V.** 1997. Morphology of homogeneous copolymers of ethene and 1-octene. I. Influence of thermal history on morphology – *J. Polym. Sci., Part B: Polym. Phys.*, 35, 2689-2713.
- Parski, M., Piorkowska, E., Galeski, A.** 2000. Crystallization of polyethylene from the melt with lowered chain entanglements. – *Macromolecules* 33, 916–932.
- Puig C.** 2001. Enhanced crystallization in branched polyethylenes when blended with linear polyethylene – *Polymer* 42, 6579-6585.
- Puig, C.; Hill, M.; Odell, J.** 1993. Absence of isothermal thickening for a blend of linear and branched polyethylene – *Polymer* 34(16), 3402-3407.
- Rastogi, S., Lippits, D.R., Peters, G.W.M., Graf, R., Yao, Y.** 2005. Heterogeneity in polymer melts from melting of polymer crystals. – *Nat. Mater.* 4, 635–641.
- Razavi-Nuori, M.** 2006. Studies of comonomer distribution and molecular segregation in metallocene-prepared polyethylenes by DSC. – *Polymer Testing*, 25, 1052-1058.
- Razavi-Nuori, M., Hay, J. N.** 2001. Thermal and dynamic mechanical properties of metallocene polyethylene. – *Polymer*, 42, 8621-8627.
- Reiter G., Strobl G.R.** 2007. *Progress in Understanding of Polymer Crystallization*. Berlin Heidelberg, Springer-Verlag.

- Robelin-Souffache, E., Rault, J.** 1989. Origin of the long period and crystallinity in quenched semicrystalline polymers. I. – *Macromolecules* 22, 3581–3594.
- Rousseaux, F., Lemonnier, M.** 1980. Crystallization of polymers. Part II: Fractionated polyethylene quenched from the liquid state. – *J. Physique* 41, 1469–1474.
- Schultz, J. M., Scott, R. D.** 1969. Temperature dependence of secondary crystallization in linear polyethylene – *J. Polym. Sci. A-2*, 7, 659-666.
- Shanks, R.; Amarasinghe, G.** 2000. Crystallisation of blends of LLDPE with branched VLDPE – *Polymer* 41, 4579-4587.
- Sharma R.K., Mandelkern L.** 1969. The Density of Polyethylene Crystallized in the Bulk and from Dilute Solution – *Macromolecules*, 2, 266-271.
- Simanke, A.G., Alamo, R.G., Galland, G.B., Mauler, R.S.** 2001 Wideangle X-ray scattering of random Metallocene–Ethylene copolymers with different types and concentration of comonomer. – *Macromolecules* 34, 6959–6971.
- Smith, P., Manley, J.** 1979. Solid solution formation and fractionation in quasi-binary systems of polyethylene fractions. – *Macromolecules* 12, 483–491.
- Storks, K.H.** 1938. An Electron Diffraction Examination of Some Linear High Polymers – *J. Am. Chem. Soc.* 60, 1753-1761.
- Strobl G.** 2000. From the melt via mesomorphic and granular crystalline layers to lamellar crystallites: A major route followed in polymer crystallization? – *Eur. Phys. J. E*, 3, 165-183.
- Subramaniam C.** 1999. Morphology, crystallization and melting behaviors of random copolymers of ethylene with 1-butene, 1-pentene and 1-hexene. – PhD thesis.
- Zhang F., J. Liu, F. Xie, Q. Fu, T. He.** 2002. Polydispersity of ethylene sequence length in metallocene ethylene/ $\alpha$ -olefin copolymers. II. Influence on crystallization and melting behaviour – *J. Polym. Sci. Polym. Phys.*, 40, 822-830.
- Zhao, Y.; Liu, S.; Yang, D.** 1997. Crystallization behavior of blends of high-density polyethylene with novel linear low-density polyethylene – *Macromolecular Chemistry and Physics* 198(5), 1427-1436.
- Tanem, B.; Stori, A.** 2001a. Blends of single-site linear and branched polyethylene. I. Thermal characterisation – *Polymer* 42(12), 5389-5399.
- Tanem, B.; Stori, A.** 2001b. Blends of single-site linear and branched polyethylene. II. Morphology characterisation – *Polymer* 42, 6609-6618.
- Tanem, B.; Stori, A.** 2000. Thermal analysis of single-site polymers in binary blends of low-molecular-weight linear polyethylene and high-molecular-weight branched polyethylene – *Thermochimica Acta* 345, 73-80.
- Tashiro, K.; Imanishi, K.; Izuchi, M.; Kobayashi, M.; Itoh, Y.; Imai, M.; Yamagichi, Y.; Ohashi, M.; Stein, R.** 1995. Cocrystallization and Phase Segregation of Polyethylene Blends between the D and H Species. 8. Small-Angle Neutron Scattering Study of the Molten State and the Structural Relationship of

Chains between the Melt and the Crystalline State – *Macromolecules* 28(25), 8484-8490.

**Tashiro, K.; Izuchi, M.; Kobayashi, M.; Stein, R.** 1994a. Cocrystallization and Phase Segregation of Polyethylene Blends between the D and H Species. 3. Blend Content Dependence of the Crystallization Behavior – *Macromolecules* 27(5), 1221-1227.

**Tashiro, K.; Izuchi, M.; Kobayashi, M.; Stein, R.** 1994b. Cocrystallization and Phase Segregation of Polyethylene Blends between the D and H Species. 4. The Crystallization Behavior As Viewed from the Infrared Spectral Changes – *Macromolecules* 27(5), 1228-1233.

**Tashiro, K.; Stein, R.; Hsu, S.** 1992. Cocrystallization and phase segregation of polyethylene blends. 1. Thermal and vibrational spectroscopic study by utilizing the deuteration technique – *Macromolecules* 25(6), 1801-1808.

**Till, P.H.** 1957. The growth of single crystals of linear polyethylene – *J. Polym. Sci.*, 24, 301-306.

**Ueda, M.; Register, R.** 1996. Crystallization-induced phase separation in mixtures of model linear and short-chain branched polyethylenes – *Journal of Macromolecular Science, Part B Physics*, 35(1), 23-36.

**Usami, T., Takayama, Sh.** 1984. Identification of branches in low density polyethylenes by Fourier transform infrared spectroscopy. – *Polym. J.* 16, 731-738.

**Weber, C. H. M., Chiche, A., Krausch, G., Rosenfeldt, G., Ballauff, M., Harnau, L., Göttker-Schnetmann, I., Tong, Q., Mecking, S.** 2007. Single lamellae nanoparticles of polyethylene. – *Nano Letters*, 7, 2024-2029.

**Wignall, G.; Alamo, R.; Londono, J.; Mandelkern, L.; Kim, M.; Lin, J.; Brown, G.** 2000. Morphology of Blends of Linear and Short-Chain Branched Polyethylenes in the Solid State by Small-Angle Neutron and X-ray Scattering, Differential Scanning Calorimetry, and Transmission Electron Microscopy – *Macromolecules*, 33, 551-561.

**Wignall, G.; Londono, J.; Lin, J.; Alamo, R.; Galante, M.; Mandelkern, L.** 1995. Morphology of Blends of Linear and Long-Chain-Branched Polyethylenes in the Solid State: A Study by SANS, SAXS, and DSC – *Macromolecules* 28, 3156-3167.

**Wilfong D. L.** LLDPE TREF fractions, crystallization behavior and morphology. 1989. – *Polym. Mater. Sci. Eng.*, 61, 743-747.

**Wilfong, D., Knight, G. W.** 1990. Crystallization mechanisms for LLDPE and its fractions. – *J. Polym. Sci. Polym. Phys.*, 28, 861-870.

**Wunderlich, B.** 1980. *Macromolecular Physics: 3. Crystal Melting.* New York and London, Academic Press

**Wunderlich, B., Mellilo, J.** 1968. Morphology and growth of extended chain crystals of polyethylene – *Macromol. Chem.*, 118, 250-264.

# KOKKUVÕTE

## Polüetüleenilise kopolümeeride ja nende segude kristallisatsioonikäitumise termiline analüüs

Polüetüleen on väga laialdaselt kasutatav polümeer. Suures ulatuses määravad tema omadused molaarmass, molaarmassiline jaotus ja lühikeseharuliste hargnemiste jaotus.

Vaatamata sellele, et polüetüleenilise kristallisatsiooni on väga palju uuritud, on seal siiani ebaselgeid nüansse. Enamus polüetüleenilise makromolekulidest kristallub temperatuuril 110-120°C (niinimetatud kõrge temperatuuri kristallisatsioon). Tihti kaasneb selle protsessiga täiendav kristallisatsioon ~90°C juures, niinimetatud madala temperatuuri kristallisatsioon. Kahte eelpool mainitud protsessi kokku nimetatakse primaarseks kristallisatsiooniks, kus moodustuvad kristalsed superstruktuurid. Kristalliitide vahele jäävas amorfses osas toimub kristallisatsioon edasi ning tihti esineb temperatuurivahemikus 60-75°C sekundaarne kristallisatsioon. Polüetüleenilise primaarse kristallisatsiooni temperatuuri silmas pidades võib sekundaarse kristallisatsiooni temperatuuri nimetada väga madalaks. Selle väga madalal temperatuuril toimuva kristallisatsiooni olemus ja tekkepõhjused on siiani ebaselged.

Töö eesmärk oli uurida lineaarse madaltiheda polüetüleenilise (LLDPE) kristallisatsioonikäitumist väga madalal temperatuuril, 60-75°C juures, kasutades selleks diferentseerivat skaneerivat kalorimeetriat. Uuriti kuidas mõjutavad väga madalal temperatuuril toimuvat kristallisatsiooni materjali struktuur, molaarmass, molaarmassiline jaotus, komonomeeri tüüp ja sisaldus. Väga madala temperatuuri kristallisatsiooni nähtuse uurimiseks valiti üheksa kaubanduslikku LLDPE-d. Lisaks fraktsioneeriti osad nendest materjalidest molaarmassi (komonomeeri sisaldus on fraktsioonidel sarnane) ja koostise järgi (molaarmass on fraktsioonidel sarnane) ning uuriti saadud fraktsioone. Lisaks valmistati erinevad segud, et mõista kuidas mõjutavad materjali erinevad koostisosad kristallisatsioonikäitumist selles temperatuurivahemikus.

Termilise analüüsi tulemused näitasid, et kõikidel valitud materjalidel toimus väga madalal temperatuuril täiendav kristallisatsioon. Samas ei näidanud termiline analüüs ühelgi materjalil sellele kristallisatsioonipiigile vastavat sulamispiiki.

Tulemustest võib järeldada, et 60-75°C juures toimuv täiendav kristallisatsioon ei sõltu materjali komonomeeri sisaldusest ja -tüübist, vaid on sõltuv molaarmassist. Molaarmassi tõustes suureneb temperatuurivahemikus 60-75°C termogrammil esineva kristallisatsiooni piigi pindala. Sellise käitumise põhjuseks võib olla amorfse faasi suurenemine lamellide vahel ning molekulide

takerdumine, mis takistab neil kristalluda esmase kristallisatsiooni käigus. Hiljem võivad nad aga moodustada kimbutaolisi struktuure lamellide vahel.

Seda oletust aitab kinnitada segude uurimine, kus segati kokku suure komonomeeri sisaldusega materjal, millel esineb täiendav kristallisatsioon väga madalal temperatuuril ning materjal, millel seda ei esine. Sellise segu termiline analüüs näitab selgelt väga madalal temperatuuril toimuvat kristallisatsiooni. Samuti esineb selliste segude termogrammidel täiendav sulamispiik 60-75°C juures. Seega võib väita, et kõige enam mõjutab väga madalal temperatuuril toimuvat kristallisatsiooni materjali molaarmass ning molekulide omavaheline takerdumine.

## ABSTRACT

### **Thermal analysis of crystallization behaviour of polyethylene copolymers and their blends**

PE is a commodity polymer that has become widely used over the past several decades because of its low price and good mechanical properties. The properties are largely determined by the characteristics of the polymer such as MM, MMD, comonomer type and content. The relationship between microstructure and properties of polymers requires, among other factors, investigation of melting and crystallization behaviours. DSC has been the main technique used to study melting and crystallization behaviour and this method is enough powerful to analyze very small quantities, sometimes only 1-2mg of material and to detect very small changes in crystallinity.

Despite the fact that polyethylene crystallization is very widely studied there are still some questions which need to be answered. Polyethylene crystallizes at the temperatures around 110-120°C (high temperature crystallization). Often this HTCP in DSC has a shoulder around 90°C, so called LTCP. This is primary crystallization where crystal superstructures are formed. Between crystallites exists amorphous region. In certain conditions additional crystallization at temperatures around 60-75°C takes place. What causes this phenomenon of VLTC is not clear and not satisfactorily studied. Therefore, the main objective of the present study was to examine the crystallization behaviour of LLDPE at very low temperature using DSC. For better understanding what causes the VLTCP some materials were fractionated according to MM and composition to get samples with narrow MMD and CD. Some components with different comonomer content were blended together to understand how different macromolecular constituents influence crystallization process at very low temperature.

DSC curves of whole copolymers, MM and compositional fractions of SS and ZN materials uniquely show the presence of an additional crystallization process occurring at temperatures around 60–75°C. The VLTCP was not detected in the fractions having lowest MM. The melting curves do not show any additional peaks clearly related to the VLTCP. Results of this work give a better understanding of the matter compared to the mixed opinions in literature. Based on DSC measurements can be said that VLTCP in copolymers is not caused by highly branched component of the materials but due to the entanglements of high MM chains.



**APPENDIX I:  
PUBLICATIONS**



## PAPER I

T. Poltimäe, E. Tarasova, A. Krumme, A. Lehtinen, A. Viikna. 2009. Behaviour of the very-low-temperature crystallization peak of linear low-density polyethylene. *Proceedings of the Estonian Academy of Sciences*, 58 (1), 58-62.





## Behaviour of the very-low-temperature crystallization peak of linear low-density polyethylene

Triinu Poltimäe<sup>a\*</sup>, Elvira Tarasova<sup>a</sup>, Andres Krumme<sup>a</sup>, Arja Lehtinen<sup>b</sup>, and Anti Viikna<sup>a</sup>

<sup>a</sup> Department of Polymeric Materials, Tallinn University of Technology, Ehitajate tee 5, 19086 Tallinn, Estonia

<sup>b</sup> Borealis Polymers OY, P.O. Box 330, FIN-06101, Porvoo, Finland

Received 29 May 2008, revised 10 September 2008, accepted 8 October 2008

**Abstract.** The crystallization behaviour of Ziegler–Natta (ZN) and single-site catalyst based ethylene–1-butene and ethylene–1-hexene copolymers with different comonomer content were studied by differential scanning calorimetry. In addition to a high-temperature crystallization peak, and for ZN copolymers in addition to a low-temperature crystallization peak, quite often a very-low-temperature crystallization peak (VLTCP) was observed at temperatures in between approximately 330 and 345 K. It was found that the VLTCP temperature decreased with increasing comonomer content and did not depend on the type of catalyst used. The fractional degree of crystallinity calculated from the VLTCP was independent of the chemical nature and content of the comonomers present as well as of the polydispersity of molar mass within the used range of magnitudes. However, crystallinity as related to the area of the VLTCP was strongly catalyst type dependent and was higher for the single-site catalyst used compared to the ZN catalyst used.

**Key words:** materials technology, linear low-density polyethylene, copolymers, low-temperature crystallization peak, differential scanning calorimetry.

### INTRODUCTION

Polyethylene (PE) is available with a wide array of engineering properties to provide toughness, ease of processing, shrinkage rates, chemical abrasion, impact resistance, etc. The properties are largely determined by the characteristics of the polymer such as molar mass (MM), molar mass distribution (MMD), and degree of branching.

One method for providing the special properties is the copolymerization of ethylene and  $\alpha$ -olefins, which has become increasingly important in the last two decades. These materials, collectively termed linear low-density polyethylene (LLDPE), have been synthesized using different types of catalysts and comonomers. Usually, 1-butene, 1-hexene, or 1-octene is used as the  $\alpha$ -olefin comonomer. Random ethylene– $\alpha$ -olefin copolymers obtained by homogeneous single-site catalysts (SSC) show a homogeneous comonomer distribution (CD) and a narrow MMD [1], in contrast to traditional

Ziegler–Natta (ZN) catalysts, which lead to broad MMD and CD [2,3].

The crystallization in copolymers is markedly different from the crystallization of linear or slightly branched polymers, such as linear PE and high-density PE respectively [4]. In copolymers ethylene sequences of varying lengths (determined by branching frequency) are present abundantly. These sequences can only crystallize below certain temperatures, determined by their lengths. Therefore, a broad range of melting temperatures may be expected for the copolymers. The crystallization process in copolymers is further influenced by the fact that branches longer than methyl are predominantly excluded from the growing crystal [5]. However, it should be mentioned here that ethyl (1-butene as comonomer), being a ‘border case’ branch, is excluded from the crystal lattice at low cooling rates, and can be included at high cooling rates. The crystals formed under such conditions are much thinner and less perfect compared to those formed in the corresponding non-branched material.

Differential scanning calorimetry (DSC) has been the main technique used to study melting and crystal-

\* Corresponding author, [triinu.poltimae@ttu.ee](mailto:triinu.poltimae@ttu.ee)

lization behaviour. The results from the thermal analysis of heterogeneous, ZN ethylene- $\alpha$ -olefin copolymers [6–9] clearly indicate the existence of a triple crystallization mechanism in the ethylene copolymers: a sharp, high-temperature crystallization peak (HTCP), a broad low-temperature crystallization peak (LTCP) next to HTCP, and often a very-low-temperature crystallization peak (VLTCP) are observed. For SSC copolymers, and in general for homogeneous copolymers [7], just HTCP and, often, VLTCP are observed (see for an example [6, Ch. 9, fig. 9.11]).

One of the hypotheses of the origin of VLTCP is proposed in [10,11] for SSC-based LLDPEs. As it was mentioned above, the crystallization process in copolymers is predominantly governed by the length distribution of the crystallizable sequence. In a random copolymer, the frequent occurrence of branches along the polymer backbone fragments the chain into a number of shorter sequences. Taking this into account, Zhang et al. [10] and Mirabella [11] suggested that HTCP corresponds to the crystallization of ethylene with a large average sequence length (ASL) and VLTCP is related to the crystallization with a relatively short ASL.

Another point of view on the problem of VLTCP arises from the investigation of the homogeneous nucleation of PE. For this purpose in [12] low MM PEs were emulsified to separate the nucleation from the growth process and to remove macroscopic heterogeneous nucleation sites. Both a VLTCP and a HTCP were observed for the emulsified samples during DSC cooling scans. The degree of undercooling from the equilibrium melting temperature of linear PE (417 K) for the VLTCP was several tens of degrees (80–100 K) in contrast to non-emulsified samples, which had only a HTCP at a few degrees of undercooling. It was suggested that the HTCP in the cooling scans is due to heterogeneous nucleation of aggregated droplets and the VLTCP is related to the homogeneous nucleation of the un-aggregated emulsion droplets.

The same degree of undercooling (as mentioned above) was pointed out for single nanocrystals homogeneously grown from solution, consisting of a single crystalline lamella with a thickness of 6.3 nm covered by thin amorphous layers [13]. Therefore, it can be concluded that the VLTCP phenomenon can be caused by homogeneous nucleation as it has the same undercooling as pointed out above.

However, the origin of the VLTCP in ethylene-containing polymers is not clear yet. Therefore, the main aim of the present study was to examine the effect of the structure of materials, polydispersity of MM of the polymers, and comonomer type and its concentration on the behaviour of the VLTCP.

## EXPERIMENTAL

### Materials

The LLDPEs used in this study were commercial ethylene-1-butene and ethylene-1-hexene copolymers produced by ZN and SSC. The polymers will be referred to as ZN and SSC samples. The comonomer content,  $C_{\text{comon}}$ , in the copolymers varied. All these materials had similar density and weight average MM ( $\bar{M}_w$ ). Molecular characteristics of the studied samples are listed in Table 1.

### Methods

A Perkin Elmer Diamond differential scanning calorimeter (DSC) was used for thermal analysis. The instrument was calibrated using indium and tin at the applied cooling rate. Helium was used for furnace purge. Plates of  $55 \times 65 \times 1$  mm were pressed from the materials at 453 K and cooled to room temperature. Flat samples of approximately 1 mg were cut from the plates and packed into aluminium foil to maximize thermal contact between the sample and the calorimetric furnace. During the measurement, the sample was first held at 453 K for 5 min for deleting its thermal history. Then it was cooled to 273 K at a rate of 100 K/min, held at 273 K for 5 min, and then heated to 453 K at a rate of 100 K/min. The fractional degree of crystallinity,  $w_c$ , was calculated by dividing the crystallization enthalpy of VLTCP by the enthalpy of the fusion of 100% crystalline PE,  $\Delta H_m^0 = 293$  J/g. Crystallinity is, however, only to be used for comparison between the materials. The overall crystallinity ( $w_{c,h}$ ) was obtained by dividing the overall melting enthalpy by 293 J/g.

The MMD was measured in Borealis Polymers OY by gel permeation chromatography (GPC) using trichlorobenzene as a solvent at 140°C.

The comonomer content was measured in Borealis Polymers OY by Fourier transform infrared spectroscopy (FTIR).

**Table 1.** Molecular characteristics of linear low-density polyethylenes

| LLDPE sample | Type of comonomer | $C_{\text{comon}}$ , wt. % | Density, kg/m <sup>3</sup> | $M_w$ , kg/mol | Polydispersity $M_w/M_N$ |
|--------------|-------------------|----------------------------|----------------------------|----------------|--------------------------|
| SSC-1        | 1-Hexene          | 5.4                        | 923                        | 84             | 2.1                      |
| SSC-2        | 1-Hexene          | 3.6                        | 927                        | 140            | 3.1                      |
| SSC-3        | 1-Hexene          | 5.0                        | 923                        | 140            | 2.3                      |
| SSC-4        | 1-Hexene          | 6.9                        | 920                        | 115            | 2.4                      |
| SSC-5        | 1-Butene          | 2.3                        | 922                        | 136            | 2.3                      |
| ZN-1         | 1-Hexene          | 5.6                        | 930                        | 125            | 4.5                      |
| ZN-2         | 1-Hexene          | 7.6                        | 924                        | 125            | 4.4                      |
| ZN-3         | 1-Hexene          | 8.5                        | 917                        | 150            | 3.8                      |
| ZN-4         | 1-Butene          | 7.2                        | 920                        | 122            | 4.0                      |

## RESULTS AND DISCUSSION

The nonisothermal crystallization and melting thermograms for one of the materials (SSC-1) are shown in Fig. 1 as an example.

Figure 1 illustrates the presence of two distinct peaks in the crystallization curves of SSC-1 copolymer: a sharp HTCP and a much broader and less in magnitude VLTCP at temperatures around 340 K. Similar heating/cooling scans are observed for all the samples studied. In contrast, the melting of the materials has only one endothermic peak corresponding to their HTCP. It should be mentioned that for ZN as well as for SSC copolymers no clearly evident LTCPs were observed, except for sample ZN-3, where an additional small LTCP was clearly detected. Along with it an additional broad melting peak is present in DCS melting curves of this sample. For copolymers produced using ZN catalyst it was suggested [14] that HTCP is due to the crystallization of high MM polymers having a low branching content, whereas the LTCP and also VLTCP are caused by low MM polymers with a high branching content. However, the branching distribution is homogeneous in materials synthesized by SSC, without the clustering of the branch along the main chain as in ZN copolymers, and there should be no relation between MM and the branch content. However, the experimental results uniquely indicate that there was still a low-temperature crystallization process, leading to a VLTCP, as it is obvious from Fig. 1.

Figure 2 shows the dependence of the peak temperature of VLTCP,  $T_{c,vi}$ , on the comonomer content,  $C_{comon}$ , for ethylene-1-hexene copolymers. It is seen that as  $C_{comon}$  increases,  $T_{c,vi}$  decreases, which is in agreement with the finding reported in [7]. An interesting fact is that  $T_{c,vi}$  vs.  $C_{comon}$  for copolymers that have the same comonomer type can be represented by a single line, irrespective of the catalyst type by which

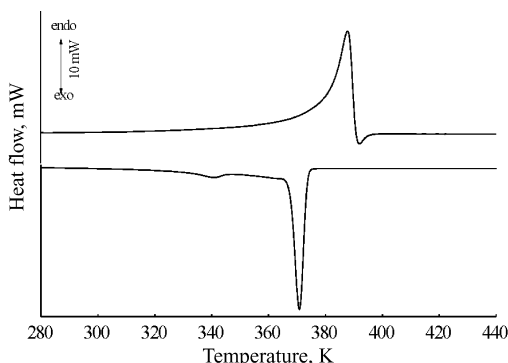


Fig. 1. DSC cooling and subsequent heating curves of sample SSC-1.

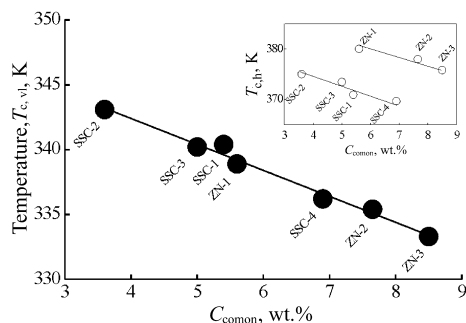
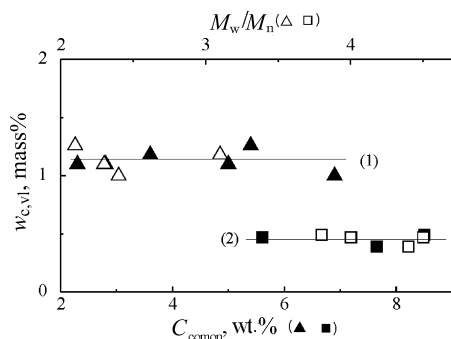


Fig. 2. Plots of peak crystallization temperatures of the VLTCP ( $T_{c,vi}$ ) as a function of the comonomer content ( $C_{comon}$ ) for the ethylene-1-hexene copolymers. The inset shows temperature dependence of the HTCP ( $T_{c,h}$ ) on  $C_{comon}$  for the same copolymers.

the materials were produced. This differs from the behaviour of the HTCP. The temperatures of the main peak ( $T_{c,h}$ ) for SSC materials were essentially lower than for ZN materials as is clearly seen from the inset in Fig. 2. The ZN copolymers are known to be structurally heterogeneous both at inter- and intramolecular level. Therefore, more and longer ethylene sequences are available leading to thicker lamellae and consequently to higher crystallization and melting temperatures according to the Thompson–Gibbs equation. Taking into account the above-mentioned difference in the behaviour of peak temperatures with catalyst type, one can suggest that it is not only the presence of long ethylene sequences that influences the thermal behaviour of VLTCP.

However, on further comparison between copolymers of different catalyst types, it was found that the type of catalyst, ZN and SSC, influences the crystallization process in the low-temperature range. These observations were further verified by comparing the fractional degree of crystallinity of VLTCP  $w_{c,vi}$  vs.  $C_{comon}$ . Plots for all the copolymers are shown in Fig. 3. It was found that  $w_{c,vi}$  did not depend either on the comonomer type and its content or on the polydispersity of MM within the same type of catalyst. The overall degree of crystallinity is known to be independent of the nature of the comonomer (except for methyl branches), while being largely determined by the crystallizable sequence length distributions [15,16]. In turn, the sequence distributions are influenced by the type of catalyst (e.g., ZN-based systems result in broader distributions compared to SSC-based copolymers).

The fractional degree of crystallinity calculated from VLTCP is two times higher for the SSC copolymers than for the ZN materials as is seen from Fig. 3. It is evident that homogeneous CD facilitates the formation of a VLTCP. However, thermal analysis alone is not sufficient for explaining this behaviour.



**Fig. 3.** The degree of crystallinity  $w_{c,vi}$  vs. comonomer content  $C_{comonomer}$  (solid signs, bottom of  $X$ -axis) and polydispersity  $M_w/M_n$  (open signs, top of  $X$ -axis) for SSC (1) and ZN (2) copolymers.

An interesting and important fact detected in calorimetric cooling and heating scans is that no low-temperature melting peaks corresponding to the VLTCP were found for the studied LLDPE materials. Hence, the origin and properties of the VLTCP cannot be explained only in terms of the crystallization of ethylene sequences having a relatively short ASL. In this case the lamellae population formed at low temperature should be thin [11] and therefore should melt at a considerably low temperature. This is not observed for the studied materials, which have essentially large VLTCs at undercoolings  $\sim 80$  K. The same degrees of undercoolings were detected in [12,13] for homogeneously grown crystals of PE. Probably, the VLTCP is associated with homogeneous nucleation, which occurs spontaneously by undercooling only.

## CONCLUSIONS

On the basis of the DSC experimental results on the low-temperature crystallization behaviour of SSC- and ZN-based ethylene- $\alpha$ -olefin copolymers the following conclusions can be drawn:

- DSC curves uniquely indicate that in the studied copolymers an additional crystallization process occurred at very low temperatures around 330–345 K. This VLTCP is much broader and less in magnitude than the main sharp HTCP. Moreover, the melting curves do not show any additional peaks clearly related to the VLTCP.
- No dependences of the fractional degree of crystallinity calculated from the VLTCP on the comonomer content and polydispersity of MM were observed at least within the studied range of magnitudes. The degree of crystallinity was also independent of the chemical nature of the comonomers (1-butene or 1-hexene).

- The fractional degree of crystallinity was in turn strongly influenced by the type of catalyst. For the SSC materials the degree of crystallinity was higher than for the ZN samples.
- The crystallization temperatures of the VLTCP,  $T_{c,vi}$ , decreased with the increasing comonomer content in the LLDPEs. At the same time,  $T_{c,vi}$  did not depend on the catalyst type used for producing the LLDPE materials.

## ACKNOWLEDGEMENTS

The Estonian Science Foundation is acknowledged for support under grant No. 6553 and Borealis Polymers OY for structural characterization of the studied materials.

## REFERENCES

1. Pino, P., Oschwald, A., Ciardelli, F., Carlini, C., and Chiellini, E. *Coordination Polymerization of  $\alpha$ -Olefins* (Chien, J. C. W., ed.). Elsevier, New York, 1975.
2. Ziegler, K., Holzkamp, E., Breil, H., and Martin, H. Das Mülheimer Normaldruck-Polyäthylen-Verfahren. *Angew. Chem.*, 1955, 541–547.
3. Natta, G. Une nouvelle classe de polymères d' $\alpha$ -olefines ayant une régularité de structure exceptionnelle. *J. Polym. Sci.*, 1955, **16**, 143–154.
4. Hsieh, E. T., Tso, C. C., Byers, J. D., Johnson, T. W., Fu, Q., and Cheng, S. Z. D. Intermolecular structural homogeneity of metallocene polyethylene copolymers. *J. Macromol. Sci. Phys.*, 1997, **36**, 615–628.
5. Flory, P. J. Theory of crystallization in copolymers. *Trans. Faraday Soc.*, 1954, **51**, 848–857.
6. Hussein, I. A. Nonisothermal crystallization kinetics of linear metallocene polyethylenes. *J. Appl. Polym. Sci.*, 2008, **107**, 2802–2809.
7. Mathot, V. B. F. *Calorimetry and Thermal Analysis of Polymers* (Mathot, V. B. F., ed.). Hanser Publishers, Munich, 1994.
8. Mathot, V. B. F., Scherrenberg, R. L., and Pijpers, T. F. J. Metastability and order in linear, branched and copolymerized polyethylenes. *Polymer*, 1998, **39**, 4541–4559.
9. Minick, J., Moet, A., Hiltner, A., Baer, E., and Chum, S. P. Crystallization of very low density copolymers of ethylene with  $\alpha$ -olefins. *J. Appl. Polym. Sci.*, 1995, **58**, 1371–1384.
10. Zhang, F., Liu, J., Xie, F., Fu, Q., and He, T. Polydispersity of ethylene sequence length in metallocene ethylene/ $\alpha$ -olefin copolymers. II. Influence on crystallization and melting behaviour. *J. Appl. Polym. Sci. Polym. Phys.*, 2002, **40**, 822–830.
11. Mirabella, F. M. Crystallization and melting of a polyethylene copolymer: in situ observation by atomic force microscopy. *J. Appl. Polym. Sci.*, 2008, **108**, 987–994.

12. Kraack, H., Sirota, E. B., and Deutsch, M. Homogeneous crystal nucleation in short polyethylenes. *Polymer*, 2001, **42**, 8225–8233.
13. Weber, C. H. M., Chiche, A., and Krausch, G. Single lamella nanoparticles of polyethylene. *Nano Lett.*, 2007, **7**, 2024–2029.
14. Wilfong, D. and Knight, G. W. Crystallization mechanisms for LLDPE and its fractions. *J. Polym. Sci. Polym. Phys.*, 1990, **28**, 861–870.
15. Kim, M. and Philips, P. J. Nonisothermal melting and crystallization studies of homogeneous ethylene/ $\alpha$ -olefin random copolymers. *J. Appl. Polym. Sci.*, 1998, **70**, 1893–1905.
16. Alamo, R. G. and Mandelkern, L. Thermodynamic and structural properties of ethylene copolymers. *Macromolecules*, 1989, **22**, 1273–1277.

## Lineaarse madaltiheda polüetüleeni väga madala temperatuuri kristallisatsiooni piigi olemus

Triinu Poltimäe, Elvira Tarasova, Andres Krumme, Arja Lehtinen ja Anti Viikna

Diferentsiaalse skaneeriva kalorimeetriaga on uuritud Ziegleri-Natta (ZN) ja ainuasendi (SSC) katalüsaatoritega saadud erineva komonomeeri sisaldusega etüleen/1-buteen- ning etüleen/1-hekseenkopolümeeride kristallisatsioonikäitumist. Lisaks kõrge temperatuuri kristallisatsiooni piigile (KTKP) ja ZN-i kopolümeeride puhul lisaks madala temperatuuri kristallisatsiooni piigile (MTKP) on tuvastatud tihti ka väga madala temperatuuri kristallisatsiooni piik (VMTKP) temperatuurivahemikus ligikaudu 330–345 K. On leitud, et VMTKP maksimumi temperatuur väheneb koos komonomeeri sisalduse kasvuga kopolümeeris ja ei sõltu kasutatud katalüsaatori liigist. VMTKP põhjal arvatud kristalsusmäär ei sõltu uuritud materjalide puhul komonomeeri keemilisest koostisest (1-buteen või 1-hekseen), komonomeeri sisaldusest ega molaarmassilise jaotuse polüdisperssusest. Siiski sõltub VMTKP kristalsusmäär tugevalt kopolümeeri valmistamiseks kasutatud katalüsaatori liigist ja on kõrgem SSC katalüsaatori puhul, võrreldes ZN-i katalüsaatoriga.



## PAPER II

E. Tarasova, T. Poltimäe, A. Krumme, A. Lehtinen, A. Viikna. 2009. Study of very low temperature crystallization process in ethylene/ $\alpha$ -olefin copolymers. *Macromolecular Symposia*, 282 (1), 175–184.



# Study of Very Low Temperature Crystallization Process in Ethylene/ $\alpha$ -Olefin Copolymers

*E. Tarasova,\*<sup>1</sup> T. Poltimäe,<sup>1</sup> A. Krumme,<sup>1</sup> A. Lehtinen,<sup>2</sup> A. Viikna<sup>1</sup>*

**Summary:** The crystallization behavior of Ziegler-Natta (ZN) and single site (SS) based ethylene/1-butene and ethylene/1-hexene copolymers and SS copolymer fractionated by composition and molar mass (MM) has been studied by differential scanning calorimetry. It was observed that in addition to the high temperature crystallization peak (HTCP), and for ZN copolymers in addition also to low temperature crystallization peak (LTCP), a very-low temperature crystallization peak (VLTCP) is present at temperatures in between 60–75 °C. Peak temperature of VLTCP,  $T_{\text{VLTCP}}$ , decreases with increasing comonomer content ( $C_{\text{comon}}$ ) at fixed MM. If  $C_{\text{comon}}$  is kept approximately constant,  $T_{\text{VLTCP}}$  increases with increasing MM. It turns out that  $T_{\text{VLTCP}}$  does not depend on the type of catalyst used. The degree of crystallinity calculated from the VLTCP is independent of the chemical nature of the comonomers present, but slightly changes with  $C_{\text{comon}}$ . It also steeply increases with MM and levels off at MM around 50 kg/mol. It was found that the crystallinity as related to the area of the VLTCP is catalyst type dependent, and is higher for the SS catalyst used compared to the ZN catalyst.

**Keywords:** crystallization at very low temperature; differential scanning calorimetry; ethylene/ $\alpha$ -olefins; linear low-density polyethylene

## Introduction

The crystallization of copolymers is markedly different from the crystallization of linear or slightly branched polymers, such as linear polyethylene and high-density polyethylene, respectively.<sup>[1]</sup> In copolymers ethylene sequences of varying lengths (determined by branching frequency) are present abundantly. These sequences can only crystallize below certain temperatures, determined by their lengths. Therefore, a broad range of melting temperatures may be expected for the copolymers. The crystallization process in copolymers is further influenced by the fact that branches longer than the methyl are predominantly excluded from the growing crystal.<sup>[2]</sup>

Differential scanning calorimetry (DSC) has been one of the main techniques used to study melting and crystallization behavior of polymers. The results from the thermal analysis study on heterogeneous, Ziegler-Natta (ZN) ethylene/ $\alpha$ -olefin copolymers<sup>[3–6]</sup> clearly indicate the existence of a triple crystallization mechanism in the ethylene copolymers: a sharp, high temperature crystallization peak (HTCP), a broad low-temperature crystallization peak (LTCP) next to HTCP, and often a very-low temperature crystallization peak (VLTCP). For single site catalyzed (SS) copolymers, and in general homogeneous copolymers,<sup>[4]</sup> the high temperature crystallization peak and the very-low temperature crystallization peak are usually detected.

The presence and behavior of VLTCP in copolymers is interesting, because there is a possibility of correlation between this secondary crystallization process and the mechanical properties of the samples. One of the hypotheses of the origin of VLTCP is

<sup>1</sup> Tallinn University of Technology, Ehitajate tee 5, 19086 Tallinn, Estonia  
E-mail: tarasova\_elvira@mail.ru

<sup>2</sup> Borealis Polymers OY, P.O. Box 330, FIN-06101, Porvoo, Finland

proposed in Ref. [7–9] for SS based linear low-density polyethylenes (LLDPE). As it was mentioned above, the crystallization process in copolymers is predominantly governed by the crystallizable sequence length distribution. In a random copolymer, the frequent occurrence of branches along the polymer backbone fragments the chain into a number of shorter sequences. While the longest sequences form part of the lamellar crystals, they impose a constraint on the remaining crystallizable sequences in these chains. As the number of segments participating in lamellar formation increases, so do the restrictions imposed on the mobility of the remaining sequences. At very high degrees of constraint, the shorter sequences are unable to participate in the reeling-in process required for chain-folded crystal formation. The easiest route available for this short segments to crystallize without violating spatial requirements is to simply aggregate into thin bundles.<sup>[9]</sup> Accordingly, they aggregate with neighboring sequences to form stable clusters or bundled crystals. It is also suggested that the bundled crystals may act as cross-linking points in the amorphous phase. H. Teng et al.<sup>[10]</sup> stated by means of atomic force microscopy that there is a clear regular structure between spherulites and a lot of bundle-like bridges spanning the neighboring spherulites in bulk-crystallized polyethylene (PE). With increasing the branch component in the blend of linear and branched PEs the regular structure between spherulites disappeared.

However, the origin of the VLTCP in ethylene-containing polymers is not clear up to now. It is well known that many properties of crystalline random copolymers are very dependent on molar mass (MM) and crystallization conditions.<sup>[11–13]</sup> Consequently, to get appropriate properties of copolymers, along with the sequence distribution (SD) and concentration of comonomer ( $C_{\text{common}}$ ) the MM and crystallization condition have to be specified and independently assessed. Therefore, the major focus of the present study is to examine the effect of structure of materials,

co-monomer type and its content, MM and different cooling/heating rates on the behavior of the VLTCP. Moreover, one of the SS catalyzed copolymer was fractionated by MM and composition to analyze the contribution of MM and  $C_{\text{common}}$  as independent variables.

## Experimental Part

### Materials

The LLDPE's used in this study were commercial ethylene/1-butene and ethylene/1-hexene whole copolymers, produced by ZN<sup>[14]</sup> or SS<sup>[15]</sup> catalyst types. The molecular characteristics of the investigated ethylene copolymers are listed in Table 1. The samples are identified with the initials SS or ZN followed by a number corresponding to the comonomer content,  $C_{\text{common}}$ , expressed in weight percent. All these materials (obtained in pellet form) had about the same density and weight average MM ( $\overline{M}_w$ ). One of the SS materials, namely SS-6.9, was fractionated according to both MM and composition. All the fractionations were carried out on polymer in powder form. For this purpose, the sample pellets were dissolved in xylene. The solution obtained was allowed to cool to room temperature and the polymer was precipitated in acetone, filtered and dried at room temperature. Fractionation by MM was carried out according to the Holtrup technique which is a solvent/non-solvent extraction.<sup>[16]</sup> In the experiment 10 g of polymer powder was extracted in a solvent/non-solvent mixture of xylene and ethylene glycol monoethyl ether in different ratios at 116 °C. Dissolution time of 10 min was used at each dissolution step, and 10 fractions were collected. Fractionation according to short chain branching (composition) was carried out using multiple solvent extraction<sup>[17]</sup> technique. The sample amount fractionated was about 15 g and dissolution time was 30 min. The solvents used in the fractionation were: n-pentane at 35 °C, n-hexane at 65 °C, n-heptane at 75 °C and 90 °C, n-octane at 100 °C, toluene at 105 °C

**Table 1.**

Molecular characteristics of single site (SS) and Ziegler-Natta (ZN) catalyzed copolymers.

|                                |             | Sample       | Comonomer type | $C_{\text{comon}}$ | $\bar{M}_w$ | $\bar{M}_w/\bar{M}_n$ |
|--------------------------------|-------------|--------------|----------------|--------------------|-------------|-----------------------|
|                                |             |              |                | (wt%)              | (kg/mol)    | arbitrary units       |
| Whole polymers                 |             | ZN-5.6       | hexene         | 5.6                | 125         | 4.5                   |
|                                |             | ZN-7.2       | butene         | 7.2                | 122         | 4.0                   |
|                                |             | ZN-7.6       | hexene         | 7.6                | 125         | 4.4                   |
|                                |             | ZN-8.5       | hexene         | 8.5                | 150         | 3.8                   |
|                                |             | SS-2.3       | butene         | 2.3                | 136         | 2.3                   |
|                                |             | SS-3.6       | hexene         | 3.6                | 140         | 3.1                   |
|                                |             | SS-5.0       | hexene         | 5.0                | 140         | 2.3                   |
|                                |             | SS-5.4       | hexene         | 5.4                | 84          | 2.1                   |
|                                |             | SS-6.9 (6.2) | hexene         | 6.9 (6.2)          | 115         | 2.4                   |
| Fractions of<br>SS-6.9(6.2) by | molar mass  | M1           | hexene         | NA                 | 5.1         | 2.1                   |
|                                |             | M2           | hexene         | NA                 | 13.6        | 1.6                   |
|                                |             | M3           | hexene         | NA                 | 20.1        | 1.6                   |
|                                |             | M4           | hexene         | NA                 | 25.4        | 1.5                   |
|                                |             | M5           | hexene         | 5.6                | 35.0        | 1.4                   |
|                                |             | M6           | hexene         | 5.8                | 43.4        | 1.5                   |
|                                |             | M7           | hexene         | 6.3                | 66.5        | 1.5                   |
|                                |             | M8           | hexene         | 6.2                | 82.4        | 1.6                   |
|                                |             | M9           | hexene         | 6.2                | 128         | 1.8                   |
|                                |             | M10          | hexene         | 6.4                | 117         | 1.8                   |
|                                | composition | C1           | hexene         | 6.5                | 98.5        | 2.5                   |
|                                |             | C2           | hexene         | 5.9                | 100         | 2.3                   |
|                                |             | C3           | hexene         | 5.4                | 96          | 2.2                   |
|                                |             | C4           | hexene         | 3.9                | 99.5        | 2.1                   |

'NA' means 'not analyzed'; M1, M2, ... C1, C2 ... are the numbers of fractions.

and xylene at 130 °C. The first two fractions were separated by evaporation of the solvent in a rotavapor and the other ones by precipitation in acetone. Due to the reasonably narrow composition distribution of sample SS-6.9, the first three compositional fractions were too small for further analyses. For comparison with LLDPE fractions the commercial Ziegler-Natta catalysed high-density polyethylene (HDPE) with  $M_w = 94500$  and polydispersity  $\bar{M}_w/\bar{M}_n = 8.3$  was fractionated according to MM. The fractions of HDPE have approximately similar polydispersity equal 1.7 in average.

As it follows from the fractionation description the whole SS-6.9 was dissolved, dried and obtained in powder form. Probably, due to the dissimilarity in material form (pellet or powder) there was a difference in melting and crystallization temperatures as well as in the degree of crystallinity of SS-6.9. Moreover, the value of  $C_{\text{comon}}$  for powder SS-6.9 was estimated to be about 6.2 wt%. The difference in  $C_{\text{comon}}$  may be connected with the different material forms (determi-

nation of  $C_{\text{comon}}$  was calibrated with pelletized samples). Therefore, this material was identified as SS-6.9(6.2). For comparison with the fractions the fluffy SS-6.9(6.2) powder was chosen as the reference material. The MM fractions have similar polydispersity  $\bar{M}_w/\bar{M}_n$  and approximately identical  $C_{\text{comon}}$ . The  $C_{\text{comon}}$  for the first four fractions was not analyzed due to their small amount. The compositional fractions used in this work have about the same molar mass distribution and  $\bar{M}_w$ .

### Methods

Perkin Elmer Diamond differential scanning calorimeter (DSC) and DSC-7 were used for thermal analysis at scanning rates of 10, 100, 300 °C/min and 5 °C/min, respectively. The instruments were calibrated using indium and tin at all applied heating rates. In Diamond DSC helium was used as furnace purge gas and in DSC-7 nitrogen was used. 55 × 65 × 1 mm plates were pressed from the materials in pellet form at 180 °C and cooled to room temperature. For fractions powders were

manually compacted by pressure at room temperature. To avoid differences in melting and crystallization temperatures caused by variation in sample weight, a sample mass of  $1.00 \pm 0.02$  mg was used in all DSC experiments. Flat samples were packed into aluminum foil to maximize thermal contact between sample and calorimetric furnace. During the measurement, the sample was first held at  $180^\circ\text{C}$  for 5 min for deleting its thermal history. Then it was cooled to  $0^\circ\text{C}$  at a definite scanning rate, held at this temperature for 5 min and then heated to  $180^\circ\text{C}$  at the same rate. Overall degree of crystallinity  $X_{\text{overall}}$  was calculated by dividing overall melting or crystallization enthalpy by enthalpy of fusion of 100% crystalline PE,  $\Delta H_m^\circ = 293$  J/g. The partial degree of crystallinity estimated from the area of VLTCP,  $X_{\text{VLTCP}}$ , was obtained from cooling traces by dividing the crystallization enthalpy of VLTCP by  $\Delta H_m^\circ$ .

MM averages and MMD were determined by size exclusion chromatography (SEC) using 1,2,4-trichlorobenzene (TCB) as eluent at  $140^\circ\text{C}$ . Comonomer contents were measured by Fourier transform infrared spectroscopy (FTIR).<sup>[18]</sup>

## Results and Discussion

The nonisothermal crystallization and melting thermograms for all SS and ZN

whole materials were studied. Several selected exotherms of copolymers with different branch content at the constant cooling rate of  $100^\circ\text{C}/\text{min}$  are shown in Figure 1. The similar heating/cooling thermograms are observed for all the samples studied at all scanning rates used.

Figure 1 illustrates the existence of a triple crystallization mechanism in the ethylene copolymers: a sharp, high temperature crystallization peak (HTCP), a broad low-temperature crystallization peak (LTCP) close to HTCP, and a very-low temperature crystallization peak (VLTCP), extending to temperatures around  $60$ – $75^\circ\text{C}$ , are observed. For SS copolymers studied, just the HTCP and VLTCP are usually observed. It should be noticed here that for whole HDPE no VLTCP and even LTCP were observed.

Nevertheless, the melting curves of the LLDPE materials have only one or seldom two endothermic peaks corresponding to primary crystallization presented by HTCP and LTCP. No additional peaks clearly related to the VLTCP were detected for none heating rate, as it is obvious from the Inset of the Figure 1. Due to this fact no melting temperature directly corresponding to the VLTCP (and also, partial crystallinity) can be obtained from the melting traces. We suggest that the crystallization temperature of the copolymer will

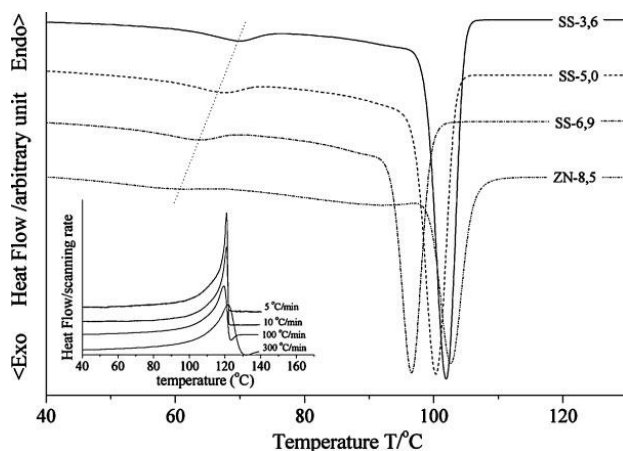


**Figure 1.**

DSC exotherms of ethylene-hexene copolymers measured at cooling rate of  $100^\circ\text{C}/\text{min}$ . Inset shows DSC endotherms divided by scanning rates of SS-3,6 copolymer at different scanning rates.

accordingly behave itself with the melting temperature and such parameters as  $C_{\text{common}}$ , MM, scanning rate etc. affects the melting and crystallization temperatures in a consistent manner. Therefore, in this work just the high and the very low temperature crystallization peaks, their crystallinity and temperatures, are mainly discussed. The temperatures used are the peak temperatures.

For copolymers produced using ZN catalyst it was suggested<sup>[19]</sup> that the HTCP is due to the crystallization of high MM polymers having low branching content, whereas the LTCP is caused by low MM polymers with high branching content. The VLTCP was also referred to the highly branched low MM chains.<sup>[7–9]</sup> However, the branching distribution is homogeneous in materials synthesized by SS catalysis, without the localization of branch along the main chain as in ZN copolymers, and there should be no relation between MM and branch content. However, the experimental results uniquely indicate that there is still a low temperature crystallization process, leading to a VLTCP, as it is obvious from Figure 1. From this figure it is also clearly seen there is some dependence of  $T_{\text{VLTCP}}$  on  $C_{\text{common}}$  of the copolymers.

Indeed, Figure 2 shows the dependence of  $T_{\text{VLTCP}}$  on scanning rate for several selected samples with different  $C_{\text{common}}$  produced by ZN and SS type of catalyst. The temperature corresponding to the main

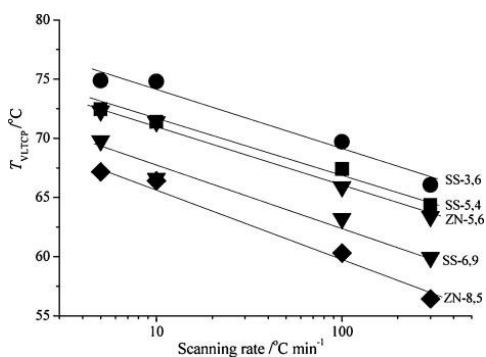


**Figure 2.**

Dependence of temperature of the VLTCP,  $T_{\text{VLTCP}}$  on scanning rate for selected SS and ZN based copolymers.

sharp crystallization peak ( $T_{\text{HTCP}}$ ) is rate-dependent, shifting to lower temperatures at higher cooling rates. The VLTCP also depends on scanning rate, as it is evident from the Figure 2: the higher the cooling rate the lower is the  $T_{\text{VLTCP}}$ .

This figure also shows the dependence of  $T_{\text{VLTCP}}$  on  $C_{\text{common}}$  of copolymers studied. It is seen, as  $C_{\text{common}}$  increases,  $T_{\text{VLTCP}}$  decreases for all scanning rates in agreement of the finding reported in works.<sup>[4,32]</sup> A decrease in  $T_{\text{VLTCP}}$  (and consequently in crystallite size) is expected with increasing the number of branches in a given chain due to the decreased number of crystallizable units. In our previous work<sup>[20]</sup> we detected that for 100 °C/min scanning rate the  $T_{\text{VLTCP}}$  vs.  $C_{\text{common}}$  for copolymers, having the same comonomer type, can be represented by a single line, irrespective of the catalyst type by which the materials were produced. The same behavior is observed in present study for all used scanning rates. Taking into account similar MM of the used materials (see Table 1), the conclusion can be reached that SS and ZN copolymers possess approximately the same thickness of crystallites associated with the VLTCP. Such behavior differs from that of HTCP. The temperatures of the main peak ( $T_{\text{HTCP}}$ ) for SS materials are essentially lower than for ZN materials if  $C_{\text{common}}$  is fixed, due to the structural heterogeneity of ZN copolymers both in inter- and intramolecular level.<sup>[20]</sup> Therefore, more and longer ethylene sequences are available in ZN materials leading to thicker lamellae and consequently to higher crystallization and melting temperatures according to the Thompson-Gibbs equation. Considering above mentioned difference in behavior of peak temperatures of HTCP and VLTCP with catalyst type, one can suggest that not only the presence of long/short ethylene sequences plays the role in thermal behavior of VLTCP.

An important element of phase structure is the degree of crystallinity. It should be noted here, that the partial degree of crystallinity calculated from VLTCP,  $X_{\text{VLTCP}}$ , displays scanning rate dependence.

Crystallinity value decreases with increasing scanning rate, and appear to reach a nearly constant value when scanning rate is higher than 100 °C/min. It is well known that at low scanning rate there is enough time for chains to be incorporated into the crystal lattice and more perfect and larger crystals are formed in comparison to those obtained at high cooling rate.

On further comparison between copolymers of different catalyst types, the interesting and unusual effect was found. For ZN materials the shape of the VLTCP is broader and less in magnitude than for SS materials having approximately the same comonomer content  $C_{\text{comon}}$  (see Figure 1). However, their peak crystallization temperatures  $T_{\text{VLTCP}}$  are similar. As is seen from the Figure 3 where the plots of  $X_{\text{VLTCP}}$  vs.  $T_{\text{VLTCP}}$  for all the copolymers are presented, in spite of identical  $T_{\text{VLTCP}}$ ,  $X_{\text{VLTCP}}$  is approximately two times higher for the SS copolymers compared to the ZN materials.

This figure also shows that  $X_{\text{VLTCP}}$  does not depend on  $T_{\text{VLTCP}}$  and comonomer type within the same type of catalyst. It should be noted that MM for all whole copolymers was approximately similar (see Table 1) and higher than 80 kg/mol. As it will be shown below for fractionated SS-6.9(6.2),  $X_{\text{VLTCP}}$  does not change with  $T_{\text{VLTCP}}$  if MM is higher than 40–50 kg/mol.

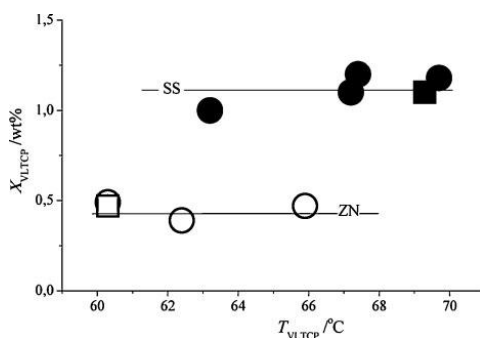


**Figure 3.**

Plots of VLTCP fractional crystallinity  $X_{\text{VLTCP}}$  vs. peak temperatures of VLTCP,  $T_{\text{VLTCP}}$ , for all used SS and ZN based ethylene/1-butene (squares) and ethylene/1-hexene (circles) copolymers. Scanning rate is 100 °C/min.

The independence of crystallinity on nature of the comonomer (except for methyl branches) is well known for the HTCP, because the degree of crystallinity mostly determined by the crystallizable sequence length distributions.<sup>[21,22]</sup> In its turn, the sequence distributions are influenced by the type of catalyst (e.g., ZN based systems result in broader distributions compared to SS based copolymers). It is evident, that homogeneous CD facilitates formation of the VLTCP. However, thermal analysis alone is not sufficient for explaining this behavior.

In Figure 4 the  $X_{\text{VLTCP}}$  is plotted as a function of  $C_{\text{comon}}$  for whole copolymers at two selected scanning rates. Data for compositional fractions of SS-6.9(6.2) are also presented in the Inset to the figure. It is evident that the introduction of the non-crystallizing co-units into the chain does not influence the level of  $X_{\text{VLTCP}}$  for whole copolymers. There is only slight tendency to decrease when  $C_{\text{comon}}$  is higher than 6 wt%. For compositional fractions having the same MM the decrease in  $X_{\text{VLTCP}}$  at  $C_{\text{comon}} > 6 \text{ wt}\%$  is a little bit steeper. It should be noted that the degree of crystallinity that is attained in an actual crystallization process is not a measure of the minimum or maximum sequence that

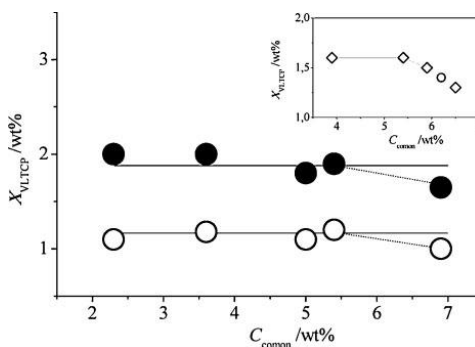


**Figure 4.**

Plots of VLTCP fractional crystallinity  $X_{\text{VLTCP}}$  vs.  $C_{\text{comon}}$  for all SS copolymers at 5 °C/min (solid circles) and 100 °C/min (open circles). The inset shows the plots  $X_{\text{VLTCP}}$  vs.  $C_{\text{comon}}$  for SS-6.9(6.2) fractions obtained by fractionation according to structure. The open circle in the Inset represents the whole unfractionated SS-6.9(6.2) copolymer at 100 °C/min.

participates in the crystallization, which is directly related to  $C_{\text{common}}$ . Rather it is the sum over all possibilities, which can lead to independence of crystallinity with  $C_{\text{common}}$  up to definite value.

Many properties of crystalline polymers are dependent on chain length.<sup>[11,13,23,24]</sup> The phase structure that defines the crystalline state can be varied by changing the MM and/or crystallization conditions.<sup>[13,25,26]</sup> Since random copolymers would be expected to behave in a similar manner, the influence of MM as an independent variable has to be investigated. The best way for studying the influence of MM on copolymer structure and properties is the fractionation of copolymer. However, for fractions of ZN copolymer the less branched fractions have the highest MM, and consequently, possible role of MM in influencing the thermal behavior and other structural properties are hard to recognize.

A definite influence of the MM on temperature and degree of crystallinity can be observed for SS based LLDPE fractions. For this purpose the whole copolymer SS-6.9(6.2) was fractionated by both MM and composition. Molar mass fractions have approximately constant branching content  $6.2 \pm 0.4$  wt%. Compositional fractions have the same  $MM = 100 \pm 2$  kg/mol and different comonomer content (see inset in Figure 4).

For all molar mass fractions, except the first one with  $MM = 5.1$  kg/mol, and all compositional fractions two (seldomly three) crystallization peaks in cooling thermograms were observed – HTCP and VLTCP (and seldomly LTCP). The first fraction does not display the VLTCP at all.

As has been stated in Ref. [11], the influence of MM on the crystallization/melting temperature of the HTCP is not specific to a given copolymer type but is a general phenomenon for all types of branches. It was observed that the influence of MM is much more marked for the copolymers, than for linear PE, especially in the range of MM between 5 and 100 kg/mol.<sup>[11,12]</sup> For our samples the  $T_{\text{HTCP}}$  (and also melting temperature  $T_m$ ) levels off

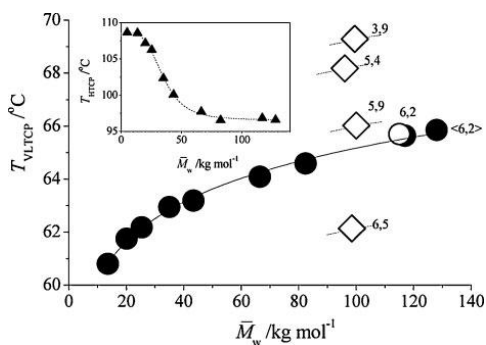


**Figure 5.**

Plot of peak temperatures  $T_{\text{VLTCP}}$  against  $\bar{M}_w$  for MM (solid circles) and compositional fractions of SS-6.9(6.2). The point for unfractionated, whole, copolymer is also included and marked as an open circle. The data labels represent the values of  $C_{\text{common}}$ . Inset shows the dependence of peak temperatures of the main crystallization peak  $T_{\text{HTCP}}$  vs.  $M_w$  for MM fractions of SS-6.9(6.2). Cooling rates are  $100$  °C/min.

above a molar mass of about 50–70 kg/mol as is seen from the inset to the Figure 5. R. Alamo et al. suggested<sup>[29,30]</sup> for fractions of ethylene/ $\alpha$ -olefin copolymers having constant branch content that the reduction of the  $T_{\text{HTCP}}$  (as well as  $T_m$ ) with increasing MM is a consequence of the decreased crystallite thickness of dominant lamellae. An explanation for the formation of smaller crystals with increasing MM is related to the slower crystallization kinetics due to the increase in entanglements. It has been demonstrated that not only crystallite thickness but also the nature of lamellae formed are affected by MM.<sup>[11]</sup> The lamellae that were long and straight at MM of 7 kg/mol have been observed to become short and highly segmented for MM of 70 kg/mol. The lateral dimensions of the lamellae are also decrease with MM.

The VLTCP behaves in absolutely opposite manner than HTCP does. As it is seen from Figure 5, while the  $T_{\text{HTCP}}$  decreases, the  $T_{\text{VLTCP}}$  grows with the increasing MM.  $T_{\text{VLTCP}}$  steeply increases in the range of MM  $5 \div 70$  kg/mol, and tends to level off at  $M_w > 70$  kg/mol.

The data for compositional fractions of SS-6.9(6.2) is also drawn in Figure 5. These plots indicate that the less branched

copolymers display the higher values of  $T_{\text{VLTCP}}$ . It is in agreement with the data for whole copolymers shown in Figures 1 and 2. Probably, the data for compositional fractions will generate a family of curves in plots  $T_{\text{VLTCP}}(M_w)$ , each dependent on  $C_{\text{common}}$  and having the functional form as presented for  $C_{\text{common}} = 6.2 \text{ wt\%}$  (drawn with solid line in Figure 5).

Since we have studied the influence of MM as an independent variable on the crystallization temperature of the VLTCP, we examined next its influence on the degree of crystallinity. Figure 6 represents the dependences of the degrees of overall ( $X_{\text{overall}}$ ) and partial VLTCP ( $X_{\text{VLTCP}}$ ) crystallinities of MM fractions of LLDPE SS-6.9(6.2) on  $M_w$ . For comparison in the given figure the data for MM fractions of HDPE are also included.

The decrease in the overall crystallinity of the fractions with MM agrees with that observed in works<sup>[13,29,30]</sup> for copolymer and linear polymer fractions. As it was supposed<sup>[11,29,30]</sup>, increasing MM increases the density of chain entanglements in the melt. It gives us the opportunity to suggest that increasing chain entanglements reduce the ability of chains to participate in the primary crystallization process at high temperature and to form large dominant crystallites. It results in a significant

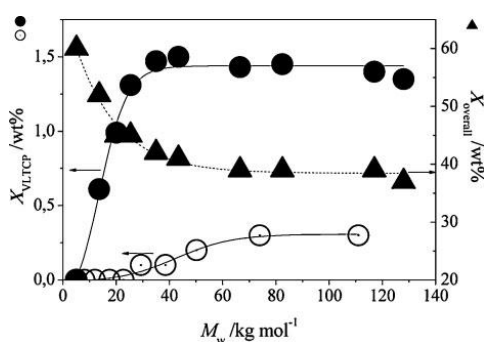


**Figure 6.**

Dependence of VLTCP crystallinity  $X_{\text{VLTCP}}$  (circles; left Y-axis) and overall crystallinity  $X_{\text{overall}}$  (triangles; right Y-axis) on  $M_w$  of SS-6.9(6.2) fractions (solid circles and triangles) and HDPE fractions (open circles), which were obtained by fractionation of whole polymers by molar mass. Cooling rate used is  $100 \text{ }^\circ\text{C}/\text{min}$ .

increase of the amorphous layer thickness.<sup>[33]</sup> This means that the proportion of non-crystallized chains in the amorphous regions, which further can participate in the secondary crystallization at lower crystallization temperature, increases. As it is evident from the Figure 6, in the range of MM from 5 up to 40–50 kg/mol  $X_{\text{VLTCP}}$  sharply increases. At  $MM > 40\text{--}50 \text{ kg/mol}$  the degree of crystallinity  $X_{\text{VLTCP}}$  does not change any more. It seems that the crystallinity of the VLTCP depends on whether the fraction of crystallizable sections of polymer macromolecules is incorporated into the main peak. Less incorporation will cause that VLTCP to grow in size or/and amount and reach some kind of equilibrium with dominant crystallites at critical  $MM \approx 40\text{--}50 \text{ kg/mol}$ . The most probable the value of critical MM is not a universal parameter and can differ with  $C_{\text{common}}$ , polydispersity of MM, etc.

Because there is some clear correlation of HTCP and VLTCP with MM, it can imply that these exotherms are consequences of melt topology defined by entanglements. However, not only the melt topology, but also the presence of the branch defines the existence and properties of VLTCP. Indeed, as it is clear seen from the comparison of the curves for LLDPE and HDPE fractions in Figure 6, for branched polymer the crystallinity of VLTCP,  $X_{\text{VLTCP}}$ , is in around 5 times higher than for approximately linear polymer (having a few branches).

An identical behavior as presented in Figure 6 for VLTCP is observed for the dependence of  $X_{\text{VLTCP}}$  on  $T_{\text{VLTCP}}$ .

On this stage of our investigation it is hard to suggest the morphology structure of VLTCP crystallites. According to the model for copolymer crystallization proposed in *Introduction* section, two distinct modes of crystallization can be a result of two vastly different morphologies operated in the copolymers – lamellae and bundled crystals.<sup>[8,9]</sup> Following this model the HTCP can be attributed to crystallization of polymer chains having high MM and low branching content, while VLTCP is

comprised of the less crystallizable, lower MM, more highly branched chains.<sup>[7]</sup> If there was the case, for ZN fractions the polymer molecules associated with the VLTCP would be eluted first in the temperature rising elution fractionation (TREF) process. Hence, fractions with higher MM would be expected to exhibit only the HTCP. However, as it was shown in work,<sup>[32]</sup> all the MM fractions of ZN copolymer, obtained by preparative TREF, displayed both the HTCP and the VLTCP. This suggests that the polymer chains associated with the HTCP are also related to the VLTCP. D. Wilfong suggested<sup>[32]</sup> that the HTCP and the VLTCP arise from the crystallization of ethylene rich and hexene/butene rich portions of the macromolecule, respectively. That is, the HTCP can be associated with crystallization of the linear portions of the macromolecule into the chain folded lamellae. Highly branched molecular segments of these lamellae are exiled to the interlamellar or interfacial regions of the crystal and crystallized upon further undercooling.

However, the origin and properties of VLTCP cannot be explained only in terms of the crystallization of ethylene sequences having a relatively short average sequence length. In this case the lamellae population formed at low temperature should be thin<sup>[8]</sup> and therefore should melt at considerable low temperature. This is not observed for the studied materials. Following the results, presented in Figure 6, the melt topology (in other words, entanglements) also has to be taken into account.

Unfortunately, only DSC experiments without any additional morphological study cannot provide us with full information about structure of crystallites formed at very-low crystallization temperature. It is the body of our upcoming study.

## Conclusion

On the basis of the DSC experimental results on low temperature crystallization behavior of SS and ZN based ethylene/ $\alpha$ -

olefin copolymers the following conclusions can be made:

- 1) DSC curves uniquely show the presence of an additional crystallization process occurring at very low temperatures around 60–75 °C. This VLTCP is much broader and less in magnitude than the main sharp HTCP. Moreover, the melting curves do not show any additional peaks clearly related to the VLTCP.
- 2) The peak crystallization temperature of the VLTCP,  $T_{\text{VLTCP}}$ , decreases both with increasing comonomer content (if MM is fixed) and with decreasing MM (when comonomer content is approximately constant). At the same time,  $T_{\text{VLTCP}}$  does not depend on catalyst type used for producing the copolymers.
- 3) Very slight dependences of the degree of crystallinity calculated from the VLTCP,  $X_{\text{VLTCP}}$ , on co-monomer content were observed at least within the studied range of magnitude. However, the  $X_{\text{VLTCP}}$  is independent of the chemical nature of the co-monomers (1-butene or 1-hexene).
- 4) It was observed that  $X_{\text{VLTCP}}$  sharply increases with MM in the range of 5–50 kg/mol, and levels off at higher MM. In the same time the crystallinity of HTCP decreases with MM in the range of 5–50 kg/mol. This implies a molecular correlation between the primary and secondary crystallization processes.
- 5) The  $X_{\text{VLTCP}}$  is in turn strongly influenced by the type of catalyst. For the SS materials the  $X_{\text{VLTCP}}$  is higher than for the ZN samples.

*Acknowledgements:* The Estonian Science Foundation is acknowledged for support under grant no. 6553 and Borealis Polymers OY Finland for structural characterization of the studied materials.

[1] E. T. Hsieh, C. C. Tso, J. D. Byers, T. W. Johnson, Q. Fu, S. Z. D. Cheng, *J. Macromol. Sci. - Phys.* **1997**, 36, 615.

[2] P. J. Flory, *Trans. Faraday Soc.* **1954**, 51, 848.

[3] I. A. Hussein, *J. Appl. Polym. Sci.* **2008**, 107, 2802.

- [4] V. B. F. Mathot, "Calorimetry and Thermal Analysis of Polymers", Hanser Publishers, Munich-Germany-Vienna-New York 1994.
- [5] V. B. F. Mathot, R. L. Scherrenberg, T. F. J. Pijpers, *Polymer* **1998**, 39, 4541.
- [6] J. Minick, A. Moet, A. Hiltner, E. Baer, S. P. Chum, *J. Appl. Polym. Sci.* **1995**, 58, 1371.
- [7] F. Zhang, J. Liu, F. Xie, Q. Fu, T. He, *J. Appl. Polym. Sci. Polym. Phys.* **2002**, 40, 822.
- [8] F. M. Mirabella, *J. Appl. Polym. Sci.* **2008**, 108, 987.
- [9] A. Alizadeh, L. Richrdson, J. Xu, S. McCartney, H. Marand, *Macromolecules* **1999**, 32, 622.
- [10] H. Teng, Y. Shi, X. Jin, *Polym. J.* **2003**, 35, 436.
- [11] R. G. Alamo, L. Mandelkern, *Thermochim. Acta* **1994**, 238, 155.
- [12] R. G. Alamo, E. K. M. Chan, L. Mandelkern, *Macromolecules* **1992**, 25, 6381.
- [13] E. Ergoz, J. G. Fatou, L. Mandelkern, *Macromolecules* **1972**, 5, 147.
- [14] K. Ziegler, E. Holzkamp, H. Breil, H. Martin, *Angew. Chem.* **1955**, 541 G. Natta, *J. Polym. Sci.* **1955**, 16, 143.
- [15] P. Pino, A. Oschwald, F. Ciardelli, C. Carlini, E. Chiellini, in: "Coordination Polymerization of  $\alpha$ -Olefins", J. C. W. Chien Ed., Elsevier, New York 1975, p. 25.
- [16] W. Holtrup, *Makromol. Chem.* **1977**, 178, 2335.
- [17] A. Lehtinen, R. Paukeri, *Macromol. Chem. Phys.* **1994**, 195, 1539.
- [18] T. Usami, Sh. Takayama, *Polym. J.* **1984**, 10, 731.
- [19] D. Wilfong, G. W. Knight, *J. Polym. Sci., Polym. Phys.* **1990**, 28, 861.
- [20] T. Poltimäe, E. V. Tarasova, A. Krumme, A. Lehtinen, A. Viikna, *Proceedings of the Estonian Academy of Sciences, in press.*
- [21] M. Kim, P. J. Philips, *J. Appl. Polym. Sci.* **1998**, 70, 1893.
- [22] R. G. Alamo, L. Mandelkern, *Macromolecules* **1989**, 22, 1273.
- [23] L. Mandelkern, *J. Phys. Chem.* **1971**, 75, 3909.
- [24] L. Mandelkern, R. G. Alamo, M. A. Kennedy, *Macromolecules* **1990**, 23, 4721.
- [25] L. Mandelkern, *Acc. Chem. Res.* **1990**, 23, 380.
- [26] U. W. Gedde, J. F. Janson, G. Liljenstrom, S. Eklund, *Polym. Eng. Sci.* **1988**, 28, 1289.
- [27] R. G. Alamo, E. K. M. Chan, L. Mandelkern, I. G. Voigt-Martin, *Macromolecules* **1992**, 25, 6381.
- [28] R. G. Alamo, L. Mandelkern, *Macromolecules* **1991**, 24, 6480.
- [29] L. Mandelkern, *J. Phys. Chem.* **1971**, 75, 3909.
- [30] C. G. Vonk, H. Reynaers, *Polym. Commun.* **1990**, 31, 190.
- [31] M. Peeters, B. Goderis, C. Vonk, H. Reynaers, V. Mathot, *J. Polym. Sci. Polym. Phys.* **1997**, 35, 2689.
- [32] D. L. Wilfong, *Polym. Mater. Sci. Eng.* **1989**, 61, 743.

### PAPER III

E. Tarasova, T. Poltimäe, A. Krumme, A. Lehtinen, A. Viikna. 2011. Triple crystallization behavior of fractionated ethylene/ $\alpha$ -olefin copolymers of different catalyst type. *Journal of Polymer Research*, 18 (2), 207-216.



# Triple crystallization behavior of fractionated ethylene/ $\alpha$ -olefin copolymers of different catalyst type

E. Tarasova · T. Poltimäe · A. Krumme · A. Lehtinen · A. Viikna

Received: 22 October 2009 / Accepted: 10 February 2010  
© Springer Science+Business Media B.V. 2010

**Abstract** Non-isothermal crystallization processes in fractions of Ziegler-Natta (ZN) and single site (SS) based ethylene/1-butene and ethylene/1-hexene copolymers have been studied by differential scanning calorimetry (DSC). Fractionation of used copolymers was done according to molar mass (MM) and composition (comonomer content). It was observed in DSC scans that for fractions with high MM (larger than 10 kg/mol) in addition to the main high-temperature crystallization peak (HTCP), a very-low temperature crystallization peak (VLTCP) is present at temperatures in between 60–75 °C. Such peak is absent for the first fractions having very-low MM. The partial crystallinity and peak temperatures, obtained from VLTCP, increase with MM and level off at MM around 60–100 kg/mol. It was found that the crystallinity as related to the area of the VLTCP is catalyst type dependent, and is higher for the SS catalyst compared to the ZN. Peak temperature of VLTCP linearly decreases with increasing comonomer content at fixed MM while the partial crystallinity practically does not change with comonomer content.

**Keywords** Linear low-density polyethylene · Ethylene/ $\alpha$ -olefins · Fractions · Very-low temperature crystallization peak · Differential scanning calorimetry

## Introduction

Despite the vast amount of experimental data and thermodynamic as well as kinetic considerations, polyethylene crystallization continues to be an attractive field of research. This is illustrated by recent landmark with industrial impact—introduction of heterogeneous and homogeneous copolymers of ethylene with  $\alpha$ -olefins [1–3]. The later materials experience a revival as a result of the need to fill the gap between linear and high-density polyethylenes (LPE and HDPE, respectively) and low-density polyethylenes (LDPE). Typical commercial samples, prepared by Ziegler-Natta (ZN) polymerization, are heterogeneous copolymers of ethylene and 1-butene, 1-hexene, or 1-octene. Such samples appear to be complex blends with a wide inter- and intramolecular distribution of the side chains and are generally termed linear low-density polyethylenes (LLDPE) [1–4]. It is well known that the chain microstructure, resulting from the synthesis, determines, together with the crystallization conditions, the morphology. Hence by changing the chain microstructure (in other words, selection of suitable catalyst), new and improved properties can be obtained, as evidenced by the recent interest in using single site (SS) catalysts [5–8]. Such catalyst gives a possibility to change the molar mass (MM) and the short chain branching (SCB) distributions independently.

Differential scanning calorimetry (DSC) has been one of the main techniques used to study melting and crystallization behavior of polymers. For heterogeneous Ziegler-Natta (ZN) and homogeneous SS ethylene/ $\alpha$ -olefin copolymers the existence of a double crystallization mechanism: a sharp, high temperature crystallization peak (HTCP) and a broad low-temperature crystallization peak (LTCP) closely located to HTCP, is well known and widely studied [6–13].

However, during non-isothermal treatment in ethylene/ $\alpha$ -olefin copolymers a third very-low temperature crystal-

---

E. Tarasova (✉) · T. Poltimäe · A. Krumme · A. Viikna  
Tallinn University of Technology,  
Ehitajate tee 5,  
19086 Tallinn, Estonia  
e-mail: elvira.tarasova@ttu.ee

A. Lehtinen  
Borealis Polymers OY,  
P.O. Box 330, FIN-06101 Porvoo, Finland

lization peak (VLTCP) is detected. This peak was observed previously by several authors [6, 8, 12, 13, 28]. Unfortunately only a few papers are devoted directly to this phenomenon and it is still not satisfactorily studied. Alizadeh et al. [12] studied the copolymers of polyethylenes and also observed the third crystallization peak in DSC exotherms during the non-isothermal scan. However, to understand the origin of this VLTCP they used an isothermal treatment. After annealing at certain temperature they observed two melting peaks in endotherms: high temperature peak and low temperature peak, located just above the annealing temperature. The lower temperature melting peak was addressed by authors to correspond to the VLTCP. The similar isothermal behavior was detected in works [13–18] for polyethylene copolymers. All authors [13–18] suggested that low temperature melting peak is not related to melting-recrystallization-remelting process. Therefore they conclude that under isothermal treatment two crystal populations are formed in polyolefins. Some of the authors suggested that one of the populations is lamellae crystals formed from longest sequence lengths and another is fringed micelles [14] or small lamellae [11] formed from the shortest sequence lengths. Another authors explained the high-temperature isothermal crystallization and double melting behavior of a copolymer by a reduction in spherulitic growth rate associated with the creation of an intermediate disordered phase that only in a secondary stage converts into orthorhombic material. None of these authors, excluding Alizadeh et al. [12], claimed that the lower melting peak obtained during annealing is corresponded to the VLTCP, which is clearly observed only under non-isothermal conditions. As it is well known, due to possible time for reorganization and thickening under isothermal treatment the crystallization mechanism and the morphology of isothermally crystallized polymers are different from non-isothermal. Therefore the origin of the VLTCP is still an open question.

By our knowledge all previous studies were mostly done for whole unfractionated copolymers with wide MM (MMD) and short chain branching (SCBD) distributions and with a focus on the influence of SCBD on the melting and crystallization of LLDPEs [5–7, 12, 13, 19].

It is well known that many properties of crystalline random copolymers are very dependent MM and crystallization conditions [18–21]. That is why the influence of MM on the behavior of VLTCP under non-isothermal conditions has to be studied. Probably the main reason behind that is that it is hard to find commercial PEs with different MM but with the same comonomer content. Consequently, to get appropriate properties of copolymers, along with the sequence distribution and comonomer content ( $C_{\text{com}}$ ), the MM and crystallization condition have to be specified and independently assessed. Commercial

LLDPEs are complex blends of polyethylenes involving strongly heterogeneous copolymers with a very wide MMD containing low as well as high density like material. The need to work with better defined materials could be reached only by a strong effort in fractionation. Ziegler-Natta catalyzed LLDPEs and its fractions are heterogeneous with respect to inter- and intramolecular distribution of the side chain branches, and MM and short chain branching content are intimately related. Therefore it is not possible to study the effect of the different molecular parameters on the crystallization independently. However, SS copolymers of ethylene and several  $\alpha$ -olefins are homogeneous in that the comonomer content does not vary with MM; low and high MM fractions have essentially the same comonomer content.

It should be stated here that we define primary crystallization as the stage that ends at spherulitic impingement (i.e., when lamellar growth is no longer taking place from the melt). Since the morphology resulting from primary crystallization is kinetically controlled, it is not surprising to observe that the degree of crystallinity at the end of this stage is significantly below unity [18]. We then define the term secondary crystallization as including any process that leads to further increase in crystallinity and that is not associated with a main chain folding lamellar growth mechanism from the melt. In summary, secondary crystallization will occur below the primary crystallization temperature to an extent that decreases with decreasing temperature.

From our point of view, the behavior of VLTCP in copolymers has to be investigated more carefully because there is a possibility of correlation between this *secondary crystallization process* and the mechanical properties of the samples. The present work reports on the crystallization behavior of fractionated heterogeneous (ZN) and homogeneous (SS) copolymers of ethylene with 1-butene and 1-hexene, and fractionated high density polyethylenes. The major focus is to examine the effect of structure of materials and their MM (which has not been investigated with due attention before), co-monomer type and its content on the behavior of the VLTCP. One might be tempted to explain mentioned above triple crystallization behavior by a mechanism of fractionation during primary crystallization. To refute this explanation the SS and ZN catalyzed LLDPEs as well as ZN HDPEs were fractionated by MM and composition. Fractionation also gives the opportunity to analyze the contribution of MM and  $C_{\text{com}}$  as independent variables.

Running ahead, let us say here that the level of VLTCP crystallinity is around 2–3 wt% and if VLTCP crystallites have bundle-like structure as we suggest, the direct observation of morphology of VLTCP crystallites by such usually used for morphological study methods as atomic force microscopy, transmission electron microscopy, small

angle light scattering etc. is hardly possible in principal. Therefore, DSC seems to be the most convenient and sensitive method for studying the properties of crystallites associated with VLTCP. And mostly on the base of DSC data we are able to do some predictions on morphology of VLTCP crystallites. To our knowledge, this is at least one of the first detailed experimental attempts to study the thermal properties of crystallites associated with the VLTCP.

The additional discoveries of the present work are the observation and elucidation of the effect of MM, comonomer content, catalyst type and polymer structure on the properties of VLTCP.

## Experimental part

### Materials

The LLDPEs used in this study were commercial ethylene/1-butene and ethylene/1-hexene whole copolymers, produced by ZN [22] or SS [23] catalyst types. The molecular characteristics of the studied fractionated ethylene copolymers are listed in Tables 1 and 2. The samples are identified with the initials SS or ZN followed by a number corresponding to the comonomer content,  $C_{\text{com}}$ , expressed in weight percent (wt%). All whole materials (obtained in pellet form) had about the same density and weight average MM ( $\overline{M}_w$ ). All the materials presented in Tables 1 and 2 were fractionated to get the materials with the narrower MMD and SCBD. However, for fractions of ZN copolymer the less branched fractions have the highest MM, and consequently, possible role of MM in influencing the thermal behavior and other structural properties are hard

to recognize. A definite influence of the MM on crystallization temperature and degree of crystallinity can be observed for SS based LLDPE fractions.

All materials used in present study were fractionated according to MM. Moreover, two samples (SS-6.9 and ZN-7.6) were additionally fractionated according to composition (i.e. SCB). All the fractionations were carried out on polymer in powder form. For this purpose, the sample pellets were dissolved in xylene. The solution was cooled to room temperature and the polymer was precipitated in acetone, filtered and dried at room temperature. Fractionation by MM was carried out according to the Holtrup technique which is a solvent/non-solvent extraction [24]. In the experiment 10 g of polymer powder was extracted in a solvent/non-solvent mixture of xylene and ethylene glycol mono-ethyl ether in different ratios at 116 °C. Dissolution time of 10 min was used at each dissolution step, and 13 fractions were collected. Fractionation according to short chain branching (composition) was carried out using multiple solvent extraction technique [25]. The sample amount fractionated was about 15 g and dissolution time was 30 min. The solvents used in the fractionation were: n-pentane at 35 °C, n-hexane at 65 °C, n-heptane at 75 °C and 90 °C, n-octane at 100 °C, toluene at 105 °C and xylene at 130 °C. The first two fractions were separated by evaporation of the solvent in a rotavapor and the other ones by precipitation in acetone.

The MM fractions of samples have similar polydispersity  $\overline{M}_w/\overline{M}_n$ . As an illustration, in the Fig. 1 the selected MMD curves for SS material are shown. For MM fractions of SS materials the comonomer content  $C_{\text{com}}$  was approximately fixed while for ZN materials  $C_{\text{com}}$  varied with MM (see Tables 1 and 2). The  $C_{\text{com}}$  for the first four-five fractions was not analyzed due to a small amount of

**Table 1** Molecular characteristics of single site (SS) based molar mass and compositional fractions of LLDPEs

| Sample                | SS-5.4(5.2) (hexene) |                      | SS-6.9(6.2) (hexene) |                      | Compos. fractions |                      |
|-----------------------|----------------------|----------------------|----------------------|----------------------|-------------------|----------------------|
|                       | MM fractions         |                      | MM fractions         |                      | Compos. fractions |                      |
| Fraction number whole | $M_w$ kg/mol         | $C_{\text{com}}$ wt% | $M_w$ kg/mol         | $C_{\text{com}}$ wt% | $M_w$ kg/mol      | $C_{\text{com}}$ wt% |
|                       | 84                   | 5.4/5.2              | 115                  | 6.9/6.2              | 115               | 6.9/6.2              |
| 1                     | 9.4                  | NA                   | 5.1                  | NA                   | NA                | NA                   |
| 2                     | 14.2                 | NA                   | 13.6                 | NA                   | 56.1              | 9.2                  |
| 3                     | 23.1                 | NA                   | 20.1                 | NA                   | 98.5              | 6.5                  |
| 4                     | 32.4                 | NA                   | 25.4                 | NA                   | 100               | 5.9                  |
| 5                     | 44                   | 5.2                  | 35                   | 5.6                  | 96                | 5.4                  |
| 6                     | 54                   | 5.2                  | 43.4                 | 5.8                  | 99.5              | 3.9                  |
| 7                     | 78.8                 | 5.1                  | 66.5                 | 6.3                  | –                 | –                    |
| 8                     | 89.3                 | 5.1                  | 82.4                 | 6.2                  | –                 | –                    |
| 9                     | 86.1                 | 5.2                  | 128                  | 6.2                  | –                 | –                    |
| 10                    | 90                   | 5.2                  | 117                  | 6.4                  | –                 | –                    |
| 11                    | 90.2                 | 5.1                  | –                    | –                    | –                 | –                    |

NA means 'not analysed'

**Table 2** Molecular characteristics of Ziegler-Natta (ZN) based molar mass and compositional fractions of LLDPEs and HDPE

| Sample                | ZN-7.2 (butene) |               | ZN-7.6(7.2) (hexene) |               |                   |               | ZN-0 (HDPE)  |               |
|-----------------------|-----------------|---------------|----------------------|---------------|-------------------|---------------|--------------|---------------|
|                       | MM fractions    |               | MM fractions         |               | Compos. fractions |               | MM fractions |               |
|                       | $M_w$ kg/mol    | $C_{com}$ wt% | $M_w$ kg/mol         | $C_{com}$ wt% | $M_w$ kg/mol      | $C_{com}$ wt% | $M_w$ kg/mol | $C_{com}$ wt% |
| Fraction number whole | 122             | 7.2           | 125                  | 7.6/7.2       | 125               | 7.6/7.2       | 95           | 0             |
| 1                     | 2.1             | NA            | 5.1                  | NA            | 61                | 27.8          | 4.8          | 0             |
| 2                     | 5.3             | NA            | 8.1                  | NA            | 66.9              | 18.9          | 8.1          | 0             |
| 3                     | 9.1             | NA            | 14.3                 | NA            | 92.9              | 12.3          | 12           | 0             |
| 4                     | NA              | NA            | 17.5                 | NA            | 128               | 4.5           | 17.5         | 0             |
| 5                     | NA              | NA            | 24                   | NA            | 136               | 3.2           | 22.7         | 0             |
| 6                     | NA              | NA            | 33                   | 9.3           | 232               | 1.3           | 29.3         | 0             |
| 7                     | 29              | NA            | 42.7                 | 7.9           | 227               | 1.5           | 38.5         | 0             |
| 8                     | 35.8            | NA            | 53                   | 6.9           | –                 | –             | 50.2         | 0             |
| 9                     | 125             | NA            | 78.7                 | 6.2           | –                 | –             | 73.9         | 0             |
| 10                    | –               | –             | 152                  | 5.9           | –                 | –             | 111          | 0             |
| 11                    | –               | –             | 303                  | 5.7           | –                 | –             | 211          | 0             |
| 12                    | –               | –             | 207                  | 5.1           | –                 | –             | 571          | 0             |
| 13                    | –               | –             | 194                  | 5.2           | –                 | –             | 606          | 0             |

NA means 'not analysed'

samples. The compositional SS fractions used in this work have about the same  $\overline{M}_w$  and polydispersity.

As it follows from the fractionation description the whole SS-6.9, SS-5.4 and ZN-7.6 were dissolved, dried and obtained in powder form. Probably, due to the dissimilarity in material form (pellet or powder) there was a difference in melting and crystallization temperatures as well as in the degree of crystallinity of pellet and powder materials. Moreover, the value of averaged  $C_{com}$  for powder samples was lower than for pellets. Therefore, such materials were identified as SS-6.9(6.2), SS-5.4(5.2) and ZN-7.6(7.2), where values in brackets are for powder form of materials.

For comparison with LLDPE fractions the commercial Ziegler-Natta catalysed high-density polyethylene (ZN-0) with  $\overline{M}_w=94500$  and polydispersity  $\overline{M}_w/\overline{M}_n=8.3$  was fractionated according to MM. The fractions of HDPE have approximately similar polydispersity equal 1.7 in average.

## Methods

Perkin Elmer Diamond differential scanning calorimeter (DSC) and DSC-7 were used for thermal analysis at scanning rates of 10 and 100 °C/min. Temperature and heat flow calibrations have been done by indium and tin at all applied heating rates. In Diamond DSC helium was used as furnace purge gas and in DSC-7 nitrogen was used. 55 × 65 × 1 mm plates were pressed from the materials in pellet form at 180 °C and cooled to room temperature. For fractions powders were manually compacted by pressure at

room temperature. To avoid differences in melting and crystallization temperatures caused by variation in sample weight, a sample mass of 1.00 ± 0.02 mg was used in all DSC experiments. Flat samples were packed into aluminum foil to maximize thermal contact between sample and calorimetric furnace. During the non-isothermal measurement, the sample was first held at 180 °C for 5 min for deleting its thermal history. Then it was cooled to 0 °C (–50 °C for highly branched samples) at 100 °C/min scanning rate, held at this temperature for 5 min and then heated to 180 °C at the same rate. Overall degree of

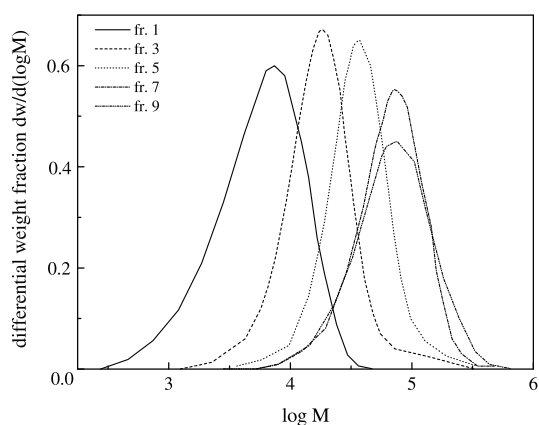


**Fig. 1** Differential molar mass distributions of the selected fractions of SS-5.4(5.2) sample obtained by SEC

crystallinity  $X_{\text{overall}}$  was calculated from the heat of fusion using the peak area determination method, i.e., by integration of the area under the normalized melting peak after subtraction of an arbitrary straight baseline; a value of  $\Delta H_{\text{m}}^{\circ} = 293 \text{ J/g}$  was used as the reference melting enthalpy of fusion for 100% crystalline PE. The partial degree of crystallinity estimated from the area of VLTCP,  $X_{\text{VLTCP}}$ , was obtained from cooling traces by dividing the crystallization enthalpy of VLTCP by  $\Delta H_{\text{m}}^{\circ}$ .

MM averages and MMD were determined by size exclusion chromatography (SEC) using 1,2,4-trichlorobenzene (TCB) as eluent at 140 °C. Comonomer contents were measured by Fourier transform infrared spectroscopy (FTIR) [26].

## Results and discussions

In our previous work [27] we studied by DSC the whole unfractionated copolymers with different  $C_{\text{com}}$  and at different scanning rates, namely 5, 10, 100 and 300 °C/min. It was found that in ethylene/ $\alpha$ -olefins at all used scanning rates three peaks of crystallization (HTCP, LTCP, and a small VLTCP) are observed and the character of dependences on the same molecular parameters is similar for all scanning rates.

As it has been found in our previous work [27] the area of VLTCP increases with decreasing scanning rate and the shape of this peak broadens. The higher the scanning rate the better is the resolution of VLTCP: the peak becomes sharper and higher. It allows obtaining the more precise values of  $X_{\text{VLTCP}}$  and peak temperatures of VLTCP. Therefore, 100 °C/min cooling/heating rate was chosen in present study for all non-isothermal experiments.

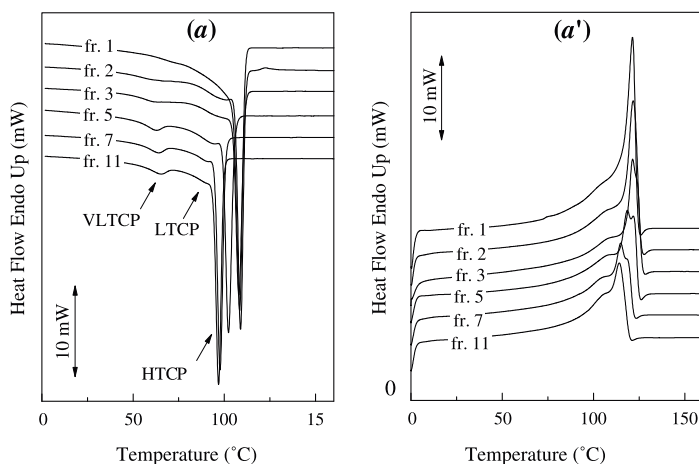
Many properties of crystalline polymers are dependent on chain length [18, 21, 28–31]. The phase structure that defines the crystalline state can be varied by changing the MM and/or crystallization conditions [21, 32–37]. Since random copolymers would be expected to behave in a similar manner, the influence of MM as an independent variable has to be investigated.

The crystallization and melting behaviour of the selected SS molar mass fractions are shown in Fig. 2. As it is clear seen from the figure, no VLTCP is detected for the first fractions of SS. The similar behaviour is observed for ZN samples. They have mostly only one main peak—HTCP. However, for the next MM fractions and all compositional fractions (not presented in the Fig. 2, but shown in Fig. 5) three crystallization peaks in cooling thermograms are observed—HTCP, LTCP and VLTCP. The crystallization behaviours of the SS and ZN fractions are rather similar. The important finding is that the identical crystallization behaviour is also detected for MM fractions of HDPE, namely ZN-0.

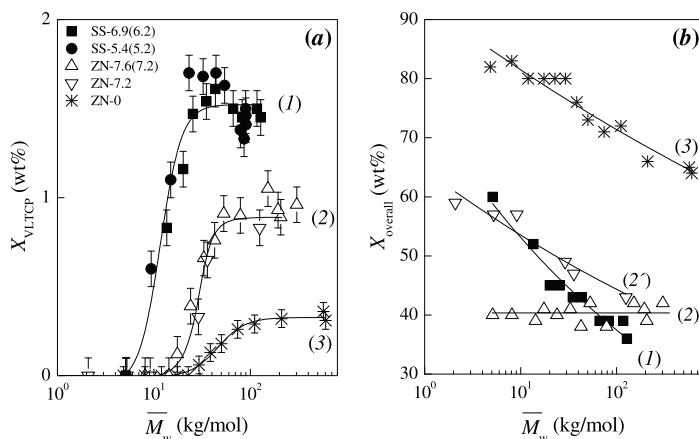
Nevertheless, the melting curves of the LLDPE materials and HDPE as well have only one or seldom two endothermic peaks corresponding to primary crystallization process presented by HTCP and LTCP. No additional very low temperature peaks unambiguously related to the VLTCP were detected, as it is obvious from the Fig. 2a and a'. Due to this fact no melting temperature and partial crystallinity directly corresponding to the VLTCP can be obtained from the melting traces. Therefore, in this work just the high and the very low temperature crystallization peaks, their crystallinities and temperatures, are mainly discussed. The temperatures used are the peak temperatures.

Figure 3 represents the dependences of the degrees of overall ( $X_{\text{overall}}$ ) and partial VLTCP ( $X_{\text{VLTCP}}$ ) crystallinities

**Fig. 2** Selected heat flow curves for MM fractions of SS-6.9(6.2) (a, a'). The numbers of fractions are listed in the plots



**Fig. 3** Dependence of VLTCP crystallinity  $X_{\text{VLTCP}}$  (a) and overall crystallinity  $X_{\text{overall}}$  (b) on  $\overline{M}_w$  of both SS and ZN fractions, which were obtained by fractionation of whole polymers by molar mass. (1)—SS samples; (2) and (2')—ZN copolymers; (3)—ZN HDPE. Cooling rate used is 100 °C/min



of MM fractions for all the samples on  $\overline{M}_w$ . The decrease in  $X_{\text{overall}}$  of the fractions with MM is well-known [21, 38, 40]. Increasing MM increases the density of chain entanglements in the melt [18–20, 40–43]. It gives us the opportunity to suggest that increasing chain entanglements reduce the ability of chains to participate in the primary crystallization process at high temperature and as a result restrict the formation of large dominant crystallites.

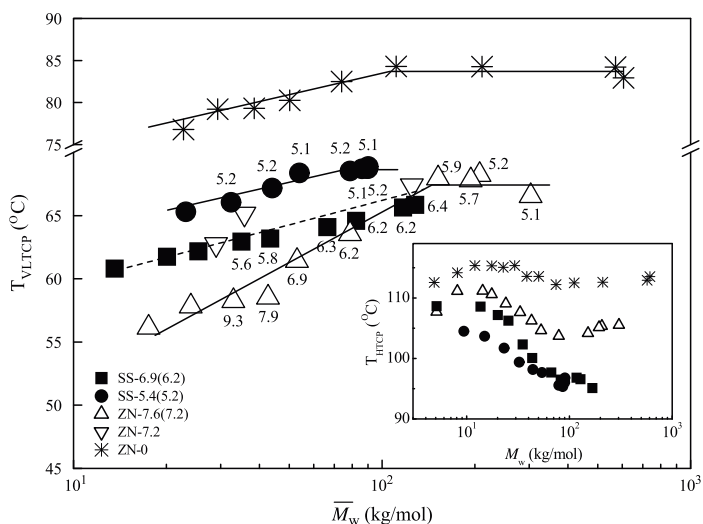
This means that the proportion of non-crystallized chains in the amorphous regions, which further can participate in the secondary crystallization at lower temperature, increases. As it is evident from the Fig. 3, in the range of MM from 5 up to 60–100 kg/mol  $X_{\text{VLTCP}}$  sharply increases. At  $\overline{M}_w > 60$ –100 kg/mol, named as critical MM, the degree of crystallinity  $X_{\text{VLTCP}}$  does not change any more or starts to decrease slightly. Everyone can see the difference in maxima level of  $X_{\text{VLTCP}}$  for LLDPEs catalyzed by Ziegler-Natta or single site techniques. Moreover, within the same catalyst type (ZN) there is an essential difference in  $X_{\text{VLTCP}}$  values for different material types—LLDPE or HDPE. It is well known that in case of HDPE in comparison with LLDPE the major part of chains takes part in primary crystallization process that gives the value of overall crystallinity for HDPE more than 70% against 30–60% for LLDPE. Therefore we can conclude that the value of critical MM and maximum level of  $X_{\text{VLTCP}}$  are sensitive to polymer (LLDPE or HDPE) and catalyst (ZN or SS) types. The most probable that the VLTCP crystallinity depends on whether the fraction of crystallizable sections of polymer macromolecules is incorporated into the primary crystallization process associated with HTCP. Less incorporation in primary crystallization will cause crystallites, creating the VLTCP, to grow in size or/and amount and reach some kind of equilibrium with dominant crystallites at critical  $\overline{M}_w \approx 60$ –100 kg/mol.

An identical behavior as presented in Fig. 3 is observed for the dependence of  $X_{\text{VLTCP}}$  on  $T_{\text{VLTCP}}$ .

Since we have studied the influence of MM as an independent variable on the degree of crystallinity, we examined next its influence on the crystallization temperature. We have got qualitatively and quantitatively the same set of results for 1-hexene and 1-butene copolymers. For the lowest MM fractions as seen from the inset to the Fig. 4, crystallization temperature of the HTCP,  $T_{\text{HTCP}}$ , slightly increases with MM due to the decrease in number of end-groups per 1000 C [8]. It should be noted here that the VLTCP is not detected for such fractions. Further, after an initial expected increase the  $T_{\text{HTCP}}$  decreases at  $\overline{M}_w \approx 10$ –20 kg/mol to become more or less constant at  $\overline{M}_w \approx 60$ –100 kg/mol. The reduction of the  $T_{\text{HTCP}}$  with increasing MM is a consequence of the decreased crystallite thickness of dominant lamellae [8, 20, 38–43]. An explanation for the formation of smaller crystals with increasing MM is related to the slower crystallization rates due to the increase in entanglements. As the number of intermolecular entanglements increases with the increase in MM, the mobility of segments is increasingly hindered. In this case, a higher undercooling is required to produce a larger driving force for crystallization to overcome the influence of entanglements, and then the crystallization temperature shifts to lower temperature [43].

VLTCP behaves in opposite manner than HTCP: while the  $T_{\text{HTCP}}$  decreases, the  $T_{\text{VLTCP}}$  grows with the increasing MM (see Fig. 4). According to Smith and Manley [44], for quenched PE fractions with  $\overline{M}_w = 4$  kg/mol, that is MM above which the entanglements are operative, the chains are extended. In the domain  $4 < \overline{M}_w < 100$  kg/mol the amorphous phase increases with the MM. For monodisperse and polydisperse samples of MM greater than 100 kg/mol, the long period and the crystalline lamellar thickness do not

**Fig. 4** Plot of peak temperatures  $T_{VLTCP}$  against  $\overline{M}_w$  for MM fractions of SS and ZN fractions. The data labels represent the values of  $C_{com}$ . Inset shows the dependence of peak temperatures of the main high temperature crystallization peak  $T_{HTCP}$  vs.  $\overline{M}_w$  for the same fractions. Cooling rates are 100 °C/min



change any more [45, 46]. Our results is in accordance with this finding. Indeed,  $T_{VLTCP}$  steeply increases in the range of MM 10–100 kg/mol, and tends to level off at  $\overline{M}_w = 60$ –100 kg/mol. Within the same catalyst and polymer types the value of critical MM depends on polydispersity: the larger is the PDI the higher is the value of critical MM.

When  $MM < 60$ –100 kg/mol the slope of the dependence  $T_{VLTCP}(\overline{M}_w)$  is defined by  $C_{com}$ . It is obvious for ZN-7.6 (7.2) sample, in which the less branched fractions have higher MM (see Table 2), that  $T_{VLTCP}$  decreases with  $\overline{M}_w$  steeper than that of SS-5.4(5.2) fractions, having the same comonomer contents.

The relationship between the crystallization peak temperatures and the comonomer content for the HTCP and VLTCP is shown in Fig. 5 for ZN and SS compositional fractions. As an illustration, the heat flow curves for compositional ZN-7.6(7.2) fractions are shown in Fig. 6. At fixed branch content the values of  $T_{VLTCP}$ , as well as  $T_{HTCP}$ , are identical for the SS and ZN fractions. Increase in  $C_{com}$  leads to decreasing of the peak temperatures. The interesting and important fact is that the temperature interval between HTCP and VLTCP remains constant. Thus, crystallization of the macromolecules associated with the VLTCP is influenced by the prior crystallization of macromolecules represented by the HTCP.

Moreover, the plots in Fig. 5 indicate that the less branched copolymers display the higher values of  $T_{VLTCP}$  and extrapolation of  $T_{VLTCP}$  to  $C_{com} = 0$  gives the value of  $T_{VLTCP} = 80$  °C, which is typical for  $T_{VLTCP}$  of ZN-0 (HDPE).

In spite of  $T_{VLTCP}$ , which is presumably related to the crystallite thickness of the very-low temperature crystallized structures, decreases with increasing  $C_{com}$ , the  $X_{VLTCP}$  does not show any systematical change with  $C_{com}$ . In Fig. 7

the  $X_{VLTCP}$  is plotted as a function of  $C_{com}$  for compositional fractions of SS-6.9(6.2) and ZN-7.6(7.2) copolymers. It is evident that the introduction of the non-crystallizing co-units into the chain does not influence strongly the level of  $X_{VLTCP}$  within the same type of catalyst. This fact is understandable if we take into account that the degree of crystallinity that is attained in an actual crystallization process is not a measure of the minimum or maximum sequence that participates in the crystallization, which is directly related to  $C_{com}$ . Rather it is the sum over all possibilities, which can lead to independence of crystallinity with  $C_{com}$  up to a definite value.

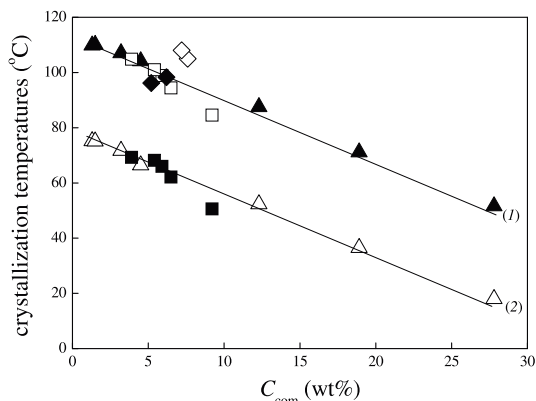
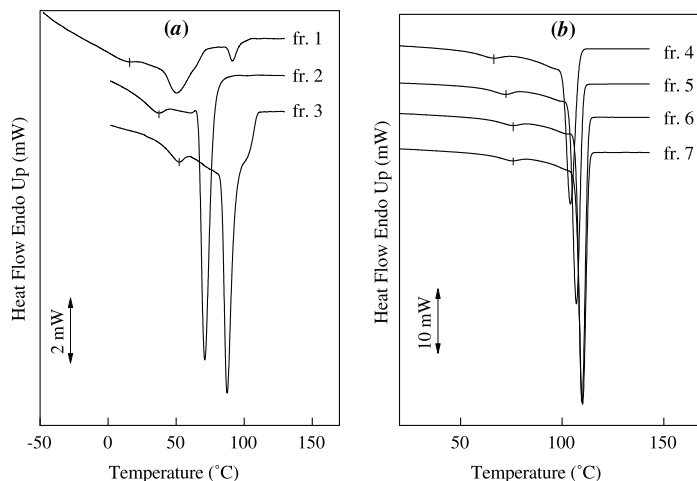


**Fig. 5** Crystallization peak temperature of the HTCP (1) and VLTCP (2) as a function of comonomer content  $C_{com}$  for the compositional SS-6.9(6.2) (solid and open squares) and ZN-7.6(7.2) (solid and open triangles) fractions. The data for whole fluffy SS-6.9(6.2) (solid rhombs) and fluffy ZN-7.6(7.2) (open rhombs) copolymers are also presented in the Figure

**Fig. 6** DSC cooling thermograms of compositional ZN-7.6 (7.2) fractions. Numbers of fractions are listed in the figure



The origin of VLTCP still remains a discussed problem. For copolymers produced using ZN catalyst the most popular point of view is that the molecular fractionation or segregation of macromolecules by MM during crystallization implies that the HTCP is due to the crystallization of high MM macromolecules having low branching content, whereas VLTCP can be comprised of the less crystallizable, lower MM, more highly branched polymer chains [10–19, 30]. However, based on our results we can say—if there was the case, for ZN fractions the polymer molecules associated with the VLTCP would be mostly present in the first fractions. Hence, fractions with higher MM would be expected to exhibit only the HTCP. However, as it is seen from the Figs. 1, 2 and 5 the first MM fractions of ZN copolymer having low MM and high  $C_{\text{com}}$  do not show any VLTCP at all. The fractions with higher MM display both the HTCP and the VLTCP. This suggests that the polymer chains associated with the HTCP are also related to the VLTCP, which is in agreement with the results on crystallization temperatures (see comments to the Fig. 4). Moreover, everyone can see from Fig. 5 that even the first highly branched compositional fractions, which presumably should have only VLTCP, demonstrate the HTCP along with VLTCP in DSC thermograms.

D. Wilfong suggested [47] that the monomers in the macromolecule may have been distributed in a blocky manner during the copolymerization of ethylene and olefin. Hence, the HTCP and the VLTCP may arise from the crystallization of ethylene rich and hexene/butene rich portions of the macromolecule, respectively. That is, the HTCP can be associated with crystallization of the linear portions of the macromolecule into the chain folded lamellae. The branched segments of macromolecule are exiled into the inter-lamellar or inter-facial regions and

crystallized there upon further undercooling into thin lamellae. However, the blocky intramolecular distribution of co-monomers in chain is recognized for ZN [48], but not for SS samples. Additionally, VLTCP has also been detected by us for HDPE having extremely low number of branches. Moreover, thin lamellar crystallites should melt at considerable low temperature and could be detected by DSC. But no melting peaks related to VLTCP were found for all the studied materials.

Because there is a clear correlation of both peaks with molar mass, it is implicit that these exotherms (especially the VLTCP) are also a consequence of melt topology; in other words, entanglements. Then, the key to the presence of this VLTCP exotherm will not be the sequence

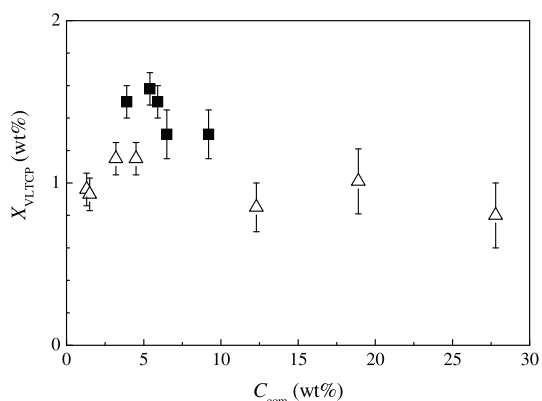


**Fig. 7** Plots of VLTCP partial crystallinity  $X_{\text{VLTCP}}$  vs.  $C_{\text{com}}$  for SS-6.9 (6.2) (solid squares) and ZN-7.6(7.2) (open triangles) fractions obtained by fractionation according to structure

distribution caused by the comonomer, but a melt topology that restricts further crystallization after a primary nucleation and further (usually spherulitic) growth in most semicrystalline polymers. The increase in  $X_{\text{VLTCP}}$  with MM leads us to suggest that inter-crystalline links are responsible for the formation of the VLTCP. During crystallization numerous tie molecules are formed especially at rather large supercooling. These tie molecules can aggregate locally to form inter-crystalline links (named us as bundles). However, the formation of inter-crystalline links also has its optimum MM limit equal to 60–100 kg/mol, above which the crystallinity level of so-named bundles does not strongly changes or even slightly decreases.

## Conclusions

On the basis of the DSC experimental results on low temperature crystallization behavior of fractionated SS and ZN based ethylene/ $\alpha$ -olefin copolymers and ZN HDPE the following conclusions can be made:

DSC curves of MM and compositional fractions of SS and ZN materials, except the first MM fractions, for which the VLTCP was not detected, uniquely show the presence of an additional crystallization process occurring at very low temperatures around 60–75 °C. The VLTCP is much broader and less in magnitude than the main sharp HTCP. Moreover, the melting curves do not show any additional peaks clearly related to the VLTCP.

In the range of  $5 < \overline{M}_w < 100$  kg/mol the partial degree of crystallinity calculated from the VLTCP ( $X_{\text{VLTCP}}$ ) and the peak crystallization temperature of the VLTCP ( $T_{\text{VLTCP}}$ ) increase with increasing MM. At the same time the crystallinity of HTCP decreases with MM that involves a molecular correlation between the primary and secondary crystallization processes. When MM is higher than 100 kg/mol, the  $X_{\text{VLTCP}}$  and  $T_{\text{VLTCP}}$  level off. Such behavior can be a result of increasing amorphous layer with MM due to the increase in number of entanglements. It implies the less incorporation of the fraction of crystallizable sections of polymer macromolecules into the primary crystallization process associated with HTCP. The chains or/and segments of chains, remaining in the melt after primary crystallization, can aggregate locally forming the bundle-like inter-crystalline links.

The comonomer content ( $C_{\text{com}}$ ) does not strongly influence on the values of  $X_{\text{VLTCP}}$  while the pronounce decrease in  $T_{\text{VLTCP}}$  with  $C_{\text{com}}$  is observed. However, the  $X_{\text{VLTCP}}$  and  $T_{\text{VLTCP}}$  are independent of the chemical nature of the co-monomers (1-butene or 1-hexene).

The  $X_{\text{VLTCP}}$  is in turn strongly influenced by the type of catalyst. For the SS materials the  $X_{\text{VLTCP}}$  is in approximately 2 times higher than for the ZN samples. Moreover,

for ZN HDPE the obtained values of  $X_{\text{VLTCP}}$  are much lower than those of ZN LLDPE.

**Acknowledgments** The Estonian Science Foundation is acknowledged for support under grant no. 6553 and Borealis Polymers OY (Finland) for structural characterization of the studied materials. We also acknowledge the Targeted Financing of Estonian Ministry of Education and Research for the grant no. SF0142687s05.

## References

- Mathot VBF, Pijpers JFJ (1988) Integration of fundamental polymer science and technology. Proceedings of International Discussion Meeting, Rolduc Abbey, Netherlands, 26–30 April, 1987. Elsevier Applied Science, London, p 381
- Mathot VBF, Scherrenberg RL, Pijpers MFJ, Engelen YMT (1996) New trends in polyolefin science and technology. Hosoda S. Ed.; Research Signpost, Trivandrum, India
- Patel RM, Jain R, Story B, Chum S (2008) Polyethylene: an account of scientific discovery and industrial innovations. ACS Symposium Series. Innovations in Industrial and Engineering Chemistry 1000:71–102
- Wang C, Chu M, Lin T, Lai S, Shih H, Yang J (2001) Microstructures of a highly branched polyethylene. *Polymer* 42:1733–1741
- Minick J, Moet A, Hiltner A, Baer E, Chum SP (1995) Crystallization of very low density copolymers of ethylene with  $\alpha$ -olefins. *J Appl Polym Sci* 58:1371–1384
- Hussein IA (2008) Nonisothermal crystallization kinetics of linear metallocene polyethylenes. *J Appl Polym Sci* 107:2802–2809
- Ramos J, Peristeras LD, Theodorou DN (2007) Monte Carlo simulation of short chain branched polyolefins in the Molten State. *Macromolecules* 40:9640–9650
- Mathot VBF (1994) Calorimetry and thermal analysis of polymers. Hanser, Munich-Germany-Vienna-New York
- Mathot VBF, Scherrenberg RL, Pijpers TFJ (1998) Metastability and order in linear, branched and copolymerized polyethylenes. *Polymer* 39:4541–4559
- Zhang F, Liu J, Xie F, Fu Q, He T (2002) Polydispersity of ethylene sequence length in metallocene ethylene/ $\alpha$ -olefin copolymers. II. Influence on crystallization and melting behavior. *J Polym Sci Polym Phys* 40:822–830
- Mirabella FM (2008) Crystallization and melting of a polyethylene copolymer: in situ observation by atomic force microscopy. *J Appl Polym Sci* 108:987–994
- Alizadeh A, Richardson L, Xu J, McCartney S, Marand H (1999) Influence of structural and topological constraints on the crystallization and melting behavior of polymers. 1. Ethylene/1-Octene Copolymers. *Macromolecules* 32:6221–6235
- Marand H, Alizadeh A, Farmer R, Desai R, Velikov V (2000) Influence of structural and topological constraints on the crystallization and melting behavior of polymers. 2. Polyarylene ether ether keton. *Macromolecules* 33:3392–3403
- Crist B, Claudio ES (1999) Isothermal crystallization of random ethylene-butene copolymers: bimodal kinetics. *Macromolecules* 32:8945–8951
- Canetti M, Bertini F (2010) Crystalline and supermolecular structure evolution of poly(ethylene terephthalate) during isothermal crystallization and annealing treatment by means of wide and small angle X-ray investigation. *Euro Polym J* 46:270–276
- Rabiej S, Goderis B, Janicki J, Mathot VBF, Koch MHJ, Groeninckx G, Reynaers H, Gelan J, Wlochowicz A (2004) Characterization of the dual crystal population in an isothermally

- crystallized homogeneous ethylene-1-octene copolymer. *Polymer* 45:8761–8778
17. Tashiro K, Imanishi K, Izumi Y, Kobayashi M, Kobayashi K, Satoh M, Stein RS (1995) Cocrystallization and phase segregation of polyethylene blends between the D and H species. 7. Time-resolved synchrotron-source small-angle X-ray scattering measurements for studying the isothermal crystallization kinetics: comparison with the FTIR Data. *Macromolecules* 28:8477–8483
  18. Alamo RG, Mandelkern L (1994) The crystallization behavior of random copolymers of ethylene. *Thermochim Acta* 238:155–201
  19. Simanke AG, Alamo RG, Galland GB, Mauler RS (2001) Wide-angle X-ray scattering of random Metallocene–Ethylene copolymers with different types and concentration of comonomer. *Macromolecules* 34:6959–6971
  20. Alamo RG, Chan EKM, Mandelkern L, Voigt-Martin IG (1992) Influence of molecular weight on the melting and phase structure of random copolymers of ethylene. *Macromolecules* 25:6381–6394
  21. Ergoz E, Fatou JG, Mandelkern L (1972) Molecular weight dependence of the crystallization kinetics of linear polyethylene. I. Experimental results. *Macromolecules* 5:147–157
  22. Natta G (1955) Une nouvelle classe de polymeres d'  $\alpha$ -olefines ayant une régularité de structure exceptionnelle. *J Polym Sci* 16:143–154
  23. Pino P, Oschwald A, Ciardelli F, Carlini C, Chiellini E (1975) In: Chien JCW (ed) *Coordination polymerization of  $\alpha$ -Olefins*. Elsevier, New York
  24. Holtrup W (1977) Zur fraktionierung von polymeren durch direktextraktion. *Makromol Chem* 178:2335–2349
  25. Lehtinen A, Paukkeri R (1994) Fractionation of polypropylene according to molecular weight and tacticity. *Macromol Chem Phys* 195:1539–1556
  26. Usami T, Takayama Sh (1984) Identification of branches in low-density polyethylenes by Fourier transform infrared spectroscopy. *Polym J* 16:731–738
  27. Tarasova EV, Poltimäe T, Krumme A, Lehtinen A, Viikna A (2009) Study of very low temperature crystallization process in ethylene/ $\alpha$ -olefin copolymers. *Macromol Symp* 282:175–184
  28. Kim M, Philips PJ (1998) Nonisothermal melting and crystallization studies of homogeneous ethylene/ $\alpha$ -olefin random copolymers. *J Appl Polym Sci* 70:1893–1905
  29. Alamo RG, Mandelkern L (1989) Thermodynamic and structural properties of ethylene copolymers. *Macromolecules* 22:1273–1277
  30. Mandelkern L (1971) Thermodynamic and morphological properties of crystalline polymers. *J Phys Chem* 75:3909–3920
  31. Mandelkern L, Alamo RG, Kennedy MA (1990) The interphase thickness of linear polyethylene. *Macromolecules* 23:4721–4723
  32. Failla MD, Lucas JC, Mandelkern L (1994) Supermolecular structure of random copolymers of ethylene. *Macromolecules* 27:1334–1337
  33. Liu W, Yang H, Hsiao BS, Stein RS, Liu S, Huang B (1999) Real-time crystallization and melting study of ethylene-based copolymers by SAXS, WAXD, and DSC techniques. *ACS Symposium Series: Scattering from Polymers* 739:187–200
  34. Mandelkern L (1990) The structure of crystalline polymers. *Acc Chem Res* 23:380–386
  35. Gedde UW, Janson JF, Liljenstrom G, Eklund S (1998) Molecular structure, crystallization behavior, and morphology of fractions obtained from an extrusion grade high-density polyethylene. *Polym Eng Sci* 28:1289–1303
  36. Fatou JG, Mandelkern L (1965) The effect of molecular weight on the melting temperature and fusion of polyethylene. *J Phys Chem* 69:417–428
  37. Alamo RG, Mandelkern L (1991) Crystallization kinetics of random ethylene co-polymers. *Macromolecules* 24:6480–6493
  38. Alamo RG, Domszy R, Mandelkern L (1984) Thermodynamic and structural-properties of copolymers of ethylene. *J Phys Chem* 88:6587–6595
  39. Basiura M, Gearba RI, Ivanov DA, Janicki J, Reynaers H, Groeninckx G, Bras W, Goderis B (2006) Rapidly cooled polyethylenes: on the thermal stability of the semicrystalline morphology. *Macromolecules* 39:8399–8411
  40. Rastogi S, Lippits DR, Peters GWM, Graf R, Yao Y (2005) Heterogeneity in polymer melts from melting of polymer crystals. *Nat Mater* 4:635–641
  41. Lippits DR, Rastogi S, Hhne G, Mezari B, Magusin P (2007) Heterogeneous distribution of entanglements in the polymer melt and its influence on crystallization. *Macromolecules* 40:1004–1010
  42. Psarski M, Piorowska E, Galeski A (2000) Crystallization of polyethylene from the melt with lowered chain entanglements. *Macromolecules* 33:916–932
  43. Fan Z, Wang Y, Bu H (2003) Influence of intermolecular entanglements on crystallization behavior of ultra-high molar mass polyethylene. *Polym Eng Sci* 43:607–614
  44. Smith P, Manley J (1979) Solid solution formation and fractionation in quasi-binary systems of polyethylene fractions. *Macromolecules* 12:483–491
  45. Robelin-Souffache E, Rault J (1989) Origin of the long period and crystallinity in quenched semicrystalline polymers. I. *Macromolecules* 22:3581–3594
  46. Rousseaux F, Lemonnier M (1980) Crystallization of polymers. Part II: Fractionated polyethylene quenched from the liquid state. *J Physique* 41:1469–1474
  47. Wilfong DL (1989) LLDPE TREF fractions, crystallization behavior and morphology. *Polym Mater Sci Eng* 61:743–747
  48. Hosoda S (1988) Structural distribution of linear low-density polyethylenes. *Polym J* 20:383–386

#### PAPER IV

T. Poltimäe, E. Tarasova, A. Krumme, J. Roots, A. Viikna. Thermal analyses of blends of hyperbranched LLDPE with HDPE and LLDPE prepared by dissolving method. *Material Science (Medžiagotyra)*, accepted 03 December 2010.



## Thermal Analyses of Blends of Hyperbranched Linear Low-density Polyethylene (LLDPE) with High-density Polyethylene and LLDPE Prepared By Dissolving Method

Triinu POLTIMÄE<sup>1\*</sup>, Elvira TARASOVA<sup>1</sup>, Andres KRUMME<sup>1</sup>, Jaan ROOTS<sup>2</sup>, Anti VIKNA<sup>1</sup>

<sup>1</sup> Tallinn University of Technology, Ehitajate tee 5, 19086 Tallinn, Estonia

<sup>2</sup> University of Oslo, Department of Chemistry, P.O. box 1033 Blindern, N - 0315 Oslo, Norway

Received 17 August 2010; accepted 03 December 2010

Blends of high-density polyethylene (HDPE), moderate and hyper-branched LLDPEs (LLDPE and HbPE, respectively) have attained widespread commercial applications, though the understanding of the mechanical and melt-flow properties of such blends has been handicapped by the absence of a consensus concerning the degrees of mixing of the components. Moreover, usually the blends are obtained by melt blending, which may not ensure the initial homogeneity of the components. In our work the mixtures were prepared by dissolving the conventional LLDPE having branching content 7.2 wt% with HbPE with comonomer content 17.8 wt% in xylene at 130°C and stirring for 2 hours. The same procedure was applied for the blending of HDPE with HbPE. After dissolving the mixtures were cooled in liquid nitrogen and after that freeze dried in vacuum line. The ratio of components in the blends was varied. Differential scanning calorimetry has been used to investigate the miscibility and thermal behavior of the blends. For this purpose isothermal and non-isothermal treatment of prepared blends were conducted. By preliminary study the double melting peaks in non-isothermal endotherms have been observed in all the studied blends. The presence of two peaks in DSC scan can be attributed to the formation of separated crystals from both the high density/linear low density and highly branched components. However, certain limited degree of co-crystallization is detected in all the LLDPE/HbPE blends and HDPE/HbPE blend rich in HbPE component

*Keywords:* blends, hyper-branched linear low density PE, thermal behaviour, differential scanning calorimetry.

### 1. INTRODUCTION

Blends of linear low density polyethylene (LLDPE) with different types of polyethylenes have been widely investigated from scientific as well as industrial interests and attained widespread commercial applications.

One of the most important problems that have to be solved is the phase segregation between the components of the blends. For example as it is known from the literature the blend of high density polyethylene (HDPE) with low density polyethylene (LDPE) shows segregation between these two components when cooled slowly from the melt [1-3]. Only quenching of the melts showed a uniformly mixed crystalline sample, or a co-crystallized sample. But the phenomenon is limited to the sample with high HDPE content or to those with a low degree of branching in branched PE [4, 5]. For the blend of LDPE with LLDPE a formation of separated crystals of phase segregation was suggested [6]. For the blend between HDPE and slightly branched LLDPE the co-crystallization was reported even under the condition of slow cooling [7-10]. Therefore the crystal segregation and co-crystallization are dependent in a complicated manner upon the couples of the selected PEs, the crystallization conditions, etc.

The molecular weight of the components in the blends, as it has been suggested elsewhere [8, 11], is of secondary importance in determining the occurrence or extent of co-crystallization. At the same time the amount of short chain branching (SCB) and type of catalyst seems to be

important factors [12-14]. The higher the branching content, the lower is the possibility of co-crystallization between the components. Zhao et al. [15] conclude that the upper branching limit still allowing co-crystallization to occur probably is much lower in blends with single-site materials than in blends with Ziegler-Natta based materials. Zhao et al. argue that in Z-N LLDPE there exists long segments between branches that can easily co-crystallize with HDPE or LPE, but the more uniform SCB distribution in single site LLDPE makes co-crystallization more difficult.

Much of the works present in literature has been focused on blends between LPE or HDPE and the LLDPE, which is a lightly branched ethylene-butene copolymer, obtained by single site catalyst [7-11, 16, 17]. Moreover, in performed works the mixtures are generally prepared by melt-blending, which may not ensure the initial homogeneity of the components, because it is not certain that sufficient time was allowed for the molecules to inter-diffuse to the homogeneous state.

In present work we prepared the blends of hyper-branched LLDPE with HDPE and moderate branched LLDPE. These blends were prepared with mixing of components in solution and keeping them for several hours in that state before drying. Although HDPE, LLDPE and hyper-branched LLDPE differ in the amount and distribution of the comonomer, chemically they should be miscible. To our knowledge this is the first study of thermal behavior of hyper-branched LLDPE blends. Blends were analyzed with a view to determine the extent to which the polymers either co-crystallize or crystallize independently.

\* Corresponding author. Tel.: + 372-620-2906; fax.: + 372-620-2903  
E-mail address: triinu.poltimae@ttu.ee (T. Poltimäe)

## 2. EXPERIMENTAL PART

### 2.1. Materials

All materials used in this study are commercial materials kindly supplied from Borealis, Finland. Single site catalyzed hyper-branched LLDPE (HbPE) is used as common component for all the blends. HbPE is a copolymer of ethylene with 1-butene. The Ziegler-Natta catalyzed polyethylene samples with different degrees of branching, i.e., fractionated high-density polyethylene (HDPE) having presumably low amount of branches and linear low density polyethylene moderately branched (marked in text as just LLDPE) were used as the second component in the blends. LLDPE is a copolymer of ethylene with 1-hexene. HDPE sample was fractionated by molar mass (MM) according to Holtrup technique which is a solvent/non-solvent extraction [18]. In the present study the first fraction of fractionated HDPE was used in order to have the high-density sample with a few branches. The molecular parameters of pure components are listed in Table 1.

**Table 1.** Molecular characteristics of the pure components used for preparation of blends.

| Material | Comonomer content (wt%) | Weight average MM (kg/mol) | MM polydispersity |
|----------|-------------------------|----------------------------|-------------------|
| HbPE     | 17.8                    | 88                         | 2                 |
| LLDPE    | 7.2                     | 125                        | 4.4               |
| HDPE     | <i>not analyzed</i>     | 5                          | 2                 |

### 2.2. Blending

Blends were prepared by dissolving different ratios of components in xylene at 130°C and stirring for 2h. After dissolving the mixtures were quenched in liquid nitrogen and then freeze dried in vacuum line for 48h. Blends were obtained as powders/fluffy materials. Ratios of components in blends were varied: 20/80, 50/50 and 80/20 wt% was taken for LLDPE/HbPE, 20/80 and 80/20 for HDPE/HbPE.

### 2.3. Methods

For all isothermal and non-isothermal experiments at cooling rates 1 and 10°C/min Perkin Elmer differential scanning calorimeter DSC-7 was used with nitrogen as furnace purge gas. For non-isothermal experiments at cooling rate 200°C/min Perkin Elmer Diamond DSC was used with helium as furnace purge gas. Temperature and heat flow calibrations were done with indium and tin standards. To avoid differences in melting and crystallization temperatures caused by variation in sample weight, a sample mass of 1.00±0.02mg was used in all DSC experiments. Samples were manually compressed and packed into aluminium foil to maximize thermal contact between sample and calorimetric furnace.

During non-isothermal measurements the sample was first held at 180°C for deleting its thermal history. Then it was cooled to -40°C at cooling rate 1, 10 or 200°C/min, held at -40°C for 2 minutes and heated to 180°C at heating rate 10°C/min. Degree of crystallinity  $\lambda$  was calculated

from the heat of fusion using the peak area determination method, i.e., by integration of the area under the normalized melting peak after subtraction of an arbitrary straight baseline; a value of  $\Delta H_m^0 = 293$  J/g was used as the reference melting enthalpy of fusion for 100% crystalline PE.

For isothermal treatment sample was first held at 180°C, then quenched to an annealing temperature and held there 30 minutes and then heated to 180°C at heating rate 10°C/min. Annealing temperatures were between melting temperatures of pure components: 80, 90, 100 and 115°C.

MM and polydispersity were determined by size exclusion chromatography using 1,2,4-trichlorobenzene (TCB) as eluent at 140°C. Comonomer contents were measured by Fourier transform infrared spectroscopy.

## 3. RESULTS AND DISCUSSION

It has been presented elsewhere that blends similar to the blends presented here show extended regions of phase separation (in temperature and composition) in the melt [12-17]. Based on those results it is expected that our blends will show two separate crystal populations. DSC melting endotherms of the blends HDPE/HbPE with various ratios of components are shown in Fig. 1. The heating and cooling rates were 10°C/min. The DSC result clearly indicates the existence of two crystal populations in these blends. Two melting peaks are found in all studied blends. The mixtures with a high concentration of the high-density polymer (>50%) show a sharp high-temperature peak with a small peak in the low-temperature region. This low-temperature peak further develops into a well-defined peak for the mixtures with high concentration of the hyper-branched component. The form and position of the low-temperature peak indicates that this peak represents melting of mainly the component rich in HbPE. The high-temperature melting peak seems to represent the HDPE-rich component. It should be noticed that high temperature melting peak has a small shoulder, sub-peak, generated at slightly lower temperature. Similar behavior is detected for all the blends of LLDPE with HbPE, as is obvious from the Fig. 2 where their crystallization and melting thermograms are shown.

The origin of sub-peak observed at high temperatures can be understood from the thermograms of pure components, also presented in Figs. 1 and 2. Pure HDPE component has mainly one melting peak but the shoulder extent to lower temperatures is present, indicating some degree of heterogeneity in sequence lengths. The same is found for pure LLDPE. If the compositional and molar mass (MM) heterogeneity of conventional whole LLDPE is expected, the heterogeneity of HDPE seems to be unusual. As it was mentioned in Experimental part the HDPE used in this study is the first fraction of the whole HDPE obtained by fractionation according to MM. Taken into account that HDPE is catalyzed by Ziegler-Natta technique, first fractions of such polymers after fractionation by MM usually contain branched chains with low MM. The degree of branching in the first fraction is therefore higher than present in whole polymer. Therefore

HDPE can contain chains that can be excluded from the largest lamellae during primary crystallization and generate a secondary crystal population. This can result in an appearance of sub-peak in melting traces. Presence of chains forming the secondary crystals gives the possibility of mixing them with the HbPE chains having very low branch content. As seen from the Figs. 1 and 2, the increase in the amount of HbPE component in the blends results in a better separation of two high-temperatures melting peaks. The position and broadness of these peaks change indicating partial chain segregation of HDPE-rich peak and possibility of a formation of mix crystals.

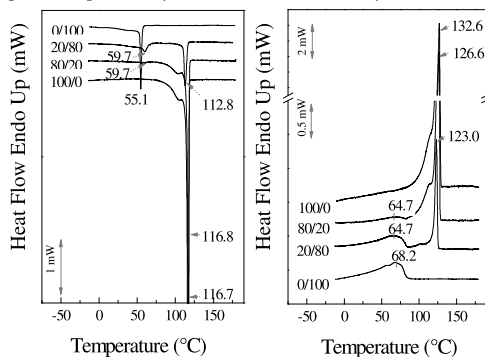


Fig. 1. DSC cooling (left) and melting (right) traces of the HDPE/HbPE blends with various component ratios. Cooling and heating rates are 10°C/min.

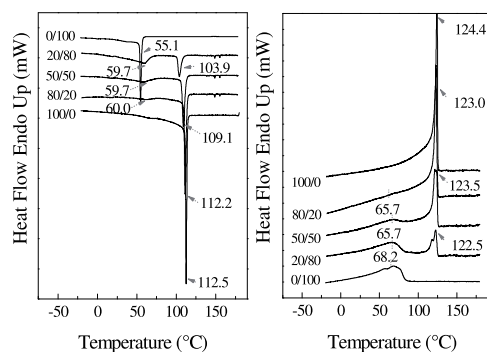


Fig. 2. DSC exotherms (left) and endotherms (right) of the HDPE/HbPE blends with various component ratios. Cooling and heating rates are 10°C/min.

In order to understand the origin of low temperature and high temperature melting peaks the cooling rate during the cooling scans was varied. The heating rate is constant, 10°C/min. The thermograms of the blends at 1 and 200°C/min cooling rates show identical behavior as it was observed for cooling rate of 10°C/min. It is clear seen from the Fig. 3 where melting traces of 20/80 HDPE/HbPE and 50/50 LLDPE/HbPE blends at different cooling rates are shown as illustrations. Two main melting peaks with additional sub-peak at high temperature are recorded.

From the heat of fusion, the degree of crystallinity  $\lambda$  by weight was obtained for low and high temperature peak.

These values are given in Table 2 for the 20/80 HDPE/HbPE blend as example. First of all the degree of crystallinity of each peak does not depend on scanning rate indicating that the observed peaks are not associated with the recrystallization or reorganization process but consistent with the formation of separate crystals from both components. The other blends of HDPE/HbPE and LLDPE/HbPE are found to possess a similar behavior and the same conclusion can be done for them. Thus, in comparison with HDPE/LLDPE and LDPE/LLDPE discussed in literature [1-14], in our types of blends two crystal populations are forming even in rapidly crystallized mixtures at 200°C/min similar to slowly cooled samples at 1°C/min.

**Table 2.** Degree of crystallinities  $\lambda$  for 20/80 HDPE/HbPE blends obtained from melting thermograms at various cooling rates.

| Cooling rate °C/min | $\lambda$ overall (wt%) |       | $\lambda$ (low temperature peak) wt% |       | $\lambda$ (high temperature peak) wt% |       |
|---------------------|-------------------------|-------|--------------------------------------|-------|---------------------------------------|-------|
|                     | exptl                   | calcd | exptl                                | calcd | exptl                                 | calcd |
| 1                   | 27                      | 37    | 11                                   | 18    | 16                                    | 19    |
| 10                  | 26                      | 31    | 11                                   | 12    | 15                                    | 19    |
| 200                 | 25                      | 35    | 10                                   | 16    | 15                                    | 19    |

\* *exptl* means measured from DSC melting endotherms  
*calcd* means calculated assuming independently crystallized crystals

To find out whether the observed melting peaks corresponds to completely separated crystallites, formed independently, the degree of crystallinity of low and high temperature peak was compared with the expected value in the blends if both components had crystallized independently. Table 2 shows that the crystallinity of the HbPE-rich low-temperature peaks is lower than that calculated assuming independent crystallites. Overall degree of crystallinity of both peaks is also lower than that calculated by mentioned above method. Lower crystallinity of the blends compared to the pure blend components has been taken elsewhere as an argument in favor of co-crystallization [3, 7-16]. The observed melting behavior of the blends therefore suggests that slight co-crystallization to some limited extent is present in the blends.

Furthermore, the low-temperature peak in all the blends has almost the same melting point which is around 4°C lower than observed for the pure HbPE component as also obvious from the Figs. 1 and 2. This result might indicate that even in HbPE there are chain segments that are able to co-crystallize with branched chains of HDPE or LLDPE [17]. In that case remaining HbPE chains, not incorporated in HDPE- (LLDPE-) rich crystals, are suggested to have a higher overall content of branches than the pure HDPE (LLDPE) and should melt consequently at a lower temperature; and this is in fact observed from Figs. 1 and 2.

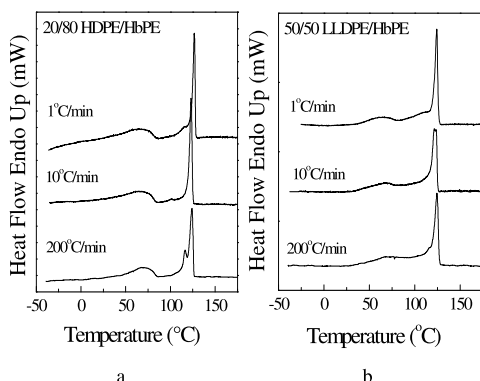


Fig. 3. DSC melting thermograms for 20/80 HDPE/HbPE (a) and 50/50 LLDPE/HbPE (b) blends crystallized at various cooling rates.

The melting point of the high-temperature peak in the HDPE/HbPE and LLDPE/HbPE is significantly lower ( $\sim 10^\circ\text{C}$  and  $2^\circ\text{C}$  maximum, respectively) compared to that of the pure HDPE and LLDPE component. Other authors have observed a similar depression of the melting temperature of the high-temperature peak in a blend of LPE/LDPE [13, 19] and LPE/LLDPE [12, 16] and suggest that such behavior can be explained by both the co-crystallization of the branched component into the LPE crystal and a lower lamellae thickness of the LPE component in the blend. Based on this conclusion, the depression of the high-temperature peak in the blends most probably has a complex reason but could be explained, at least partly, from a limited degree of co-crystallization among the blend components.

Therefore, a limited degree of co-crystallization is believed to be present in blends used in this work, at least in the blends rich in HbPE ( $\geq 50\%$ ).

One more interesting behavior can be seen from the crystallization traces of the blends. From Fig. 1 it is observed that the crystallization temperature of the HbPE-rich component in separated blends locates at a higher temperature than the crystallization point of the corresponding pure HbPE component. This observation seems to be in a conflict with the observation of melting point behavior. We will explain this effect based on comments and observations made by others [12]. Crystallization curves for both pure blend components show sharp leading edges, characteristic of primary crystallization. Additionally, both components have an extended tail to lower temperatures, reflecting a secondary crystallization process into thinner lamellae. In the blends it is obvious from Figs. 1 and 2 that the HDPE- as well as LLDPE-rich component crystallizes first. The crystallization curves show rather sharp and narrower peak at high temperature. The low-temperature peak, however, reflecting a secondary crystallization process of mainly HbPE-rich component, shows rather broad leading edge very different from the sharp peak observed for pure HbPE. Therefore it was suggested that the primary crystallization in blend is associated with the

crystallization of HDPE-rich or LLDPE-rich component in HDPE/HbPE and LLDPE/HbPE blends, respectively. HbPE-rich component crystallizes in a secondary crystallization processes within the structure determined by crystallization of HDPE- or LLDPE-rich component [20]. Therefore as others have suggested the crystallization of HDPE or LLDPE will generate the crystallization of HbPE at higher temperature than the pure HbPE would otherwise crystallize. The lamellae thickness of the resulting HbPE-rich component in the blends and the subsequent melting behavior indicate that this enhanced crystallization at higher temperature occurs without forming thicker lamellae, as normally would be expected due to higher crystallization temperature.

To confirm the presence of partial co-crystallization in used blends, assuming for the sake of argument that one could initially assign the double melting to the formation of independent LLDPE (or HDPE) and hyper-branched crystal, it follows that isothermal crystallization of blends especially with a high amount of HbPE at temperatures intermediate between both melting peaks should give rise to completely segregated LLDPE (or HDPE) crystals represented by a single peak in DSC thermograms [1].

To test this hypothesis, isothermal crystallizations were carried out in all the blends. The blends were equilibrated in the melt at  $180^\circ\text{C}$  and rapidly cooled to the annealing temperature ( $T_a$ ). The melt endotherms were subsequently recorded starting from  $T_a$  i.e., without further cooling. The example is shown in Fig. 4 for the 50/50 LLDPE/HbPE blend crystallized at different  $T_a$ . The endotherms of a similar mass of the pure components, crystallized at the same temperatures are demonstrated in the inset to the Fig. 4. The melting after crystallization at different  $T_a \leq 100^\circ\text{C}$  shows two well-defined peaks at about  $116$  and  $123^\circ\text{C}$  and a low-temperature sub-peak in the  $T_a$  region that shifts toward the melting temperature of the main peak. This sub-peak, observed also in scans at  $T_a = 115^\circ\text{C}$ , is often observed for the annealed crystalline polymers: the small crystallites of the size intrinsic of  $T_a$  are generated when the sample is annealed at  $T_a$  [8]. In the heating process these small crystallites melt in the temperature region close to  $T_a$  and can recrystallize into a larger crystallite of the main melting point. In other words, the sub-peaks in Fig. 4 are not considered to come from the co-crystal or phase segregated crystals of the blend.

The crystallization at  $T_a$  of the pure HbPE for the same time does not show any melting peak in heating scans as it is clear seen from the inset to the Fig. 4. The pure LLDPE component shows only one main melting peak at around  $123^\circ\text{C}$  and a sub-peak in  $T_a$  region. Therefore, no chain segregation of LLDPE during annealing is detected. Taken into account the medium peak of the 50/50 blend, around  $116^\circ\text{C}$ , cannot be associated with the melting of segregated crystals formed from the pure HbPE or chain segregated LLDPE. The interesting observation is that the position of medium melting peak of LLDPE/HbPE blend almost does not change with increasing  $T_a$ . Consequently, the peak is believed to be associated with the melting of limited co-crystals formed with molecules from the both components of the blend. The crystallization of shorter sequences of the hyper-branched component, unable to co-crystallize with LLDPE, takes places at lower crystallization temperatures.

These crystals melt at  $T < T_a$ . The high peak at  $\sim 123^\circ\text{C}$  is associated with melting of pure LLDPE crystals which probably were formed above  $T_a$  during the cooling process.

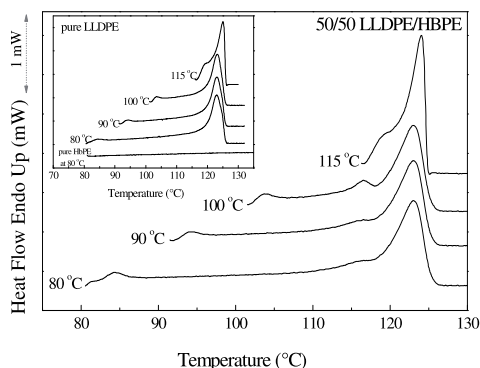


Fig. 4. DSC thermograms measured for 50/50 LLDPE/HbPE blend annealed at various temperatures. Inset shows isothermal DSC thermograms for pure LLDPE and HbPE components.

The possibility of melting with further recrystallization of a single species during the heating run is believed to be minor for the following reasons. The 50/50 LLDPE/HbPE mixture was crystallized at  $100^\circ\text{C}$  for 30 min and the melting followed at different heating rates (5, 10, and  $40^\circ\text{C}/\text{min}$ ) was recorded. The relative areas of both melting peaks are practically independent of heating rate within experimental error, indicating that both species are formed mainly during crystallization and not in the melting process [1]. However some degree of recrystallization process is still possible.

High annealing temperatures,  $T_a > 100^\circ\text{C}$ , hinder the co-crystallization process; for example, crystallization of the 50/50 mixture at  $115^\circ\text{C}$  (see Fig. 4) results in single melting peaks around  $125^\circ\text{C}$  corresponding to the pure LLDPE species.

These experiments clearly indicate that there is partial co-crystallization of both components in the 50/50 LLDPE/HbPE blend crystallized at temperatures at which the crystallization of the pure hyper-branched component is completely retarded.

A similar behavior is found from the analysis of the melting peaks after isothermal crystallization of the 20/80 and 80/20 LLDPE/HbPE mixtures, and 20/80 HDPE/HbPE blends, as it is obvious from the Fig. 5. Therefore it is believed that the limited co-crystallization is occurred in all LLDPE/HbPE blends, and in HDPE/HbPE blends rich in hyper-branched component.

HDPE-rich blends did not melt at temperatures indicative of partial co-crystallization. Only a single endotherm was observed for 80/20 HDPE/HbPE blend, see Fig. 5. It is known that for the blends with high concentration of the high-density component, the crystallization rate of the HDPE in the blend is much higher than that of the pure branched polymer [1, 20-22]. Therefore segregation of the components is kinetically favored in 80/20 HDPE/HbPE blend. At high content of HbPE ( $\geq 50\%$ ) the difference in crystallization rates between HDPE and HbPE becomes smaller, favoring co-

crystallization. The results on HDPE/HbPE blends are consistent with the interpretation from the experiments after isothermal crystallization done by other authors for various types of blends [8-10, 17, 21, 22].

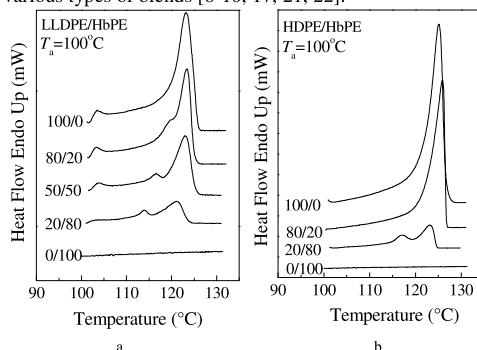


Fig. 5. DSC thermograms measured for LLDPE/HbPE (a) and blends HDPE/HbPE (b) with different component ratios annealed at  $100^\circ\text{C}$ .

### 3. CONCLUSIONS

The data of rapidly and slowly cooled blends of HDPE and LLDPE with hyper-branched LLDPE indicate that both components form two crystal populations. However, the limited degree of co-crystallization is believed to be present in all LLDPE/HbPE blends and HDPE/HbPE blends having the content of HbPE component of 80%. The DSC thermograms of all mixtures, excepting 80/20 HDPE/HbPE, annealed between the melting temperatures of both components show double melting peaks that were interpreted in terms of partial co-crystallization for all studied blends. 80/20 HDPE/HbPE blend shows only single melting peak in isothermal thermograms, which seems to be associated with completely segregated crystals.

### Acknowledgements

The Estonian Science Foundation is acknowledged for support under grant no. ETF8134

### REFERENCES

- Wignall, G.; Londono, J.; Lin, J.; Alamo, R.; Galante, M.; Mandelkern, L. Morphology of Blends of Linear and Long-Chain-Branched Polyethylenes in the Solid State: A Study by SANS, SAXS, and DSC *Macromolecules* 28 1995: pp. 3156-3167.
- Agamalian, M.; Alamo, R.; Kim, M.; Londono, J.; Mandelkern, L.; Wignall, G. Phase Behavior of Blends of Linear and Branched Polyethylenes on Micron Length Scales via Ultra-Small-Angle Neutron Scattering *Macromolecules* 32 1999: pp. 3093-3096.
- Morgan, R.; Hill, M.; Barham, P. Morphology, melting behaviour and co-crystallization in polyethylene blends: the effect of cooling rate on two homogeneously mixed blends *Polymer* 40 1999: 337-348.
- Martinez-Salazar, J.; Sanchez Cuesta, M.; Plans, J. On phase separation in high- and low-density polyethylene

- blends: 1. Melting-point depression analysis *Polymer* 32(16) 1991: pp. 2984-2988.
5. **Hill, M.; Barham, P.; Keller, A.** Phase segregation in blends of linear with branched polyethylene: the effect of varying the molecular weight of the linear polymer *Polymer* 33(12) 1992: pp. 2530-2541.
  6. **Kyu, T.; Hu, S.; Stein, R.** Characterization and properties of polyethylene blends II. Linear low-density with conventional low-density polyethylene *Journal of Polymer Science Polymer Physics* 25(1) 1987: pp. 89-103.
  7. **Tashiro, K.; Izuchi, M.; Kobayashi, M.; Stein, R.** Cocrystallization and Phase Segregation of Polyethylene Blends between the D and H Species. 4. The Crystallization Behavior As Viewed from the Infrared Spectral Changes *Macromolecules* 27(5) 1994: pp. 1228-1233
  8. **Tashiro, K.; Izuchi, M.; Kobayashi, M.; Stein, R.** Cocrystallization and Phase Segregation of Polyethylene Blends between the D and H Species. 3. Blend Content Dependence of the Crystallization Behavior *Macromolecules* 27(5) 1994: pp. 1221-1227.
  9. **Tashiro, K.; Stein, R.; Hsu, S.** Cocrystallization and phase segregation of polyethylene blends. 1. Thermal and vibrational spectroscopic study by utilizing the deuteration technique *Macromolecules* 25(6) 1992: pp. 1801-1808.
  10. **Wignall, G.; Alamo, R.; Londono, J.; Mandelkern, L.; Kim, M.; Lin, J.; Brown, G.** Morphology of Blends of Linear and Short-Chain Branched Polyethylenes in the Solid State by Small-Angle Neutron and X-ray Scattering, Differential Scanning Calorimetry, and Transmission Electron Microscopy *Macromolecules* 33 2000: pp. 551-561.
  11. **Tashiro, K.; Imanishi, K.; Izuchi, M.; Kobayashi, M.; Itoh, Y.; Imai, M.; Yamaguchi, Y.; Ohashi, M.; Stein, R.** Cocrystallization and Phase Segregation of Polyethylene Blends between the D and H Species. 8. Small-Angle Neutron Scattering Study of the Molten State and the Structural Relationship of Chains between the Melt and the Crystalline State *Macromolecules* 28(25) 1995: pp. 8484-8490.
  12. **Tanem, B.; Stori, A.** Blends of single-site linear and branched polyethylene. II. Morphology characterisation *Polymer* 42 2001: pp. 6609-6618.
  13. **Puig C.** Enhanced crystallization in branched polyethylenes when blended with linear polyethylene *Polymer* 42 2001: pp. 6579-6585.
  14. **Tanem, B.; Stori, A.** Thermal analysis of single-site polymers in binary blends of low-molecular-weight linear polyethylene and high-molecular-weight branched polyethylene *Thermochimica Acta* 345 2000: pp. 73-80.
  15. **Zhao, Y.; Liu, S.; Yang, D.** Crystallization behavior of blends of high-density polyethylene with novel linear low-density polyethylene *Macromolecular Chemistry and Physics* 198(5) 1997: pp. 1427-1436.
  16. **Tanem, B.; Stori, A.** Blends of single-site linear and branched polyethylene. I. Thermal characterisation *Polymer* 42(12) 2001: pp. 5389-5399.
  17. **Shanks, R.; Amarasinghe, G.** Crystallisation of blends of LLDPE with branched VLDPE *Polymer* 41 2000: pp. 4579-4587.
  18. **Holtrup, W.** Zur fraktionierung von polymeren durch direktextraktion *Makromol. Chem* 178(8) 1977: pp. 2335-2349.
  19. **Puig, C.; Hill, M.; Odell, J.** Absence of isothermal thickening for a blend of linear and branched polyethylene *Polymer* 34(16) 1993: pp. 3402-3407.
  20. **Ueda, M.; Register, R.** Crystallization-induced phase separation in mixtures of model linear and short-chain branched polyethylenes *Journal of Macromolecular Science, Part B Physics* 35(1) 1996: pp. 23-36
  21. **Galante, M.; Alamo, R.; Mandelkern, L.** The crystallization of blends of different types of polyethylene: The role of crystallization conditions *Polymer* 39(21) 1998: pp. 5105-5119.
  22. **Gedde, U.** Crystallization and morphology of binary blends of linear and branched polyethylene *Progress in Colloid Polymer Science* 87 1992: pp. 8-15

**APPENDIX II:  
CURRICULUM VITAE**



## ELULOOKIRJELDUS

### 1. Isikuandmed

Ees- ja perekonnanimi: Triinu Poltimäe  
Sünniaeg ja koht: 19. jaanuar 1979, Tallinn  
Kodakondsus: Eesti

### 2. Kontaktandmed

Aadress: TTÜ, Polümeermaterjalide instituut, Ehitajate tee 5, 19086  
Tallinn, Eesti  
Telefon: +372 620 2906  
E-posti aadress: triinu.poltimae@ttu.ee

### 3. Hariduskäik

| Õppeasutus<br>(nimetus lõpetamise ajal) | Lõpetamise aeg | Haridus (eriala/kraad)      |
|---|----------------|-----------------------------|
| Tallinna Tehnikaülikool                 | 2007           | Tehnikateaduste magister    |
| Tallinna Tehnikaülikool                 | 2002           | Tehnikateaduste bakalaureus |

### 4. Keelteoskus

| Keel    | Tase      |
|---------|-----------|
| Eesti   | Kõrgtase  |
| Inglise | Kõrgtase  |
| Vene    | Keskstase |
| Soome   | Algtase   |

### 5. Täiendusõpe

| Õppimise aeg   | Täiendusõppe läbiviija nimetus                         |
|----------------|--|
| 2003-2006      | Tallinna Keeltekool, vene keel                         |
| 2008, apr.-mai | TTÜ, plastide töötlemine                               |
| 2008, 1 nädal  | Oslo Ülikool, katsekehade valmistamine kuumpressimisel |
| 2009, 1 nädal  | Oslo Ülikool, polümeeride lahuses segamine             |
| 2010, 1 nädal  | TTÜ, polümeeride termo-mehaaniline analüüs             |
| 2010, apr.-mai | Oslo Ülikool, polümeeride lahuses segamine             |

## 6. Teenistuskäik

| Töötamise aeg | Organisatsiooni nimetus           | Ametikoht                                |
|---------------|-----------------------------------|--|
| 2011-         | TTÜ                               | teadur                                   |
| 2006-2011     | TTÜ                               | insener                                  |
| 2005-2006     | Horizon Tselluloosi- ja Paberi AS | kvaliteediosakond,<br>juhataja           |
| 2003-2005     | Horizon Tselluloosi- ja Paberi AS | kvaliteediosakond,<br>juhataja asetäitja |

## 7. Kaitstud lõputööd

Tehnikateaduste magistrikraad (2007): Antiseptikute väljapestavus kaitseimmutautud männipuidust. Juhendaja prof. Tiit Kaps.

Tehnikateaduste bakalaureusekraad (2002): Tärglise mõju puitkiudplaatide omadustele. Juhendaja dotsent Rein Reiska.

# CURRICULUM VITAE

## 1. Personal data

Name: Triinu Poltimäe

Date and place of birth: 19th January 1979, Tallinn

Citizenship: Estonia

## 2. Contact information

Address: TUT, Department of Polymer Materials, Ehitajate tee 5,  
19086 Tallinn, Estonia

Phone: +372 620 2906

E-mail: triinu.poltimae@ttu.ee

## 3. Education

| Educational institution          | Graduation year | Education (field of study/degree) |
|----------------------------------|-----------------|-----------------------------------|
| Tallinn University of Technology | 2007            | Master of Science                 |
| Tallinn University of Technology | 2002            | Bachelor of Science               |

## 4. Language competence/skills

| Language | Level        |
|----------|--------------|
| Estonian | Fluent       |
| English  | Fluent       |
| Russian  | Average      |
| Finnish  | Basic skills |

## 5. Special Courses

| Period         | Educational or other organization                   |
|----------------|---|
| 2003-2006      | Tallinn Language School, russian language           |
| 2008, Apr.-May | TUT, plastics processing                            |
| 2008, 1 week   | University of Oslo, sample preparation              |
| 2009, 1 week   | University of Oslo, polymer solution blending       |
| 2010, 1 week   | TUT, thermo-mechanical characterization of polymers |
| 2010, Apr.-May | University of Oslo, polymer solution blending       |

## 6. Professional Employment

| Period    | Organisation             | Position                          |
|-----------|--------------------------|-----------------------------------|
| 2011-     | TUT                      | Research scientist                |
| 2006-2011 | TUT                      | Engineer                          |
| 2005-2006 | Horizon Pulp & Paper Ltd | Head of quality department        |
| 2003-2005 | Horizon Pulp & Paper Ltd | Deputy head of quality department |

## 7. Defended theses

Master of Science (2007): Leachability of Antiseptics From Preservative Treated Pinewood. Supervisor prof. Tiit Kaps.

Bachelor of Science (2002): Effect of starch on fiberboard properties. Supervisor Associate Professor Rein Reiska.

**DISSERTATIONS DEFENDED AT  
TALLINN UNIVERSITY OF TECHNOLOGY ON  
CHEMISTRY AND CHEMICAL ENGINEERING**

1. **Endel Piiraja**. Oxidation and Destruction of Polyethylene. 1993.
2. **Meili Rei**. Lihatehnoloogia teaduslikud alused. Fundamentals of Food Technology. 1995.
3. **Meeme Põldme**. Phase Transformations in Hydrothermal Sintering Processing of Phosphate Rock. 1995.
4. **Kaia Tõnsuaadu**. Thermophosphates from Kovdor and Siilinjärvi Apatites. 1995.
5. **Anu Hamburg**. The Influence of Food Processing and Storage on the N-Nitrosamines Formation and Content in Some Estonian Foodstuffs. 1995.
6. **Ruth Kuldvee**. Computerized Sampling in Ion Chromatography and in Capillary Electrophoresis. 1999.
7. **Külliki Varvas**. Enzymatic Oxidation of Arachidonic Acid in the Coral *Gersemia fruticosa*. 1999.
8. **Marina Kudrjašova**. Application of Factor Analysis to Thermochromatography and Promotion Studies. 2000.
9. **Viia Lepane**. Characterization of Aquatic Humic Substances by Size Exclusion Chromatography and Capillary Electrophoresis. 2001.
10. **Andres Trikkel**. Estonian Calcareous Rocks and Oil Shale Ash as Sorbents for SO<sub>2</sub>. 2001.
11. **Marina Kritševskaja**. Photocatalytic Oxidation of Organic Pollutants in Aqueous and Gaseous Phases. 2003.
12. **Inna Kamenev**. Aerobic Bio-Oxidation with Ozonation in Recalcitrant Wastewater Treatment. 2003.
13. **Janek Reinik**. Methods for Purification of Xylidine-Polluted Water. 2003.
14. **Andres Krumme**. Crystallisation Behaviour of High Density Polyethylene Blends with Bimodal Molar Mass Distribution. 2003.
15. **Anna Goi**. Advanced Oxidation Processes for Water Purification and Soil Remediation. 2005.
16. **Pille Meier**. Influence of Aqueous Solutions of Organic Substances on Structure and Properties of Pinewood (*Pinus sylvestris*). 2007.
17. **Kristjan Kruusement**. Water Conversion of Oil Shales and Biomass. 2007.

18. **Niina Kulik**. The Application of Fenton-Based Processes for Wastewater and Soil Treatment. 2008.
19. **Raul Järviste**. The Study of the Changes of Diesel Fuel Properties a its Long Term Storage. 2008.
20. **Mai Uibu**. Abatement of CO<sub>2</sub> Emissions in Estonian Oil Shale-Based Power Production. 2008.
21. **Valeri Gorkunov**. Calcium-Aluminothermal Production of Niobium and Utilization of Wastes. 2008.
22. **Elina Portjanskaja**. Photocatalytic Oxidation of Natural Polymers in Aqueous Solutions. 2009.
23. **Karin Reinhold**. Workplace Assessment: Determination of Hazards Profile using a Flexible Risk Assessment Method. 2009.
24. **Natalja Savest**. Solvent Swelling of Estonian Oil Shales: Low Temperature Thermochemical Conversion Caused Changes in Swelling. 2010.
25. **Triin Märtson**. Methodology and Equipment for Optical Studies of Fast Crystallizing Polymers. 2010.
26. **Deniss Klauson**. Aqueous Photocatalytic Oxidation of Non-Biodegradable Pollutants. 2010.
27. **Oliver Järvik**. Intensification of Activated Sludge Process – the Impact of Ozone and Activated Carbon. 2011.